Office of National Marine Sanctuaries
National Oceanic and Atmospheric Administration
NATIONAL MARINE SANCTUARIES CONSERVATION SCIENCE SERIES

Long-term Monitoring at East and West Flower Garden Banks: 2018 Annual Report

June 2020 | sanctuaries.noaa.gov | National Marine Sanctuaries Conservation Series ONMS-20-09

U.S. Department of Commerce
Wilbur Ross, Secretary

National Oceanic and Atmospheric Administration
Neil A. Jacobs, Ph.D.
Assistant Secretary of Commerce for Environmental Observation and Prediction

National Ocean Service
Nicole LeBoeuf, Assistant Administrator (Acting)

Office of National Marine Sanctuaries
John Armor, Director

Report Authors:

Michelle A. Johnston[1], Raven D. Blakeway[2], Kelly O'Connell[2], Jimmy MacMillan[2], Marissa F. Nuttall[2], Xinping Hu[3], John A. Embesi[2], Emma L. Hickerson[1], and G.P. Schmahl[1]

[1]Flower Garden Banks National Marine Sanctuary, Galveston, TX, USA

[2]CPC, Galveston, TX, USA

[3]Carbon Cycle Laboratory, Department of Physical and Environmental Sciences, Texas A&M University – Corpus Christi, TX, USA

Suggested Citation:
Johnston, M.A., R.D. Blakeway, K. O'Connell, J. MacMillan, M.F. Nuttall, X. Hu, J.A. Embesi, E.L. Hickerson, and G.P. Schmahl. 2020. Long-Term Monitoring at East and West Flower Garden Banks: 2018 Annual Report. National Marine Sanctuaries Conservation Series ONMS-20-09. U.S. Department of Commerce, National Oceanic and Atmospheric Administration, Flower Garden Banks National Marine Sanctuary, Galveston, TX. 124 pp.

Cover Photo:
Two great barracuda (*Sphyraena barracuda*) swim over star coral colonies at Flower Garden Banks National Marine Sanctuary in 2018. Photo: G.P. Schmahl/NOAA

About the National Marine Sanctuaries Conservation Series

The Office of National Marine Sanctuaries, part of the National Oceanic and Atmospheric Administration, serves as the trustee for a system of underwater parks encompassing more than 600,000 square miles of ocean and Great Lakes waters. The 14 national marine sanctuaries and two marine national monuments within the National Marine Sanctuary System represent areas of America's ocean and Great Lakes environment that are of special national significance. Within their waters, giant humpback whales breed and calve their young, coral colonies flourish, and shipwrecks tell stories of our nation's maritime history. Habitats include beautiful coral reefs, lush kelp forests, whale migration corridors, spectacular deep-sea canyons, and underwater archaeological sites. These special places also provide homes to thousands of unique or endangered species and are important to America's cultural heritage. Sites range in size from less than one square mile to almost 583,000 square miles. They serve as natural classrooms and cherished recreational spots, and are home to valuable commercial industries.

Because of considerable differences in settings, resources, and threats, each marine sanctuary has a tailored management plan. Conservation, education, research, monitoring, and enforcement programs vary accordingly. The integration of these programs is fundamental to marine protected area management. The Marine Sanctuaries Conservation Series reflects and supports this integration by providing a forum for publication and discussion of the complex issues currently facing the sanctuary system. Topics of published reports vary substantially and may include descriptions of educational programs, discussions on resource management issues, and results of scientific research and monitoring projects. The series facilitates integration of natural sciences, socioeconomic and cultural sciences, education, and policy development to accomplish the diverse needs of NOAA's resource protection mandate. All publications are available on the Office of National Marine Sanctuaries website (http://www.sanctuaries.noaa.gov).

Disclaimer

The scientific results and conclusions, as well as any views or opinions expressed herein, are those of the authors and do not necessarily reflect the views of NOAA or the Department of Commerce. The mention of trade names or commercial products does not constitute endorsement or recommendation for use.

Report Availability

Electronic copies of this report may be downloaded from the Office of National Marine Sanctuaries web site at http://sanctuaries.noaa.gov.

Contact

Michelle A. Johnston, Ph.D.
NOAA Flower Garden Banks National Marine Sanctuary
NOAA Galveston Laboratory
4700 Avenue U, Bldg. 216
Galveston, TX 77551
(409) 356-0392
Michelle.A.Johnston@noaa.gov

Or

Mark Belter
Bureau of Ocean Energy Management
Gulf of Mexico OCS Region, GM 673 E
1201 Elmwood Park Blvd.
New Orleans, LA 70123
(504) 736-1739
Mark.Belter@boem.gov

Table of Contents

Abstract

This report summarizes fish and benthic community observations and water quality data collected from East Flower Garden Bank and West Flower Garden Bank long-term monitoring study sites in 2018. East Flower Garden Bank and West Flower Garden Bank are part of Flower Garden Banks National Marine Sanctuary, located in the northwestern Gulf of Mexico. The annual long-term monitoring program began in 1989 and is funded by NOAA's Flower Garden Banks National Marine Sanctuary and the Bureau of Ocean Energy Management, with support from the National Marine Sanctuary Foundation. In 2018, mean coral cover was 52% within the East Flower Garden Bank study site and 56% within the West Flower Garden Bank study site. Mean macroalgae cover was 35% within the East Flower Garden Bank study site and 27% within the West Flower Garden Bank study site. Mean coral cover within repetitive study site photostations and at deep repetitive photostations ranged from 64–75% at both banks. The *Orbicella* species complex, listed as threatened under the Endangered Species Act, accounted for the majority of the coral cover within the study sites. Fish surveys conducted in 2018 indicated an abundant reef fish community, dominated by the families Labridae and Pomacentridae. During 2018, water temperatures on the reef did not exceed 30°C and coral bleaching at both banks was less than 1%.

Key Words

benthic community, coral ecosystem, coral reef, fish community, long-term monitoring, Flower Garden Banks National Marine Sanctuary, Gulf of Mexico, marine protected area, water quality

Executive Summary

A manta ray (*Manta cf. birostris*) swims through the long-term monitoring study site at East Flower Garden Bank in 2018. Photo: Emma Hickerson/NOAA

Since 1989, a federally supported long-term coral reef monitoring program has focused on two study sites on East Flower Garden Bank (EFGB) and West Flower Garden Bank (WFGB) in the northwestern Gulf of Mexico. In 29 years of nearly continuous monitoring, mean live coral cover has been approximately 50% or higher, and despite global coral reef declines in recent decades, EFGB and WFGB have suffered minimally from hurricanes, recovered from coral bleaching events, and shown no signs of disease.

This report summarizes fish and benthic community observations and water quality data from 2018, as well as nearly 29 years of historical monitoring data. The benthic and fish community surveys were conducted by a team of multi-disciplinary scientists using random transects to document components of benthic cover, repetitive photostations to document changes in the composition of benthic assemblages in shallow and deep repetitive sites, surveys for sea urchins and lobster, and modified reef fish visual census surveys to examine fish population composition within designated study sites at EFGB and WFGB. The annual long-term monitoring program is jointly funded by NOAA's Flower Garden Banks National Marine Sanctuary (FGBNMS) and the Bureau of Ocean Energy Management, with support from the National Marine Sanctuary Foundation. Key findings from data collected within long-term monitoring study sites in 2018 are described below.

Living coral is the principal component of the benthic community at EFGB and WFGB, followed by macroalgae, colonizable substrates, and sponges. Percent live coral cover was 52% and 56% within EFGB and WFGB study sites (17–27 m), respectively, and 54% for both sites combined. *Orbicella franksi* had the highest mean coral cover within EFGB (27%) and WFGB (31%) study sites, followed by *Pseudodiploria strigosa* (EFGB 8%, WFGB 7%), *Porites astreoides* (6% for both EFGB and WFGB), *Orbicella faveolata* (EFGB 5%, WFGB 4%), and *Colpophyllia natans* (EFGB 2%, WFGB 3%). The *Orbicella* species complex, including *Orbicella franksi, Orbicella faveolata*, and *Orbicella annularis* (all of which are listed as threatened species under the Endangered Species Act), made up 63% of the observed coral species within EFGB study sites and 64% of the observed coral species within WFGB study sites. Macroalgae was the second highest benthic cover component at the EFGB (35%) and WFGB (27%) study sites and has increased significantly since 1999, averaging approximately 30% since 2009.

Permanent repetitive photo stations have been established within the study sites (19–40 m) and along the deeper flanks of the coral cap (24–40 m) to document benthic changes in selected sites over time. Within repetitive photostations, increases in coral cover over time were documented, and less than 1% of the coral cover analyzed was observed to pale or bleach in 2018 at the time of surveys. In the 32–40 m depth range, repetitive deep photostation mean coral cover was 70% at EFGB and 75% at WFGB. Along with increased percent cover, coral species composition changed slightly with depth; *Orbicella franksi* (34% at EFGB, 40% at WFGB) and *Montastraea cavernosa* (11% at EFGB, 12% at WFGB) were the species with the highest percent cover in repetitive deep photostations.

A total of 16 coral species were documented in coral demographic surveys at EFGB and 18 at WFGB (22 species documented for both banks combined). Overall mean coral density was 5 corals/m^2 in both EFGB and WFGB study sites. *Porites astreoides* was the most abundant species observed in study site surveys, *Orbicella franksi* colonies occupied the greatest total area at both banks, while *Orbicella annularis* colonies were the largest colonies in EFGB surveys, and *Siderastrea siderea* colonies were the largest in WFGB surveys in 2018.

To document incremental growth or regression of coral edges, lateral margins of selected *Pseudodiploria strigosa* colonies were monitored and photographed from 2014 to 2018. Mean tissue change in the lateral growth photostations over the five-year period was positive in both EFGB and WFGB stations, reflecting marginal growth over time. Despite improved changes that have been made to this methodology over time, these stations have a short lifespan as the colony margins grow, and it is not a common method used in other coral reef monitoring programs. Therefore, BOEM and NOAA will no longer collect this data after 2018.

Long-spined sea urchin (*Diadema antillarum*) density within the EFGB study site has remained low (ranging from 0–2 per 100 m^2) since sea urchin monitoring surveys were first conducted in 2004, but densities within the WFGB study site (1–21 per 100 m^2) have been significantly higher than EFGB through 2018. Since lobster surveys began in 2004, Caribbean spiny lobster (*Panulirus argus*) and spotted spiny lobster (*Panulirus guttatus*) counts have ranged from zero to two individuals per 100 m^2 within study sites.

A total of 29 families and 70 fish species were recorded in 2018 surveys, indicating Labridae (wrasses and parrotfish) and Pomacentridae (damselfish) as the predominant fish families observed within the study sites. Bonnetmouth (*Emmelichthyops atlanticus*) and bluehead (*Thalassoma bifasciatum)* were the most abundant species within the study sites at both banks. Mean fish density (564.68 ± 126.94 SE individuals/100 m^2) and biomass (60,160.96 ± 45,822.84 SE g/100 m^2) was greatest within the EFGB study site compared to the WFGB study site (471.87 ± 146.38 SE individuals/100 m^2 and 7,104.07 ± 1,508.24 SE g/100 m^2, respectively), and piscivores had the greatest mean biomass in all surveys. For commercially and recreationally important species, both grouper and snapper density was higher within EFGB study site surveys. Lionfish densities at EFGB (0.26 individuals/100 m^2) and WFGB (0.17 individuals/100 m^2) continue to remain lower than other locations in the southeast U.S. and Caribbean region, and the non-native regal demoiselle (*Neopomacentrus cyanomos*) was observed in study site surveys (0.28 and 0.24 individuals/100 m^2 at EFGB and WFGB, respectively) for the first time in 2018.

At 24 m, reef cap mean seawater temperatures at EFGB ranged from 20.12^{o}C to 29.81^{o}C at EFGB and 19.59^{o}C to 29.85^{o}C at WFGB, never exceeding 30^{o}C in 2018. Daily mean salinity levels at the 24 m depth averaged 36 psu. Nutrients sampled in seawater (chlorophyll *a*, ammonia, nitrate, nitrite, phosphorous, and total Kjeldahl nitrogen) were below detectable limits at both banks, with the exception of elevated nitrate levels at the surface and in midwater samples at WFGB in October 2018. Carbonate chemistry indicated clear seasonality (highest DIC values in April, pCO_2 values in August, and $\Omega_{aragonite}$ values in October) within the water column around FGBNMS, but suggested that EFGB and WFGB are overall net CO_2 sinks ($\Omega_{aragonite}$ ranged from 3.58–3.92 at EFGB and WFGB).

Overall, some of the most important trends documented since monitoring began in 1989 have been significantly increasing macroalgae cover since 1999, stable or increasing coral cover, and significantly increasing seawater temperatures at the reef depth. In contrast to many other reefs in the Gulf of Mexico and Caribbean region, macroalgae at EFGB and WFGB has experienced a sustained increase, yet coral cover has not declined. This may be due to the remote offshore location and deep water surrounding the banks, providing a buffer and more stable environment than shallower reefs in the region. Other notable characteristics include increasing sea urchin populations and an abundant reef fish community.

The relatively high coral cover documented since the beginning of the monitoring program make EFGB and WFGB unique and in need of continued protection and conservation measures. Continued monitoring will document changes in reef community condition compared to the historical baseline and enable resource managers to make decisions regarding management and research amid threats such as climate change, invasive species, storms, and water quality degradation.

Chapter 1. Long-Term Monitoring at East and West Flower Garden Banks

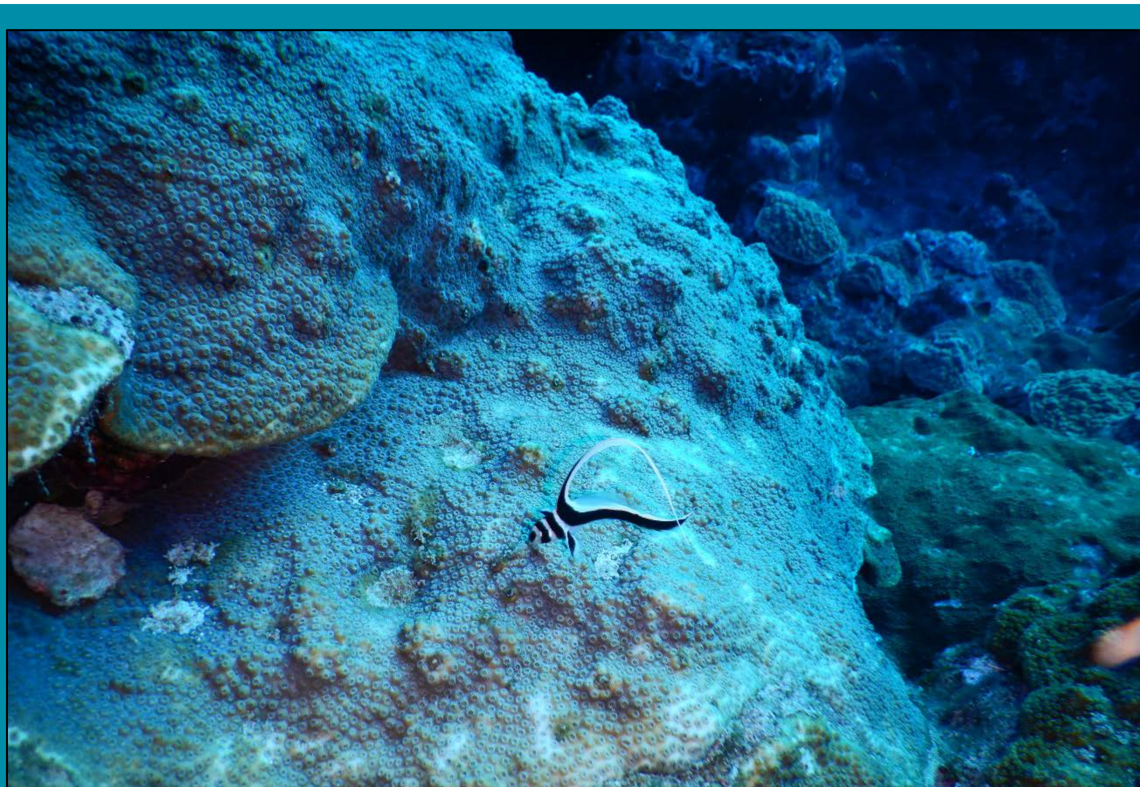

A juvenile spotted drum (*Equetus punctatus*) swims above a boulder star coral colony in the long-term monitoring study site at West Flower Garden Bank in 2018. Photo: Marissa Nuttall/CPC

Habitat Description

The coral reef-capped East Flower Garden Bank (EFGB) and West Flower Garden Bank (WFGB) are part of a discontinuous arc of reef environments along the outer continental shelf in the northwestern Gulf of Mexico (Bright et al. 1985) (Figure 1.1). These reefs occupy elevated salt domes located approximately 190 km south of the Texas and Louisiana border, containing several distinct habitats ranging in depth from 16–150 m (Bright and Rezak 1976; Schmahl et al. 2008).

The caps of the banks are approximately 20 km apart and within the photic zone, where conditions are ideal for colonization by species of corals, algae, invertebrates, and fish, similar to coral reef species found in the Caribbean region (Goreau and Wells 1967; Schmahl et al. 2008; Clark et al. 2014; Johnston et al. 2016b). The shallowest portions of each bank are topped by well-developed coral reefs, at depths ranging from 16–40 m. Although the coral species found on the EFGB and WFGB reef caps are similar to other species on Caribbean reefs, octocorals are absent and scleractinian corals of the genus *Acropora* are rare on the reefs, likely due to the latitude of the banks, as they near the northernmost limit of the coral distribution range (Bright et al. 1985; CSA 1989).

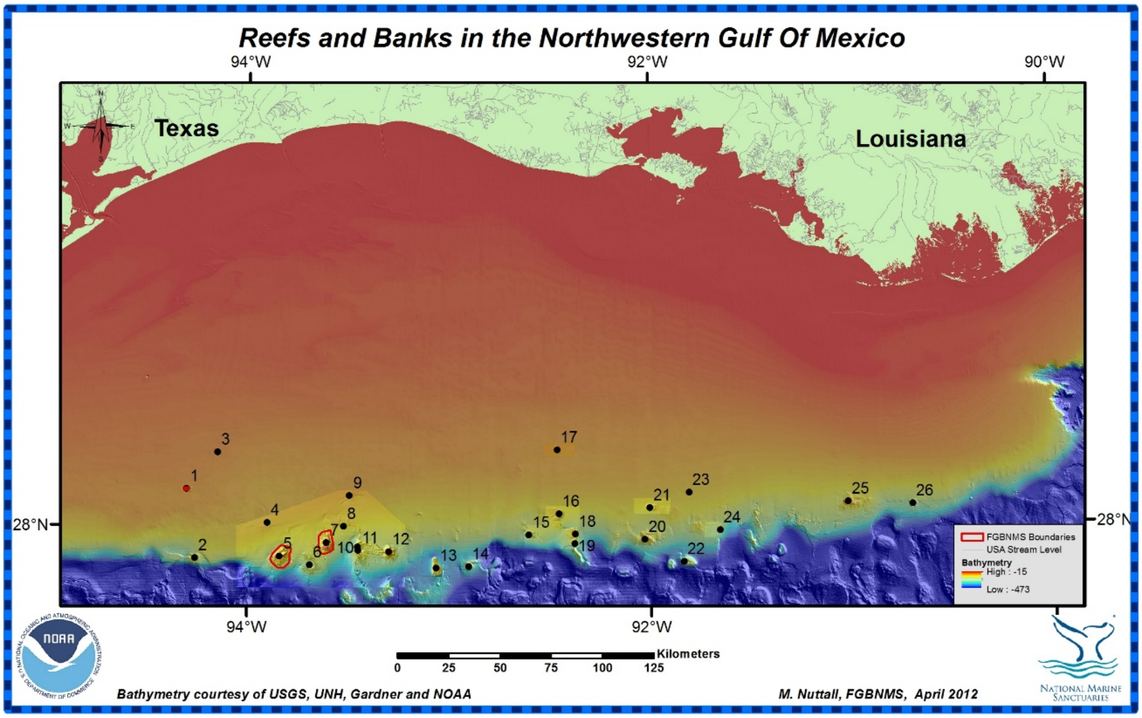

Figure 1.1. Map of EFGB, WFGB, and Stetson Bank (outlined in red) in relation to the Texas-Louisiana continental shelf and other topographic features of the northwestern Gulf of Mexico. Numbered banks include: 1. Stetson Bank, 2. Applebaum Bank, 3. Claypile Bank, 4. Coffee Lump Bank, 5. West Flower Garden Bank, 6. Horseshoe Bank, 7. East Flower Garden Bank, 8. MacNeil Bank, 9. 29 Fathom Bank, 10. Rankin Bank, 11. 28 Fathom Bank, 12. Bright Bank, 13. Geyer Bank, 14. Elvers Bank, 15. McGrail Bank, 16. Bouma Bank, 17. Sonnier Bank, 18. Rezak Bank, 19. Sidner Bank, 20. Parker Bank, 21. Alderdice Bank, 22. Sweet Bank, 23. Fishnet Bank, 24. Jakkula Bank, 25. Ewing Bank, 26. Diaphus Bank.

Long-Term Monitoring Program History

In the 1970s, due to concerns about potential impacts from offshore oil and gas development, the Department of Interior (initially through the Bureau of Land Management, then the Minerals Management Service [MMS], and now the Bureau of Ocean Energy Management [BOEM]) has supported monitoring at EFGB and WFGB to collect data and determine if the reefs are impacted by nearby oil and gas activities (Figure 1.2).

First under industry funding, then MMS funding and a partnership with Texas A&M University (TAMU), long-term monitoring study sites containing repetitive monitoring photostations were established in 1989, marking the official start of the Flower Garden Banks Long-Term Monitoring (LTM) program (CSA 1989; Gittings et al. 1992). Flower Garden Banks National Marine Sanctuary (FGBNMS) was established in 1992 (Code of Federal Regulations, 15 CFR Part 992, Subpart L, Section 922.120), and monitoring was conducted by both TAMU and environmental consulting groups through competitive contracts throughout the years. Starting in 2009, BOEM and NOAA established an interagency agreement for FGBNMS to carry out the LTM program.

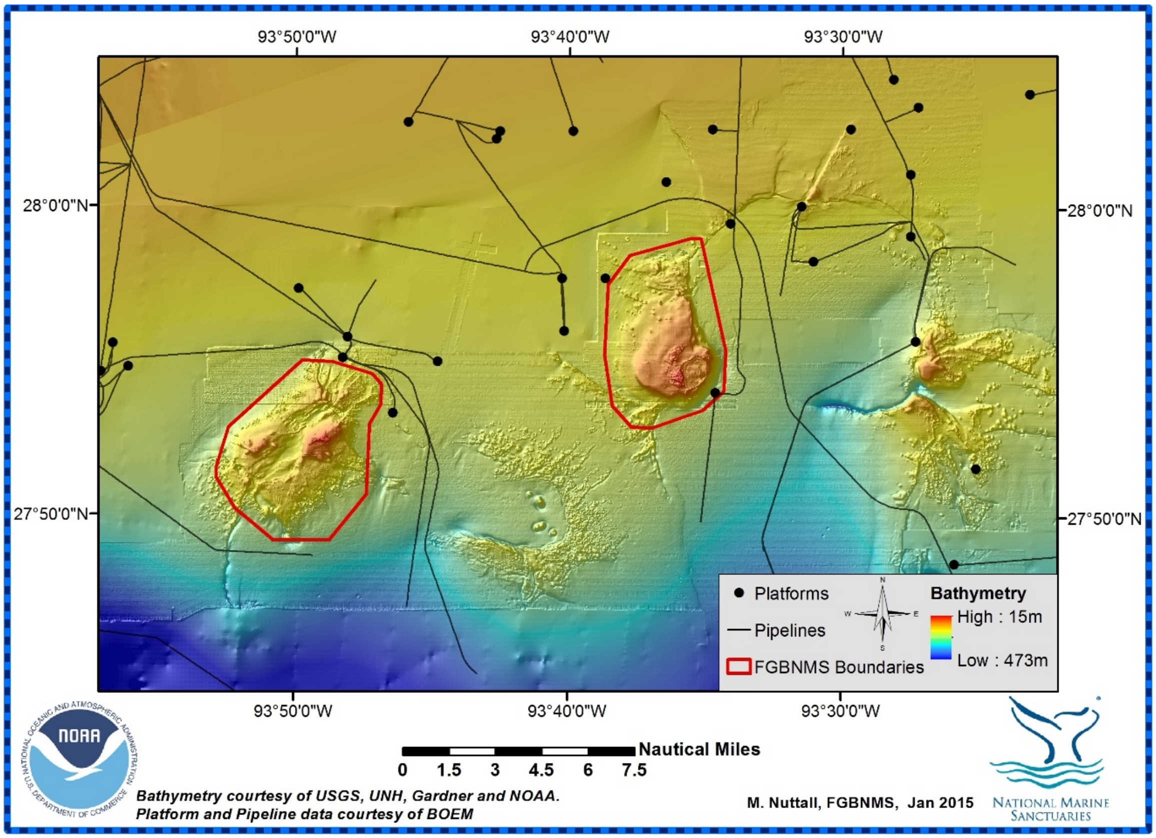

Figure 1.2. Map of oil and gas platforms and pipelines near EFGB and WFGB. FGBNMS boundaries are outlined in red.

Long-Term Monitoring Program Objectives

Priorities of FGBNMS include managing natural resources as stated in the National Marine Sanctuaries Act, and identifying threats and potential sources of impacts to coral reefs, including: overfishing, pollution, runoff, visitor impacts, disease, bleaching, invasive species, hurricanes, and oil and gas industry activities. Knowing the condition of natural resources within the national marine sanctuary and providing scientifically credible data is fundamental to NOAA’s ability to protect and manage these areas, and to evaluate management actions.

Through the interagency agreement, the LTM program is of significant interest to both NOAA and BOEM, who share responsibility to protect and monitor these important marine resources. The five objectives and subsequent indicators of the FGBNMS LTM program include:

- Monitor and evaluate environmental changes and variability in abundances of reef-associated organisms across multiple time scales.
    - Indicators: Benthic percent cover, fish community dynamics, water quality, and coral demographic analyses
- Identify changes in coral reef health resulting from both natural and human-induced stressors to facilitate management-level responses.
    - Indicators: Bleaching, disease, and invasive species
- Provide a resource to facilitate adaptive management of activities impacting reef-related resources.
    - Indicators: Maintain baseline data and image archive of damage to resources if observed
- Identify and monitor key species that may be indicative of reef and ecosystem health.
    - Indicators: Trends in sea urchin and lobster surveys
- Provide a consistent and timely source of monitoring data on environmental conditions and the status of living marine sanctuary resources.
    - Indicators: Published peer-reviewed annual reports

Long-Term Monitoring Program Components

The LTM program was designed to assess the health of the coral reefs, detect change over time, and provide baseline data in the event that natural or human-induced activities endanger the integrity of EFGB and WFGB coral communities. The high coral cover and robust fish populations compared to other reefs in the region, combined with historical data collection and the proximity to oil and gas development, make EFGB and WFGB ideal sentinel sites for continued monitoring. The following techniques listed below have been used in this monitoring program to evaluate coral reef diversity, growth rates, and community health in designated long-term monitoring 10,000 m^2 study sites at each bank:

- Random photographic transects document benthic cover;
- Repetitive photostations detect and evaluate long-term changes at the stations and in individual coral colonies;
- *Pseudodiploria strigosa* lateral growth photostations provide information on coral colony margin growth or retreat;
- Coral demographic surveys provide information on coral density and coral colony size;
- Stationary reef fish visual census surveys assess community structure of coral reef fishes;
- Long-spined sea urchin (*Diadema antillarum*) and lobster (*Panulirus argus* and *P. guttatus*) surveys establish current population levels and trends;
- Water quality datasondes record salinity, temperature, and turbidity at depth; and
- Nutrient sampling documents chlorophyll *a*, ammonia, nitrate, nitrite, total Kjeldahl nitrogen, and phosphorous levels.

Long-Term Monitoring Study Sites and Data Collection

Long-term monitoring data have been collected annually during summer months since 1989 in permanent 10,000 m² study sites (100 m x 100 m or 1 hectare) (hereafter referred to as “study sites”) at EFGB and WFGB. The corners and centers of the study sites are currently marked by large eyebolts as reference markers. Permanent mooring buoy anchors (mooring buoy #2 at EFGB and mooring buoy #5 at WFGB) have been established near the study site centers to facilitate field operations (Table 1.1; Figures 1.3 and 1.4).

Table 1.1. Coordinates and depths for permanent moorings within study sites at each bank.

Study Site Mooring Buoy Locations			
Mooring	**Lat (DDM)**	**Long (DDM)**	**Depth (m)**
EFGB Mooring #2	27° 54.516’ N	93° 35.831’ W	19.2
WFGB Mooring #5	27° 52.509’ N	93° 48.900’ W	20.7

Within the study sites, depths range from 17–27 m at EFGB and 18–25 m at WFGB. Each year during data collection, divers install reference lines to mark the perimeters of the study sites as well as north-south and east-west centerlines (hereafter referred to as the “crosshairs”). The perimeter and crosshairs divide each site into four 50 m x 50 m quadrants (Figures 1.5 and 1.6). Along with maps (Figures 1.5 and 1.6), the lines aid divers in orientation and navigation to find photostations and allow for efficient completion of monitoring tasks.

For sampling at deeper depths, permanent repetitive photostations are located outside the study sites, ranging in depth from 24–40 m (the station located at 24 m acts as a marker to the other deeper sites). Twenty-three repetitive deep photostations at EFGB are located outside the study site (east of buoy #2), ranging in depth from 32–40 m. Twenty-four repetitive deep photostations are located outside the WFGB study site (north of buoy #2), ranging in depth from 24–38 m.

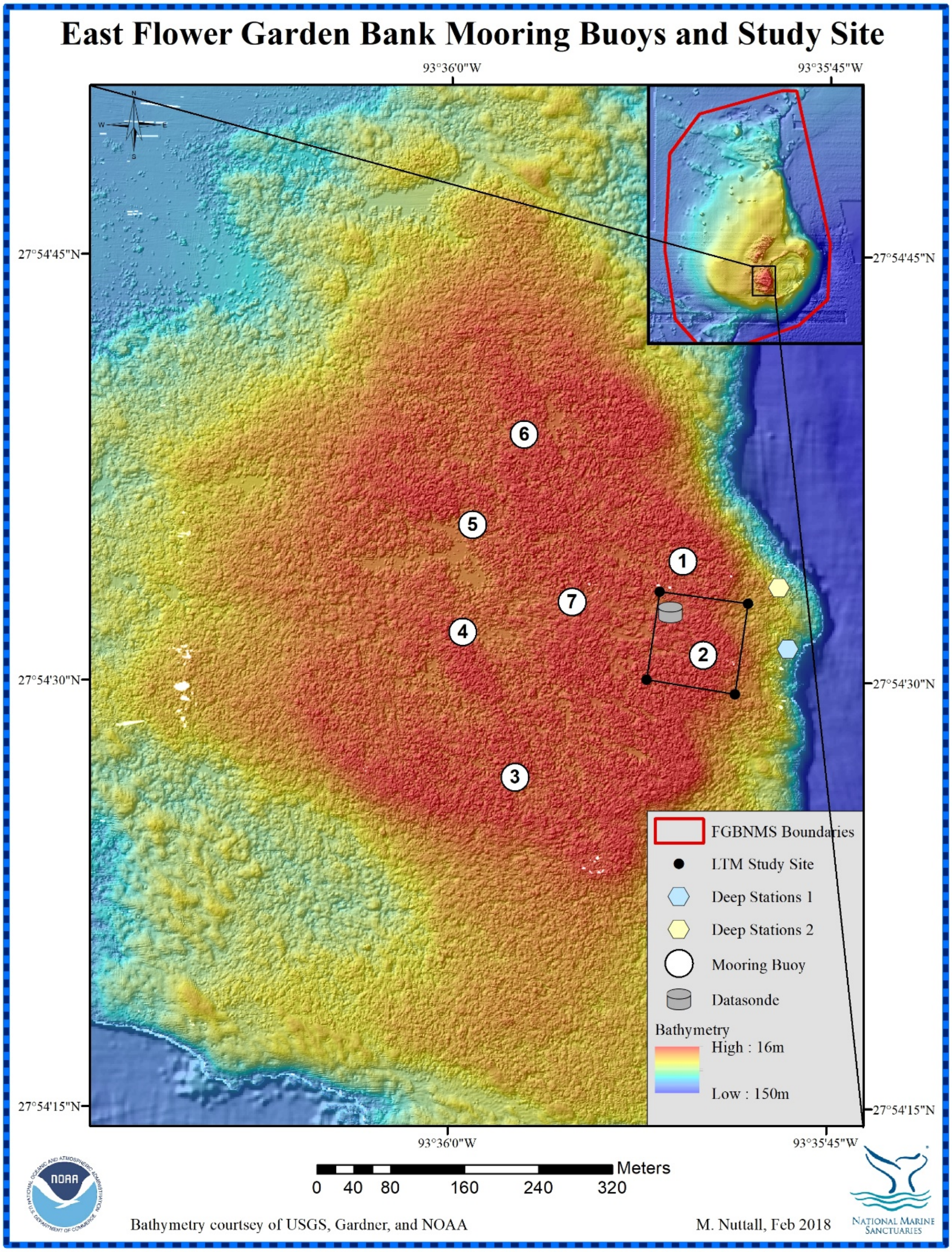

Figure 1.3. Bathymetric map of EFGB with long-term monitoring (LTM) study site, mooring buoy, water quality datasonde, and repetitive deep photostation locations.

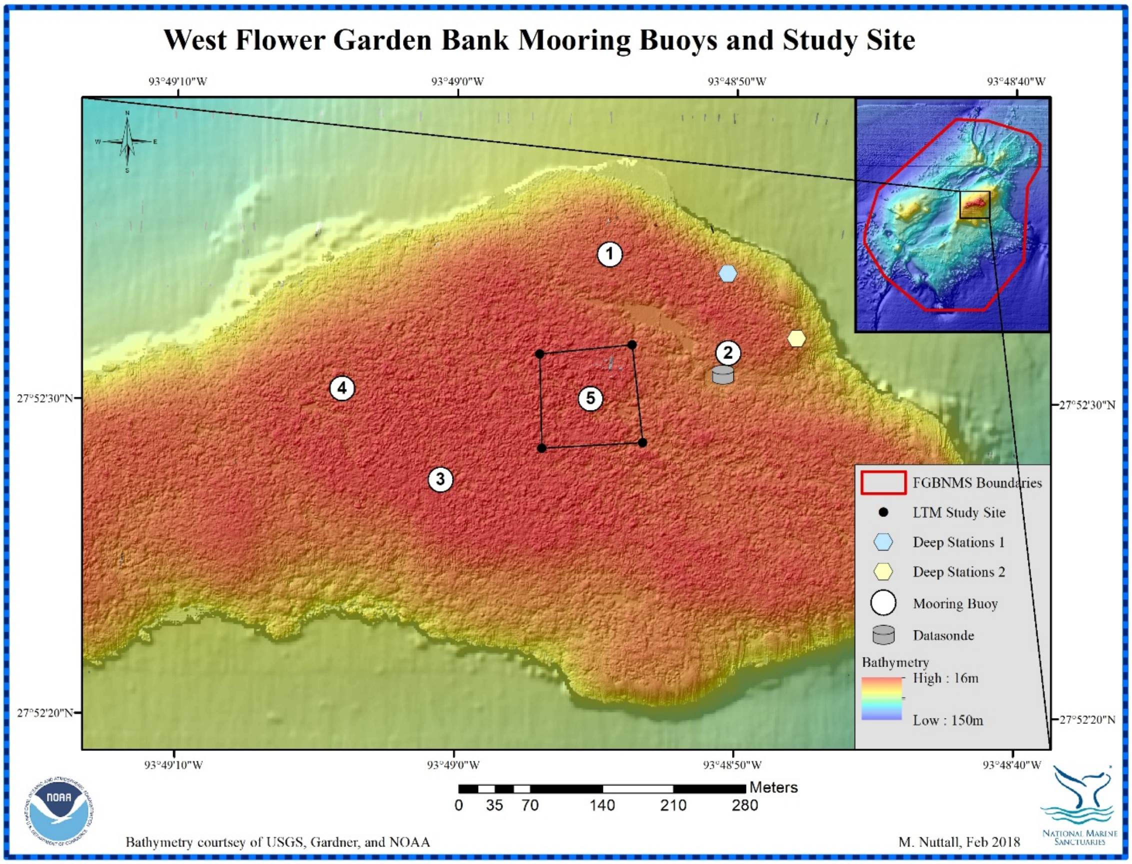

Figure 1.4. Bathymetric map of WFGB with long-term monitoring (LTM) study site, mooring buoy, water quality datasonde, and repetitive deep photostation locations.

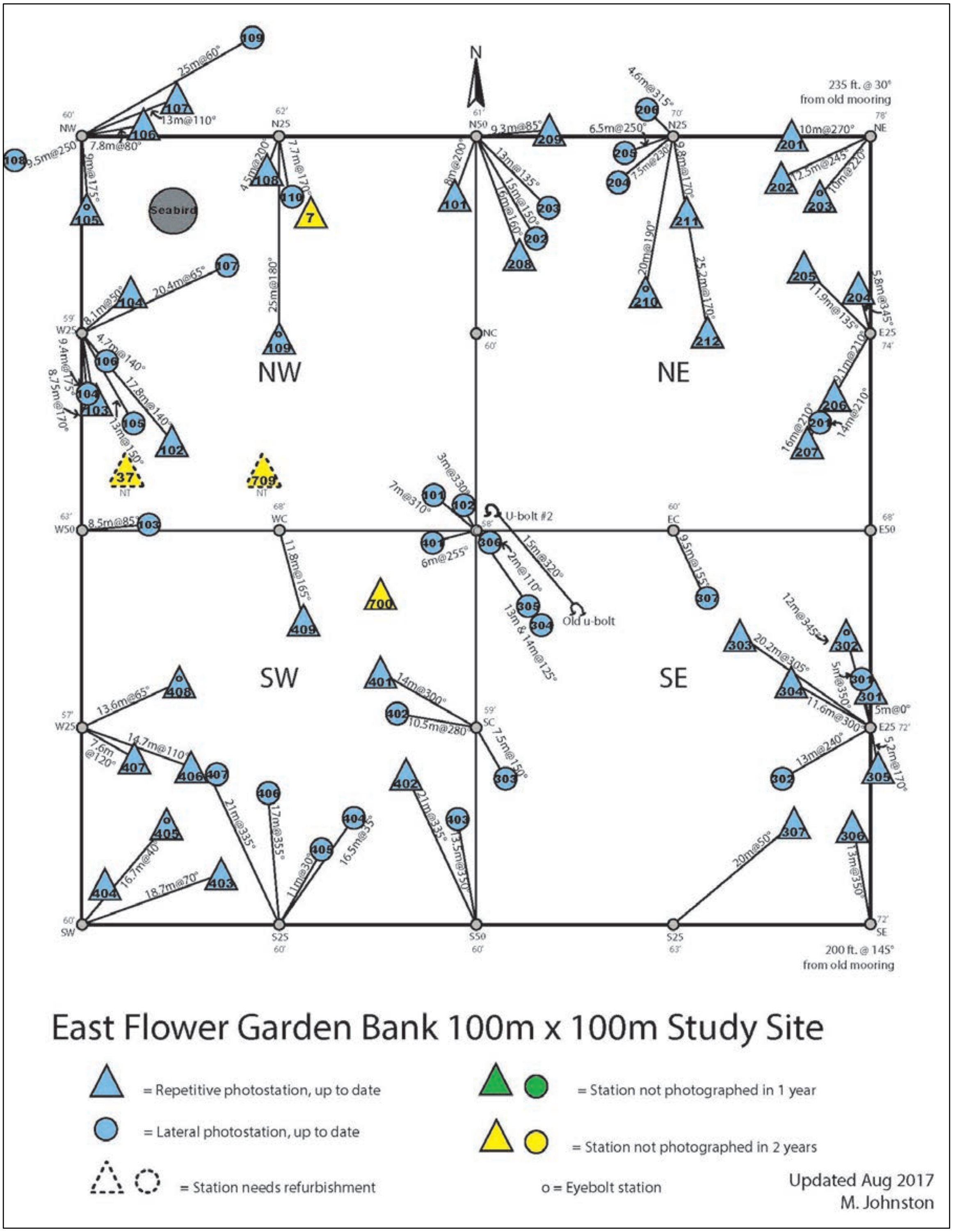

Figure 1.5. Detailed map of the EFGB study site and photostations. Permanent study site corner markers and eye-bolts are installed at 25 m intervals along each perimeter and crosshair line. Reference lines are used to mark the north-south and east-west crosshairs. Establishment of the perimeter and crosshairs divide each site into four 50 m x 50 m quadrants.

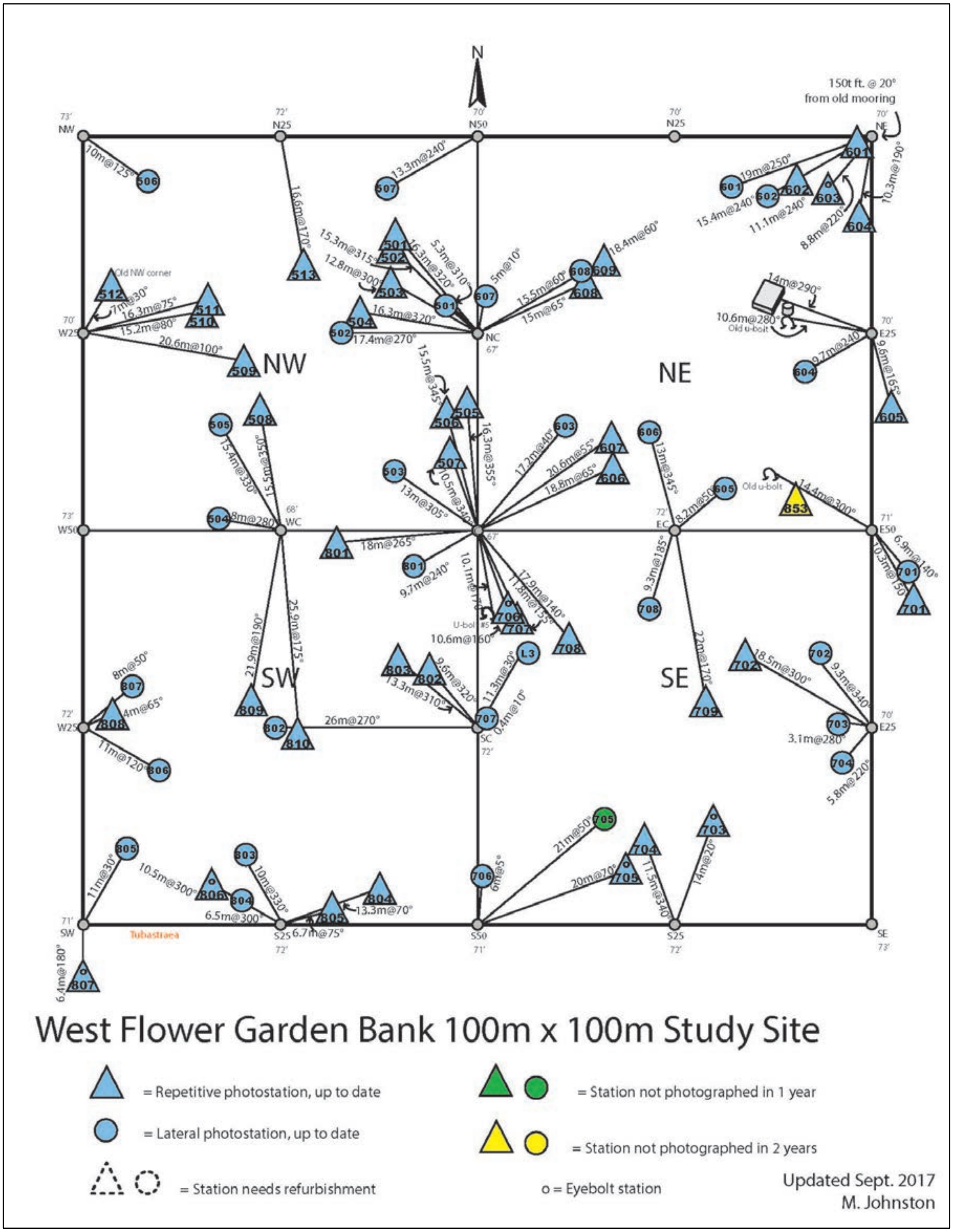

Figure 1.6. Detailed map of the WFGB study site and photostations. Permanent study site corner markers and eye-bolts are installed at 25 m intervals along each perimeter and crosshair line. Reference lines are used to mark the north-south and east-west crosshairs. Establishment of the perimeter and crosshairs divide each site into four 50 m x 50 m quadrants.

Field Operations

Long-term monitoring data were collected within the study sites at EFGB and WFGB in 2018 and SCUBA operations were conducted off the NOAA R/V *Manta* (Table 1.2). The R/V *Manta* is an 83-foot catamaran and is used primarily as a research platform, conducting research and monitoring activities in the waters of the northwestern Gulf of Mexico, mostly within marine sanctuary boundaries. The vessel's A-frame and winch were used for CTD casts on water quality cruises. The extensive dive operations during long-term monitoring cruises were supported by onboard facilities and equipment. Berthing, stowage, galley and safety equipment allowed for multiple day operations supporting four crew and ten scientists.

Table 1.2. Monitoring and response cruises completed at EFGB and WFGB in 2018.

Date	Cruise and Tasks Completed
04/24/2018	Water quality cruise: Water sample collection
06/26/2018 – 06/29/2018	Water quality cruise: Instrument exchange
08/14/2018 – 08/17/2018	Long-term monitoring cruise: WFGB study site annual monitoring and water sample collection
08/21/2018 – 08/24/2018	Long-term monitoring and water quality cruise: WFGB study site annual monitoring and water quality instrument exchange
10/30/2018	Water quality cruise: Instrument exchange and water sample collection
11/07/2018 – 11/08/2018	Deep water quality instrument exchange and deep repetitive photostation photography

Due to unfavorable weather, a quarterly cruise was not completed in the winter season (February 2018). R/V *Manta* vessel maintenance prevented dive operations in the spring of 2018; therefore, only water samples were collected by FGBNMS staff utilizing the M/V *Hull Raiser* in April 2018. Water quality instruments were exchanged and data were downloaded in June 2018.

Annual fieldwork within the WFGB study site was conducted August 14 to 17, 2018 (Table 1.2). Water quality samples were collected, but strong currents did not allow for the exchange and download of the water quality instruments on the seafloor or photography of WFGB deep repetitive photostations.

Annual fieldwork within the EFGB study site was conducted August 21 to 24, 2018 (Table 1.2). Water quality instruments were exchanged at both banks, but strong currents prevented the photography of the EFGB deep repetitive photostations.

A one-day cruise in October 2018 was conducted to exchange water quality instruments. A two-day cruise was completed in November 2018 to finish tasks not completed in August, which included EFGB and WFGB deep repetitive photostation photography and HOBO® water quality instrument exchange at the 30 m and 40 m depth locations.

Chapter 2. Random Transects

A NOAA diver with camera and strobes mounted on an aluminum t-frame takes random transect photographs within the EFGB study site. Photo: G.P. Schmahl/NOAA

Random Transect Introduction

Benthic cover, including components such as corals, sponges, colonizable substrates, and macroalgae, was assessed by analyzing a series of randomly located 8 m photo transects within study sites. The surveys were used to compare habitat and document the benthic reef community between EFGB and WFGB study sites as well as changes over time in each study site.

Random Transect Methods

Random Transect Field Methods

Sixteen non-overlapping random transects within each study site were completed in 2018. Divers were given a randomly-generated start location and heading for each survey. A Canon Power Shot® G11 digital camera in an Ikelite® housing and 28 mm equivalent wet mount lens adapter, mounted on a 0.65 m t-frame with a bubble level and two Inon® Z240 strobes was used to capture images along the transects. The bubble level mounted to the t-frame center ensured images were taken in a vertical orientation to aid in standardizing the area captured. The mounted camera was placed at pre-marked intervals 80 cm apart on a spooled 15 m measuring tape, producing 17 non-overlapping images along the transect (Figure 2.1). Each still frame image captured a 0.8 x 0.6 m area (0.48 m^2). This produced a total photographed area of 8.16 m^2 per transect, and a minimum photographed area of 130.56 m^2 per study site per year. For more detailed methods, reference Johnston et al. 2017a.

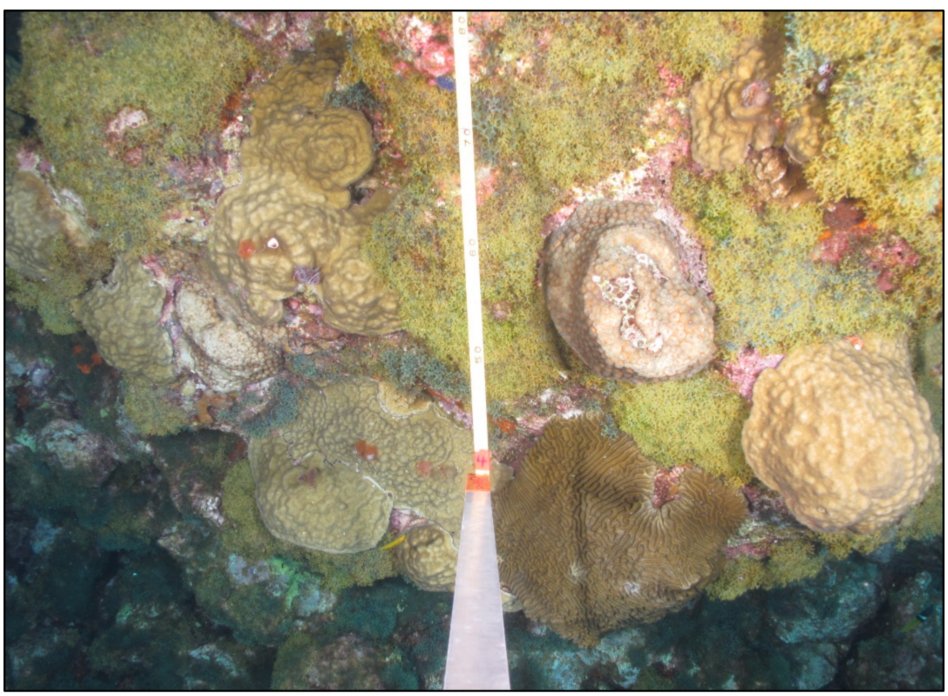

Figure 2.1. Photo taken at marked interval along random transect with camera mounted to aluminum t-frame within the EFGB study site in 2018. Photo: John Embesi/CPC

It should be noted that during the period of study, a variety of underwater camera setups were used as technology advanced from 35 mm slides (1989 to 2001), digital videography using video still frame grabs (2002 to 2009), and digital still images (2010 to 2018) (Gittings et al. 1992; CSA 1996; Dokken et al. 1999, 2003; Precht et al. 2006; Zimmer et al. 2010; Johnston et al. 2013, 2015, 2017a, 2017b, 2018b). Prior to the use of Coral Point Count with Microsoft® Excel® extensions (CPCe), percent cover was calculated with mylar traces and a calibrated planimeter from 1989 to 1995 (Gittings et al. 1992; CSA 1996). From 1996 to 2003, random dot layers were generated manually in photo software programs (Dokken et al. 1999, 2003).

Random Transect Data Processing

Mean percent benthic cover from random transect images was analyzed using CPCe version 4.1 with a 500 point overlay randomly distributed among all images within a transect (30 spatially random points per image) (Aronson et al. 1994; Kohler and Gill 2006). Organisms positioned beneath each random point were identified to the lowest possible taxonomic level, and grouped into primary functional groups: 1) coral, 2) sponges (including encrusting sponges), 3) macroalgae, and 4) "CTB," a composite substrate category of colonizable substrates including crustose coralline algae, fine turf algae, and bare rock (Aronson and Precht 2000; Aronson et al. 2005). Macroalgae included algae longer than approximately 3 mm and thick algal turfs covering underlying substrate. Additional categories included "other" (other biotic live components including ascidians, fish, serpulids, and unknown species), sand, and rubble. Abiotic features (photostation tags, tape measures, scientific equipment) and points with no data (shadows) were excluded from the analysis. Points on corals that could not be differentiated because of camera angle or camera distortion were labeled as "unidentified coral." *Orbicella* colonies that could not be identified to the species level were labeled as *Orbicella* spp.

Incidences of coral bleaching, paling, concentrated and isolated fish biting, and mortality were also recorded as "notes" in CPCe, providing additional data for each random point. Any point that landed on a portion of coral that was white with no visible zooxanthallae was characterized as "bleached." Any point that landed on coral that was pale relative to what was considered "normal" for the species, was characterized as "paling" coral (AGRRA 2012). If the colony displayed some bleaching or paling, but the point landed on a healthy area of the organism, the point was "healthy" and no bleaching or paling was noted in CPCe. To classify fish biting, any point that landed where fish biting occurred on a coral head more than once was classified as concentrated fish biting, and any point where there was only one occurrence of fish biting was classified as isolated fish biting. Mortality included any point on recently dead coral (exposed bare skeleton) with little to no algae growth so that the species could still be determined.

Point count analysis was conducted for photos within each transect and mean percent cover for all groups was determined by averaging all transects per bank study site. Results are presented as mean percent cover ± standard error.

Consistency for photographic random transect methods was ensured by training multiple scientific divers on the same camera systems for correct camera operation. Camera settings and equipment were standardized so that consistent transect images were taken annually and equipment checklists were provided in the field to ensure divers had all equipment and were confident with tasks assigned. Random transect photographs were reviewed promptly after images were taken to ensure the quality was sufficient for analysis. After all benthic components were identified in CPCe files, a separate FGBNMS staff member, different from the CPCe analyzer, independently reviewed all identified points from the random transect photographs for quality assurance/quality control (QA/QC). Any mistakes were corrected before percent cover analysis was completed.

Random Transect Statistical Analysis

Benthic community interactions in EFGB and WFGB random transects were evaluated with non-parametric distance-based analyses using Primer® version 7.0 (Anderson et al. 2008; Clarke et al. 2014). Euclidean distance resemblance matrices were calculated using untransformed percent cover data from random transect primary functional groups. Data were left untransformed so that the significance of non-dominant groups was not overinflated. Permutational multivariate analysis of variance (PERMANOVA) was based on Euclidean distance resemblance matrices and used to test for benthic community differences and estimate components of variation between bank study sites (Anderson et al. 2008). If significant differences were found, groups or species contributing to observed differences were examined using similarity percentages (SIMPER) to assess the percent contribution of dissimilarity between groups (Clarke et al. 2014).

Significant differences in coral species composition between bank study sites were tested using PERMANOVA on square root transformed coral species percent cover data with Euclidean distance similarity matrices. Diversity indices for coral species, including Margalef's species richness (d), Pielou's evenness (J'), and Shannon diversity (H'), were calculated to make comparisons between sites. Significant dissimilarities in diversity indices were tested using analysis of similarity (ANOSIM) (Clarke et al. 2014) on square root transformed data with Euclidean distance similarity matrices.

Functional group means by year and bank study sites for historical random transect mean percent cover data (1992 to 2018) were visualized using principal coordinates ordination (PCO), based on Euclidean distance similarity matrices, with percent variability explained on each canonical axis. A time series trajectory with correlation vectors (correlation >0.2) was overlaid on PCO plots to represent the direction of the variable gradients for the plot (Anderson et al. 2008; Clarke et al. 2014). Cluster analyses for year groups were performed on Euclidean distance similarity matrices with similarity profile analysis (SIMPROF) to identify significant (α=0.05) clusters within the data (Clarke et al. 2008). Significant differences between study site communities were tested using PERMANOVA. SIMPER identified groups contributing to observed dissimilarities (Clarke et al. 2014).

Mean percent benthic cover from the main random transect functional categories (coral, sponge, macroalgae, and CTB) were analyzed from 1989 to 2018. Monotonic trends in mean percent cover data were detected using the Mann-Kendall trend test in R version 2.13.2 (Hipel and McLeod 1994; Helsel and Hirsch 2002). Tests of significant correlation were completed in R version 2.13.2 with Pearson's correlation (Helsel and Hirsch 2002). It should be noted that the range of data collected has varied slightly over the years. From 1989 to 1991, only mean percent coral cover data were collected; other major functional groups were added in 1992. No data were collected in 1993.

Random Transect Results

Random Transect Mean Percent Cover

Mean coral cover within the EFGB study site was 52.37 ± 3.36%, macroalgae cover was 34.60 ± 2.38, CTB cover was 10.75 ± 1.90%, sponge cover was 0.93 ± 0.19%, and other cover was 1.35 ± 1.31% (Figure 2.2). Within the WFGB study site, mean coral cover was 55.68 ± 2.62%, macroalgae cover was 27.18 ± 2.03%, CTB cover was 14.54 ± 1.09%, mean sponge cover was 1.29 ± 0.20%, and other cover was 1.31 ± 0.51% (Figure 2.2). For both EFGB and WFGB study sites combined, mean coral cover was 54.02 ± 2.99%, macroalgae cover was 30.89 ± 2.20%, CTB cover was 12.65 ± 1.49%, sponge cover was 1.11 ± 0.19%, and other cover was 1.33 ± 0.91%.

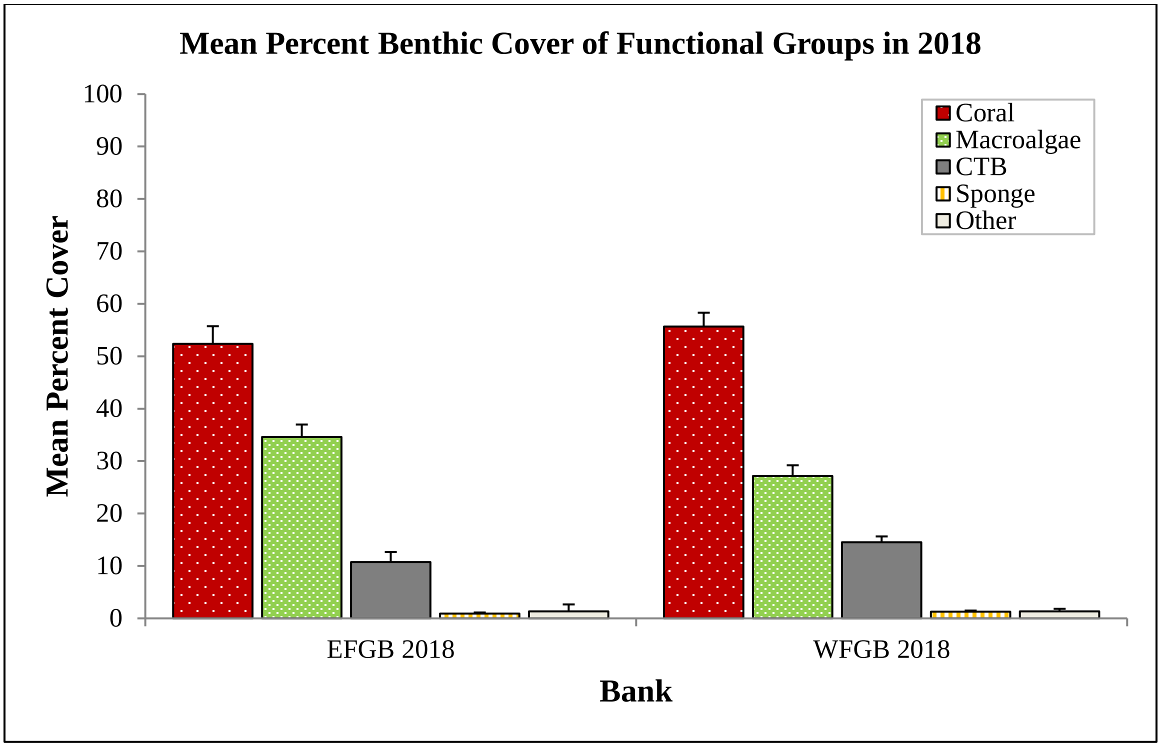

Figure 2.2. Mean percent benthic cover + SE from random transect functional groups within EFGB and WFGB study sites in 2018.

PERMANOVA analysis comparing functional groups revealed no significant differences, suggesting that EFGB and WFGB study sites were similar in benthic community composition in 2018.

Less than 1% of the coral cover analyzed within the EFGB study site was affected by bleaching or paling in August 2018, and no signs of bleaching or paling stress were observed in the WFGB study site. It is important to note that surveys occurred when water temperatures were lower than threshold levels known to trigger bleaching (Ogden and Wicklund 1988; Glynn and D'Croz 1990; Hagman and Gittings 1992; Johnston et al. 2019). In addition, less than 0.5% of fish biting and signs of mortality were observed in mean coral cover data. Fish biting that resulted in the removal of coral polyps from an affected area is most likely the result of damselfish gardening or grazing by stoplight parrotfish (*Sparisoma viride*) (Bruckner and Bruckner 1998; Bruckner et al. 2000).

Fifteen species of coral were observed within the EFGB random transect surveys and 13 species of coral were observed in the WFGB surveys in 2018, for a total of 15 coral species for both study sites (Figure 2.3). *Orbicella franksi* was the coral species with the highest mean percent cover at EFGB (27.00 ± 3.94%) and WFGB (30.97 ± 2.20%) followed by *Pseudodiploria strigosa* at EFGB (8.07 ± 1.87%) and WFGB (7.04 ± 1.15%) (Figure 2.3).

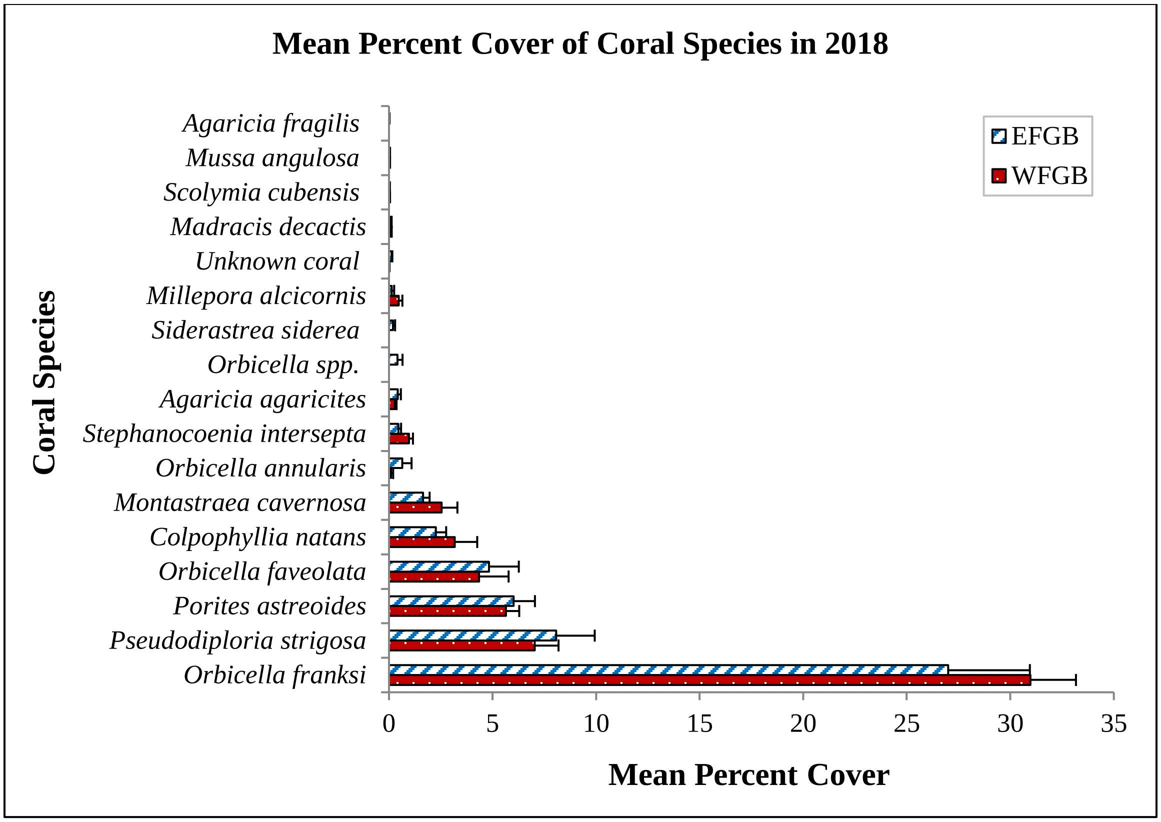

Figure 2.3. Mean percent cover + SE of observed coral species from random transects within EFGB and WFGB study sites in 2018.

The *Orbicella* species complex including *Orbicella franksi*, *Orbicella faveolata*, and *Orbicella annularis* (listed as threatened species under the Endangered Species Act in 2014) made up 62.80% of the observed coral cover within the EFGB study site and 63.62% of the observed coral cover within the WFGB study site random transect surveys (63.21% for both study sites combined). PERMANOVA analysis revealed no significant differences in coral species composition between bank study sites.

Coral species diversity measures were averaged for each study site in 2018 (Table 2.1). ANOSIM analysis revealed no significant differences in diversity measures between study site coral communities.

Table 2.1. Mean coral species diversity measures ± SE within EFGB and WFGB study sites in 2018.

Random Transect Coral Diversity Measures	EFGB	WFGB
Margalef’s Species Richness (d)	1.99 ± 0.11	1.64 ± 0.06
Pielou’s Evenness (J’)	0.62 ± 0.03	0.63 ± 0.03
Shannon Diversity (H'(loge))	1.33 ± 0.08	1.28 ± 0.05

Random Transect Long-Term Trends

Mean percent benthic cover from the main random transect functional categories (coral, sponge, macroalgae, and CTB) were analyzed from 1989 to 2018. Mean percent coral cover from 1989 to 2018 ranged from 40–64% in the EFGB study site and 37–66% in the WFGB study site, not changing significantly in the EFGB study site and significantly increasing in the WFGB study site over the time period (τ=0.26, p=0.064 and τ=0.59, p<0.001, respectively) (Figure 2.4). Coral species with the greatest mean percent cover over time were the *Orbicella* species group (31.96%) (primarily *Orbicella franksi*), followed by *Pseudodiploria strigosa* (8.43%) for both banks combined (Figure 2.5). The separate species of the *Orbicella annularis* species group complex have been quantified in recent years, but were grouped during historical data collection methods.

Prior to 1999, macroalgae cover was consistently below 5% within the study sites; however, in 1999, macroalgae cover increased to approximately 20%, and has averaged 30% the past ten years. Macroalgae and CTB cover generally varied inversely and were significantly correlated in EFGB (τ=-7.39, p<0.001) and WFGB (τ=-8.66, p<0.001) study sites, where macroalgae colonized available substrate, but did not out-compete coral. Macroalgae significantly increased within EFGB (τ=0.65, p<0.001) and WFGB (τ=0.56, p<0.001) study sites, while CTB significantly decreased within EFGB (τ=-0.49, p<0.001) and WFGB (τ=-0.48, p<0.001) study sites from 1992 to 2018 (Figure 2.4).

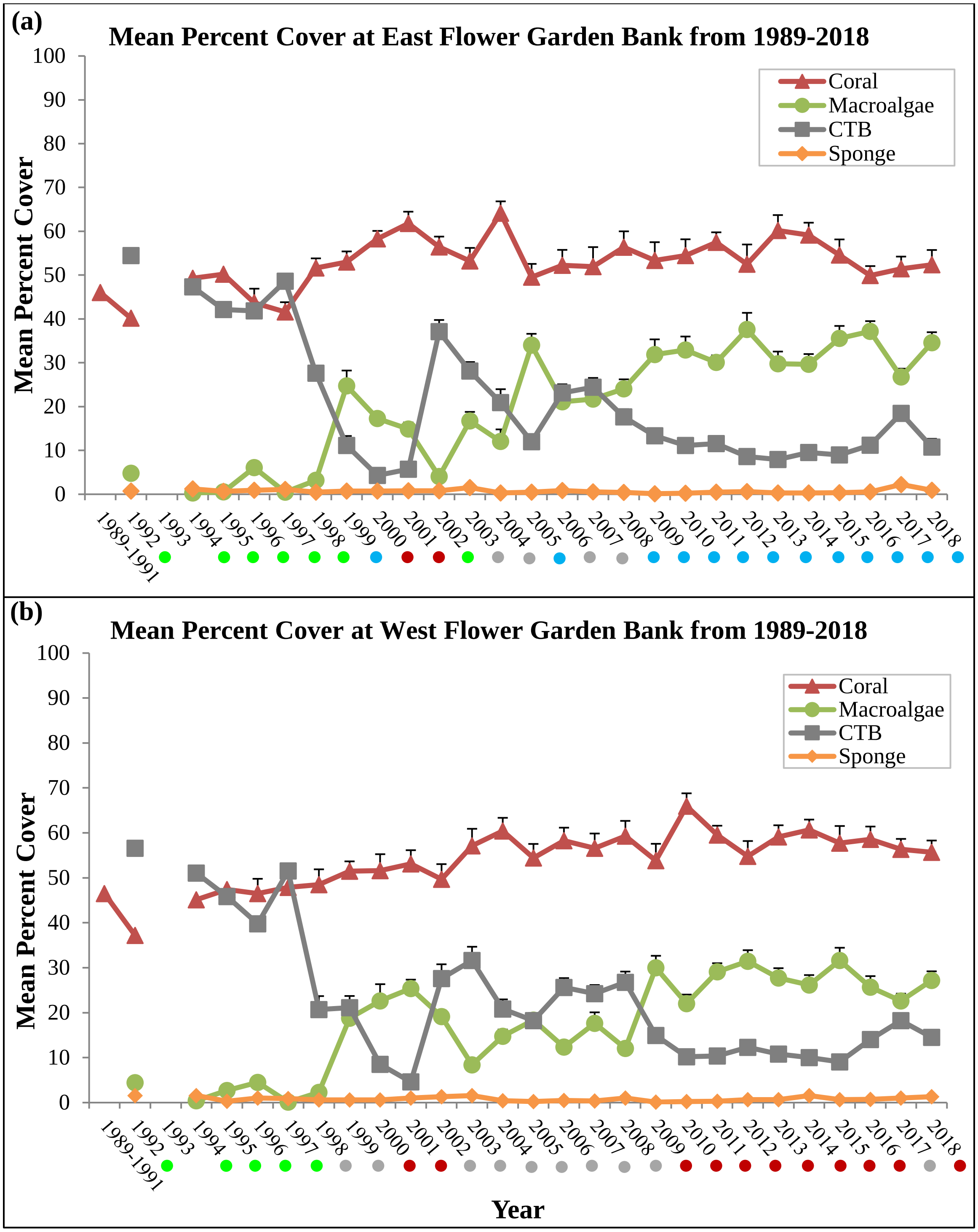

Figure 2.4. Mean percent benthic cover + SE from random transect functional groups within (a) EFGB and (b) WFGB study sites from 1989 to 2018. The colored dots represent significant year clusters corresponding to SIMPROF groups in Figures 2.6 and 2.7.

No mean percent cover data were reported in 1993. Data for 1989 to 1991 are from Gittings et al. (1992); 1992 to 1995 from Continental Shelf Associates, Inc. (CSA 1996); 1996 to 2001 from Dokken et al. (2003); 2002 to 2008 from PBS&J (Precht et al. 2006; Zimmer et al. 2010); and 2009 to 2017 from FGBNMS (Johnston et al. 2013, 2015, 2017a, 2017b, 2018b).

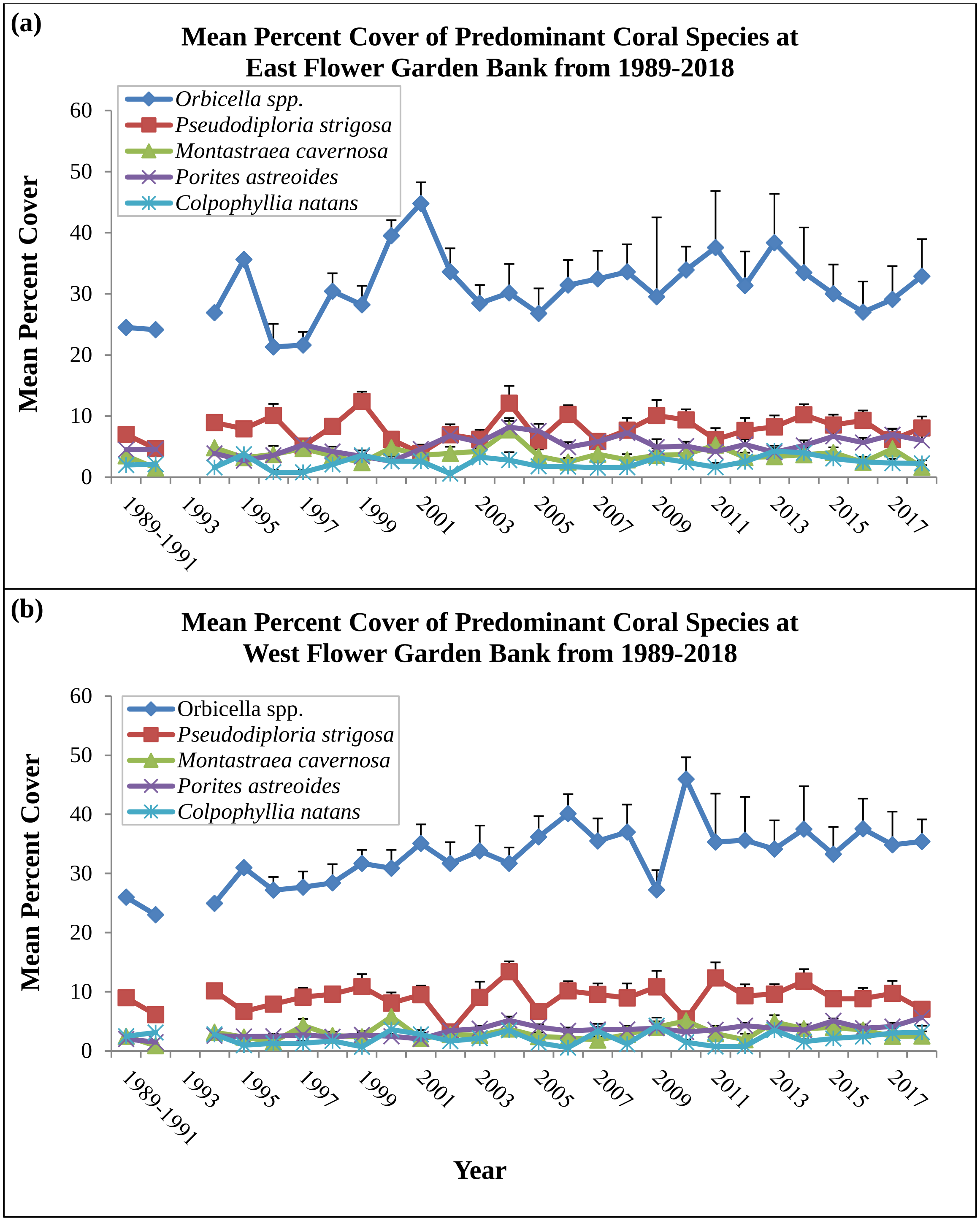

Figure 2.5. Mean percent cover of predominant coral species + SE within (a) EFGB and (b) WFGB study sites from 1989 to 2018. *Orbicella* species combines *Orbicella franksi*, *Orbicella faveolata*, and *Orbicella annularis* for historical data comparison.

No mean percent cover data were reported in 1993. Data for 1989 to 1991 are from Gittings et al. (1992); 1992 to 1995 from CSA (CSA 1996); 1996 to 2001 from Dokken et al. (2003); 2002 to 2008 from PBS&J (Precht et al. 2006; Zimmer et al. 2010); and 2009 to 2017 from FGBNMS (Johnston et al. 2013, 2015, 2017a, 2017b, 2018b).

For available yearly mean benthic percent cover data (1992 to 2018), SIMPROF analysis detected four significant year clusters in the EFGB study site (A: 1992 to 1998 and 2002; B: 2003 to 2004 and 2006 to 2007; C: 2000 to 2001; and D: 1999 and 2008 to 2018) (Figure 2.6). Between clusters A and B, CTB and macroalgae mean percent cover contributed to over 85% of the dissimilarity (53.27% and 31.76%, respectively), corresponding to the increase in macroalgae and decrease in CTB cover after 1998 (Figure 2.4). CTB was the single contributor to the dissimilarity between clusters B and C (84.10%), as well as clusters A and C (79.98%). Macroalgae and CTB mean percent cover contributed to over 90% of the dissimilarity between clusters B and D (50.91% and 40.20%, respectively), as well as between clusters A and D (42.96% and 52.74%, respectively).

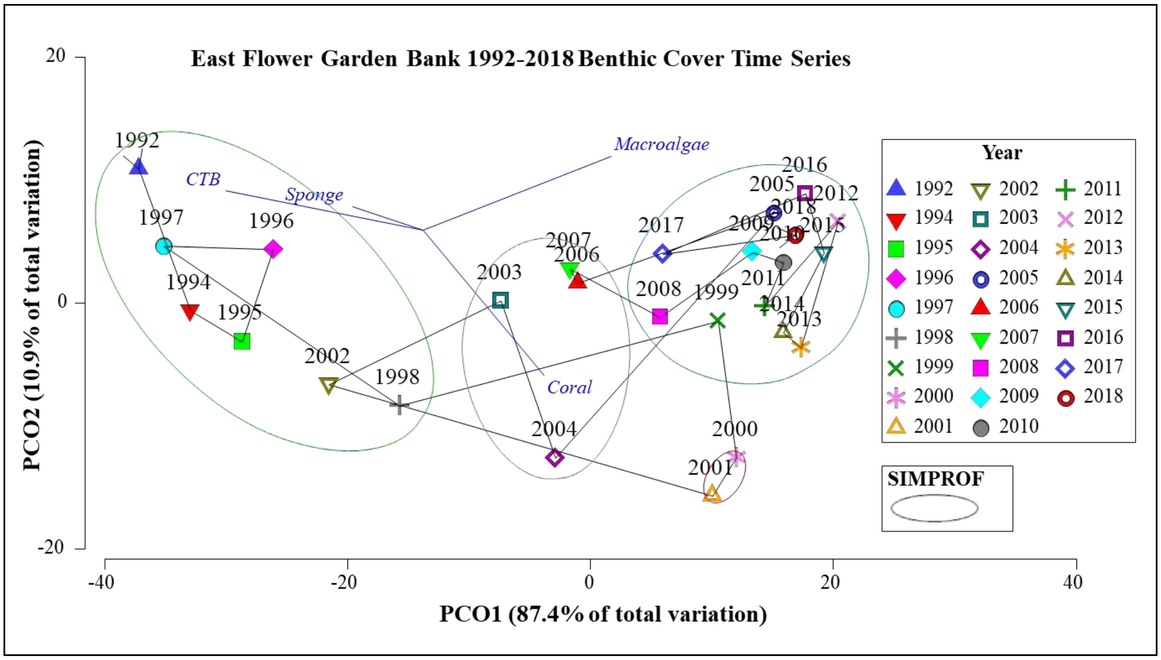

Figure 2.6. PCO for random transect benthic cover analysis from 1992 to 2018 within the EFGB study site. The ovals are SIMPROF groups representing significant year clusters grouped by color. The blue vector lines represent the directions of the variable gradients for the plot.

Yearly mean benthic percent cover data from 1992 to 2018 at the WFGB study site displayed a similar pattern to EFGB, resulting in three significant year clusters (A: 1992 to 1997; B: 1998 to 1999, 2002 to 2008, and 2017; C: 2000 to 2001, 2009 to 2010, and 2018) (Figure 2.7). Between clusters A and B, CTB and macroalgae mean percent cover contributed to over 85% of the dissimilarity (68.28% and 18.14%, respectively), corresponding to decreasing CTB cover from 1997 to 1998 (Figure 2.4). Macroalgae and CTB mean percent cover also contributed to the dissimilarity between clusters B and C (47.43% and 44.25%, respectively), corresponding to the increase in macroalgae and decrease in CTB cover after 1998 (Figure 2.4). Differences between clusters A and C were attributable to macroalgae and CTB mean percent cover (27.12% and 64.76%, respectively).

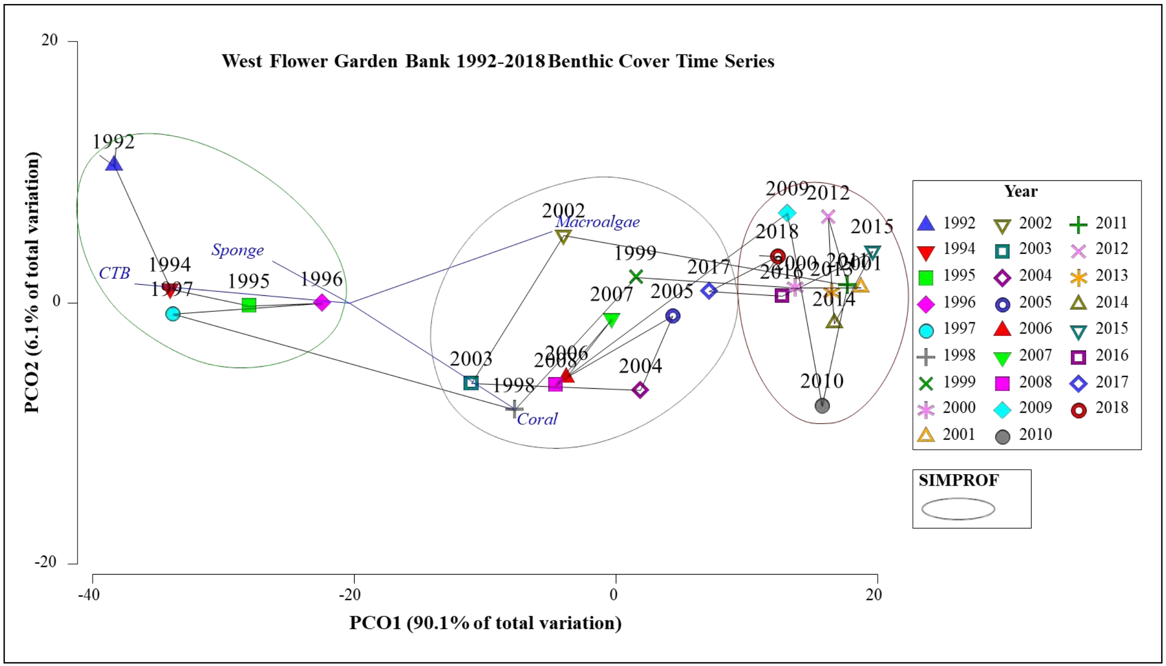

Figure 2.7. PCO for random transect benthic cover analysis from 1992 to 2018 within the WFGB study site. The ovals are SIMPROF groups representing significant year clusters grouped by color. The blue vector lines represent the directions of the variable gradients for the plot.

PERMANOVA results revealed no significant differences between study sites, suggesting that EFGB and WFGB study sites were similar to each other from 1992 to 2018 in overall benthic community composition, experiencing similar shifts though time.

Random Transect Discussion

Despite global coral reef declines in recent decades, mean coral cover within EFGB and WFGB study sites has remained near or above 50% for the combined 29 years of monitoring. Mean macroalgae percent cover increased significantly between 1998 and 1999, rising from approximately 5% to 20%, and increasing to approximately 30% over the past ten years. The inverse relationship between macroalgae and CTB observed throughout the long-term monitoring program reflects the tendency for macroalgae to grow over exposed hard bottom rather than coral or sponges. After 2008, macroalgae percent cover was greater than CTB cover, continuing to increase or remain stable within both study sites.

These trends suggest that from 1992 to 1998, the reef community within the study sites was stable, and from 1999 onward, there was an increase in macroalgae cover, as colonizable substrate was populated by macroalgae. In contrast to other shallow water reefs in the Caribbean region and many worldwide, increases in mean macroalgae cover have not been concomitant with significant coral cover decline in the EFGB and WFGB study sites (Gardner et al. 2003; Mumby and Steneck 2011; DeBose et al. 2012; Jackson et al. 2014; Johnston et al. 2016b, 2017a, 2017b, 2018b). While a portion of EFGB occurring outside the study site was affected by a localized mortality event in July of 2016, and both banks were impacted by coral bleaching in the fall of 2016, neither of these events resulted in significant coral cover declines within the study sites (Johnston et al 2018a, 2019).

Increases in macroalgae cover have also occurred on other reefs in the Gulf of Mexico and Caribbean region. Stetson Bank, located 48 km northwest of WFGB, is a series of claystone and siltstone pinnacles, once covered by a low-diversity coral and sponge community. Stetson Bank has shown an analogous, but more prominent, trend of increasing macroalgae and decreasing sponge and coral cover (DeBose et al. 2012; Nuttall et al. 2018). Also within the Gulf region, increased macroalgae cover and significant coral decline has occurred within monitoring sites at Florida Keys National Marine Sanctuary (Toth et al. 2014). Mean coral cover sanctuary-wide declined from 13% in 1996 to 7% in 2008, and was even as low as 3% in 2011 in some areas of the Florida Keys (Ruzicka et al. 2009; ONMS 2011; Toth et al. 2014). This decline in the Florida Keys was most likely due to disease, hurricane damage, and thermal stress (Toth et. al 2014). Overfishing, bleaching, algae competition, coastal development, and coral disease have also caused declines on reefs in the wider Caribbean region (Gardner et al. 2003; Steneck et al. 2011; Jackson et al. 2014).

In contrast, the EFGB and WFGB study sites have not shown a significant decline in coral cover since 1989, and have 6 to 11 times higher coral cover values than other locations in the Caribbean region (Caldow et al. 2009; Clark et al. 2014; Johnston et al. 2017a, 2017b). This may be due to the remote offshore location and deep water surrounding the banks, which provide a more stable environment than shallower reefs (Aronson et al. 2005; Johnston et al. 2015). However, despite their remote location and deeper depth compared to other Caribbean reefs, EFGB and WFGB are not impervious to impacts, as seen with the 2016 localized mortality event and bleaching event (Johnston et al. 2018a, 2019). Climate change, invasive species, storms, and water quality degradation continue to threaten the resources of the FGBNMS (ONMS 2008; Nuttall et al. 2014; Johnston et al. 2016a). As the environment in the Gulf of Mexico changes over time (Karnauskas et al. 2015), continued monitoring will be important to document ecosystem variation.

Chapter 3. Repetitive Study Site Photostations

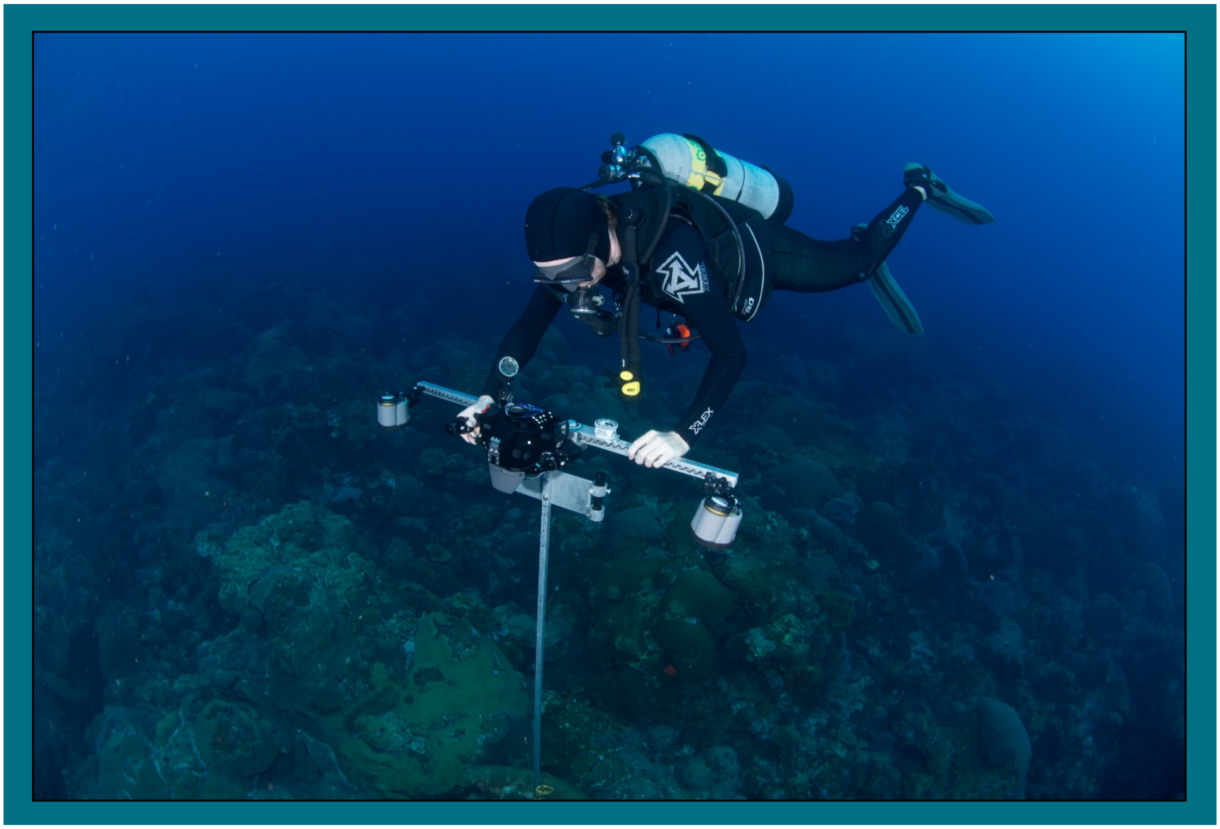

A NOAA diver photographs a repetitive photostation within the East Flower Garden Bank study site with camera and strobes mounted to aluminum t-frame. Photo: G.P. Schmahl/NOAA

Repetitive Study Site Photostation Introduction

Permanent repetitive photostations were photographed to follow specific colonies over time and to document changes in the composition of benthic assemblages in selected sites within the EFGB and WFGB study sites. The photographs were analyzed to measure percent benthic cover components using random-dot analysis.

Repetitive Study Site Photostation Methods

Repetitive Study Site Photostation Field Methods

Repetitive study site photostations, marked by permanent pins with numbered tags on the reef, were located by SCUBA divers using detailed underwater maps displaying compass headings and distances to each station within the study sites (Figures 1.5 and 1.6). After each station was located, divers photographed each one (for more detailed methods, reference Johnston et al. 2017a) (Figure 3.1). In 2018, all repetitive study site photostations were located and photographed: 37 at EFGB and 41 at WFGB.

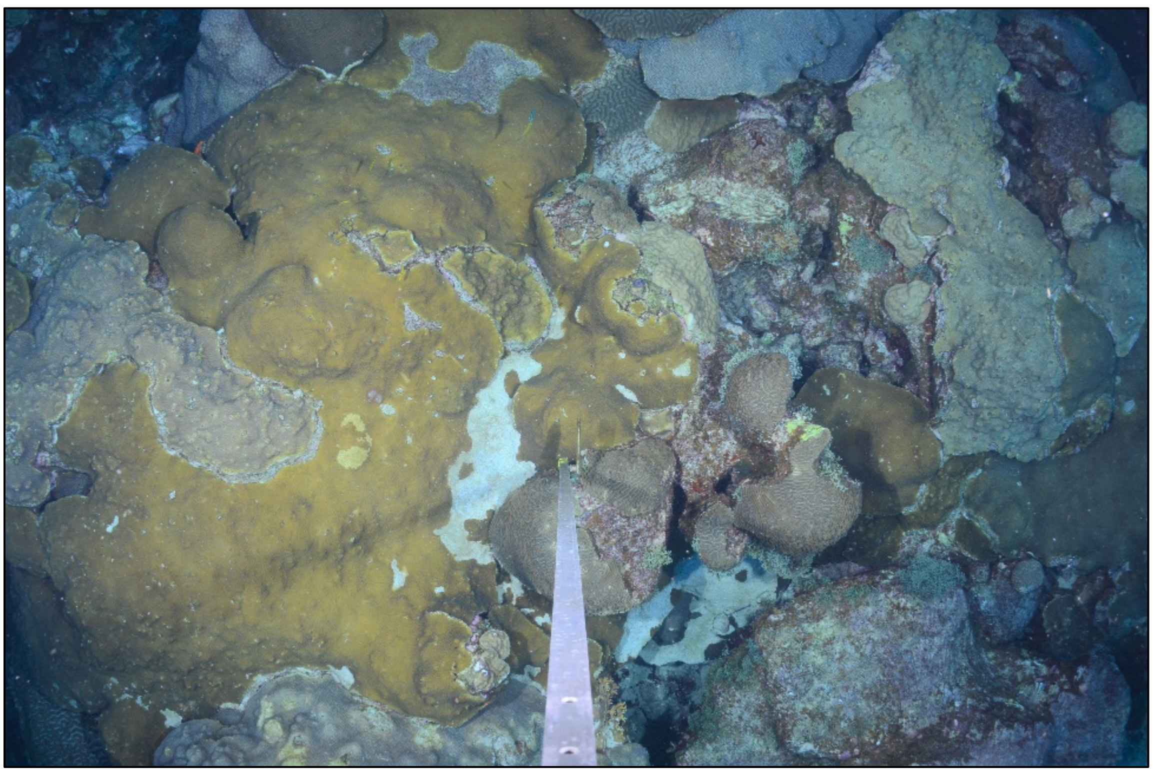

Figure 3.1. WFGB repetitive photostation #504 in 2018. Camera mounted above aluminum t-frame. Photo: Jimmy MacMillan/CPC

Stations were photographed using a Nikon® D7000® SLR camera with a 16-mm lens in a Sea&Sea® housing with a small dome port and two Inon® Z240 strobes (1.2 m apart).

The camera was mounted in the center of a T-shaped camera frame, at a distance of 2 m from the substrate. To ensure that the stations were photographed in the same manner each year, the frame was oriented in a north-facing direction and kept vertical using an attached bullseye bubble level and compass (see Chapter 3 title page image). This setup produced images covering 5 m^2.

It should be noted that since the beginning of the monitoring program, underwater camera setups used to capture benthic cover in the repetitive stations changed as technology advanced from 35 mm slides and film (1989 to 2007) to digital still images (2008 to 2018) (Gittings et al. 1992; CSA 1996; Dokken et al. 1999, 2003; Precht et al. 2006; Zimmer et al. 2010; Johnston et al. 2013, 2015, 2017a, 2017b, 2018b). From 1989 to 2009, photographs for each repetitive quadrat photostation encompassed an 8 m^2 area, but changed to a 5 m^2 area in 2009, a 9 m^2 area in 2010, and back to a 5 m^2 area from 2011 onward due to changes in camera equipment and updated technology.

Repetitive Study Site Photostation Data Processing

Mean percent benthic cover from repetitive study site photostation images was analyzed using CPCe version 4.1 (Aronson et al. 1994; Kohler and Gill 2006). A total of 100 random dots were overlaid on each photograph and benthic species lying under these points were identified and verified by QA/QC (see Chapter 2 Methods – Random Transect Data Processing for detailed methods). Point count analysis was conducted for all photos and mean percent cover for functional groups was determined by averaging all photostations per bank study site. Results are presented as mean percent cover ± standard error.

Repetitive Study Site Photostation Statistical Analysis

All nonparametric analyses for non-normal data were carried out using Primer® version 7.0 and monotonic trends were detected using the Mann-Kendall trend test in R version 2.13.2 (see Chapter 2 Methods – Random Transect Statistical Analysis).

Repetitive Study Site Photostation Results

Repetitive Study Site Photostation Mean Percent Cover

EFGB repetitive study site photostation mean coral cover was 63.94 ± 2.66%, macroalgae cover was 24.44 ± 2.04%, CTB cover was 10.32 ± 1.09%, sponge cover was 0.49 ± 0.15%, and other cover was 0.81 ± 0.29% (Figure 3.2). Within the WFGB study site, mean coral cover was 67.85 ± 2.15%, macroalgae was 15.67 ± 1.52%, CTB cover was 13.70 ± 1.21%, sponge cover was 1.34 ± 0.30%, and other cover was 1.44 ± 0.83% (Figure 3.2). For both EFGB and WFGB repetitive study site photostations combined, mean coral cover was 65.89 ± 2.41%, macroalgae cover was 20.05 ± 1.78%, CTB cover was 12.01 ± 1.15%, sponge cover was 0.91 ± 0.23%, and other cover was 1.13 ± 0.56%.

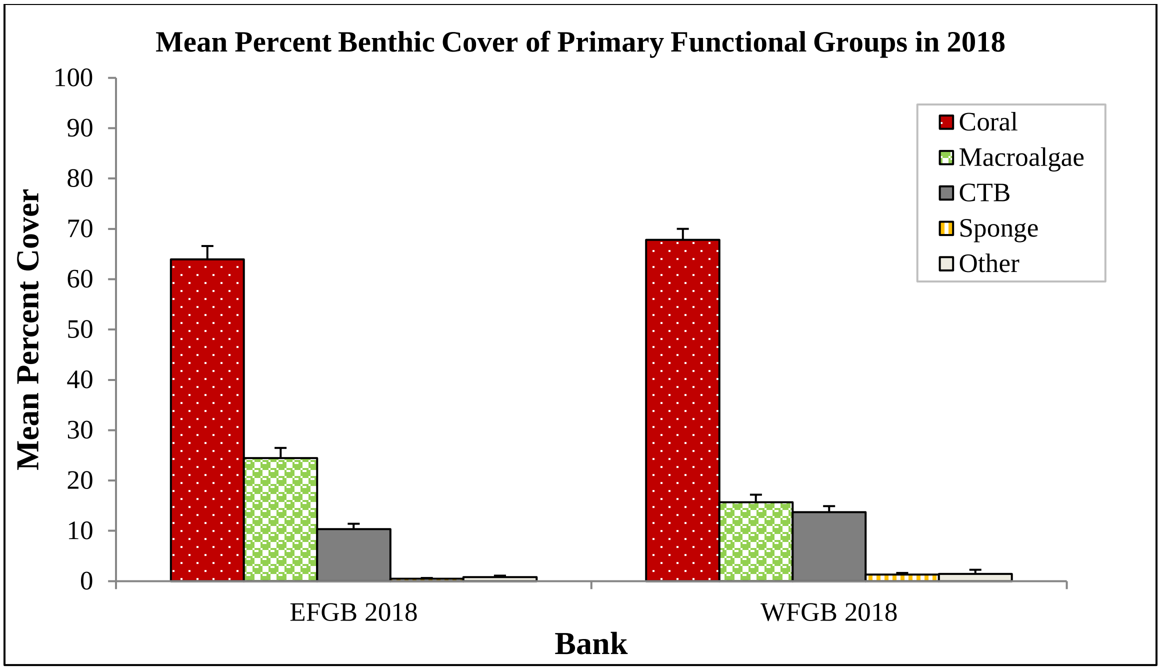

Figure 3.2. Mean percent benthic cover + SE from repetitive study site photostation functional groups within EFGB and WFGB study sites in 2018.

PERMANOVA analysis revealed significant differences among functional groups, suggesting that EFGB and WFGB repetitive photostations were dissimilar in benthic community composition in 2018 (Table 3.1). SIMPER analysis identified that the greatest contributors to the observed dissimilarity among photostations were mean coral (51%) and macroalgae (36%) percent cover.

Table 3.1. PERMANOVA results comparing repetitive study site photostation mean percent benthic cover among functional groups between EFGB and WFGB photostations in 2018. Bold text denotes significant value.

Source	Sum of Squares	df	Pseudo-F	P (perm)
Bank Photostation Cover	2060	1	5.04	**0.018**
Res	31468	77		
Total	33528	78		

Fourteen coral species were observed in EFGB repetitive study site photostations and 13 coral species were observed in WFGB repetitive study site photostations, for a total of 14 coral species for repetitive study site photostations from both banks combined (Figure 3.3). *Orbicella franksi* had the highest cover among coral species observed in EFGB (32.11 ± 2.97%) and WFGB (35.42 ± 2.64%) photostations. Followed by *Pseudodiploria strigosa* in EFGB (11.10 ± 1.91%) and WFGB (9.27 ± 1.81%) photostations (Figure 3.3). PERMANOVA analysis revealed no significant differences in coral species composition between banks in the repetitive study site photostations.

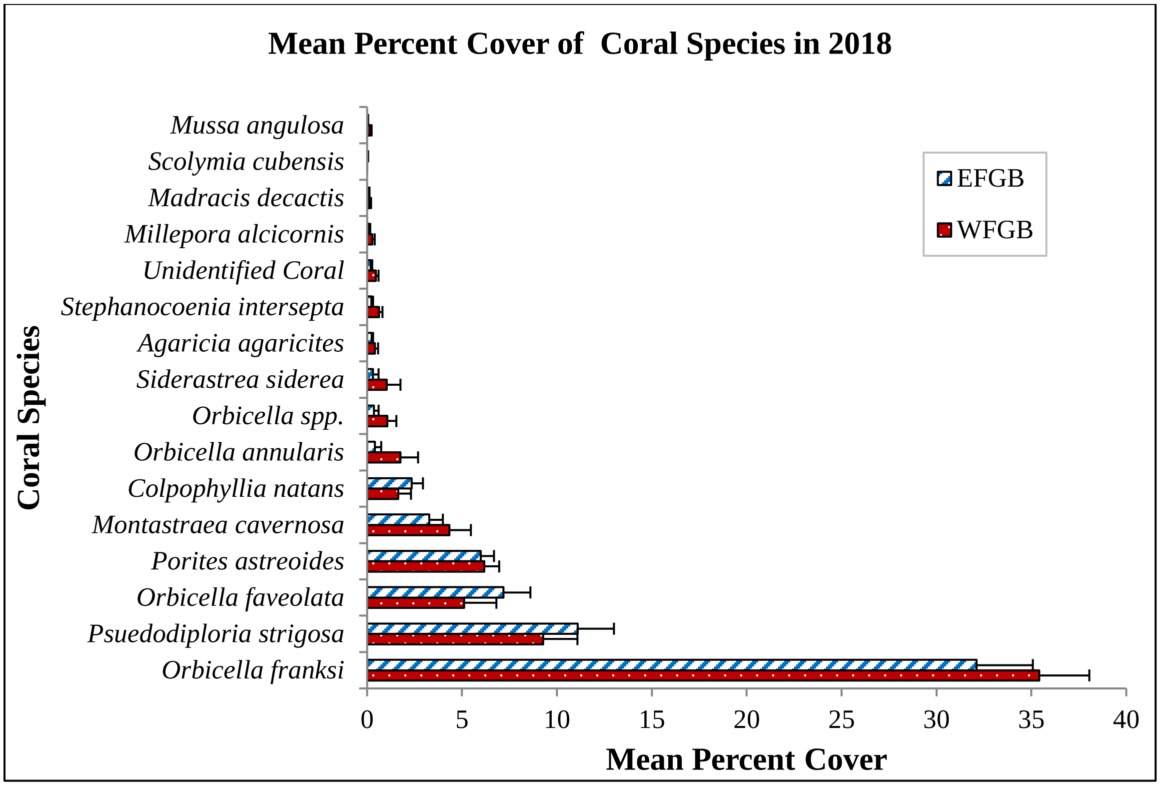

Figure 3.3. Mean percent cover + SE of observed coral species from repetitive study site photostations within EFGB and WFGB study sites in 2018.

Less than 1% of the coral cover analyzed was observed to pale, and no bleaching was observed in the repetitive study site photostations. In addition, less than 3% of corals observed were affected by fish biting or signs of recent mortality.

Repetitive Study Site Photostation Long-Term Trends

Mean percent benthic cover from the repetitive study site photostations was analyzed to measure changes over time. In repetitive study site photostations from 1989 to 2018, mean percent coral cover ranged from 49–73% at EFGB and 45–74% at WFGB, not changing significantly in the EFGB photostations (τ=0.26, p=0.064) and significantly increasing in the WFGB photostations over the time period (τ=0.59, p<0.001) (Figure 3.4). It should be noted that the change in photographic area in 2009 and 2010 due to changing camera equipment may be correlated with inflated percent coral cover estimates that resulted in these years (Figure 3.4). Percent cover data for individual coral species in repetitive study site photostations became available in 2000, as before that time, coral species were grouped together into a single "coral" category for analysis. Coral species with the highest mean percent cover in photostations from 2000 to 2018 were the *Orbicella* species group at EFGB (42.02%) and WFGB (43.44%) (primarily *Orbicella franksi*), followed by *Pseudodiploria strigosa* at EFGB (10.21%) and WFGB (8.92%) (Figure 3.5).

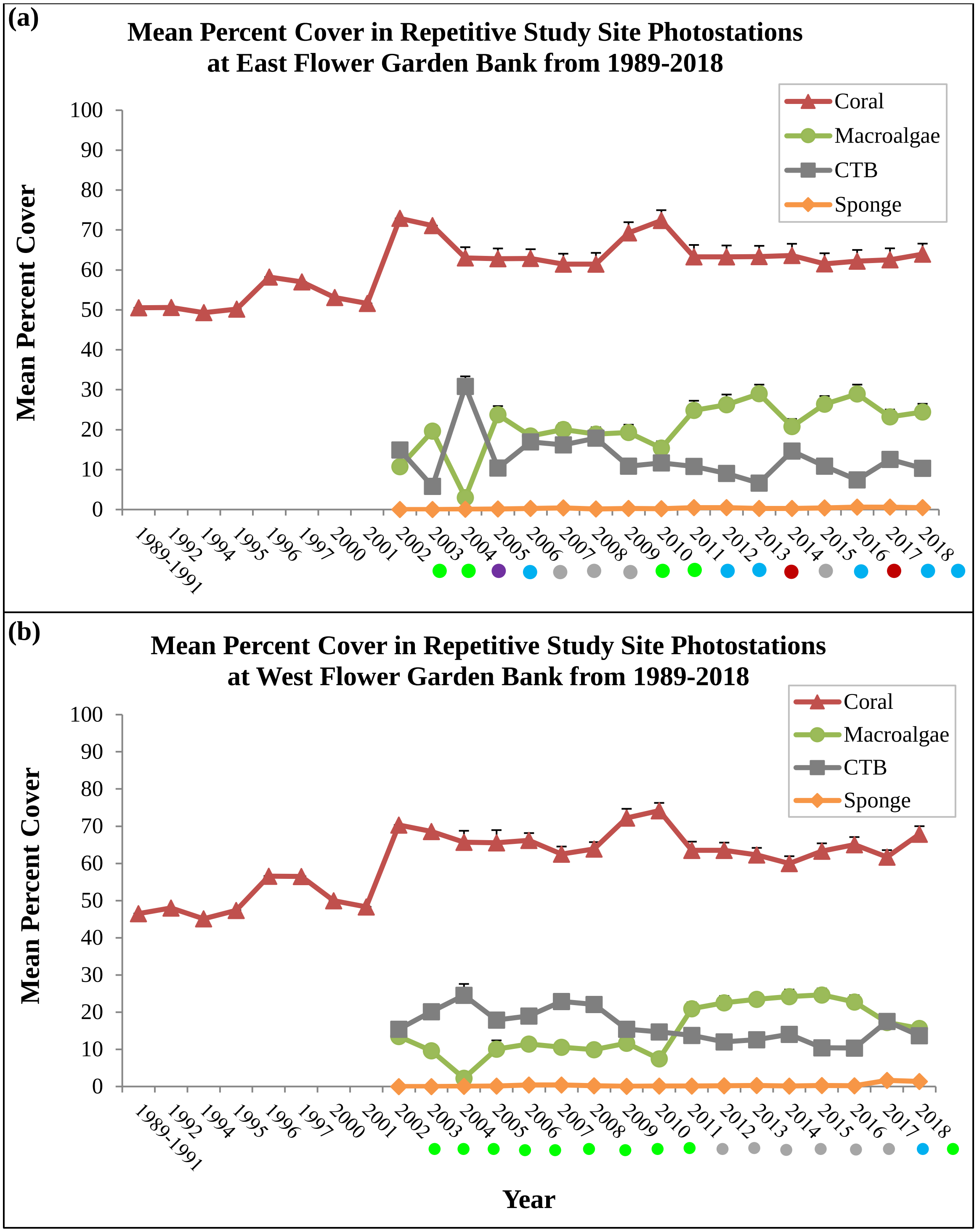

Figure 3.4. Mean percent benthic cover + SE of repetitive study site photostation functional groups within (a) EFGB and (b) WFGB study sites from 1989 to 2018. The colored dots represent significant year clusters corresponding to SIMPROF groups in Figures 3.6 and 3.7.

Sponge, macroalgae, and CTB categories were not reported until 2002. No mean percent cover data were reported in 1993. Data for 1989 to 1991 are from Gittings et al. (1992); 1992 to 1995 from Continental Shelf Associates, Inc. (CSA) (1996); 1996 to 2001 from Dokken et al. (2003); 2002 to 2008 from PBS&J (Precht et al. 2006; Zimmer et al. 2010); and 2009 to 2017 from FGBNMS (Johnston et al. 2013, 2015, 2017a, 2017b, 2018b).

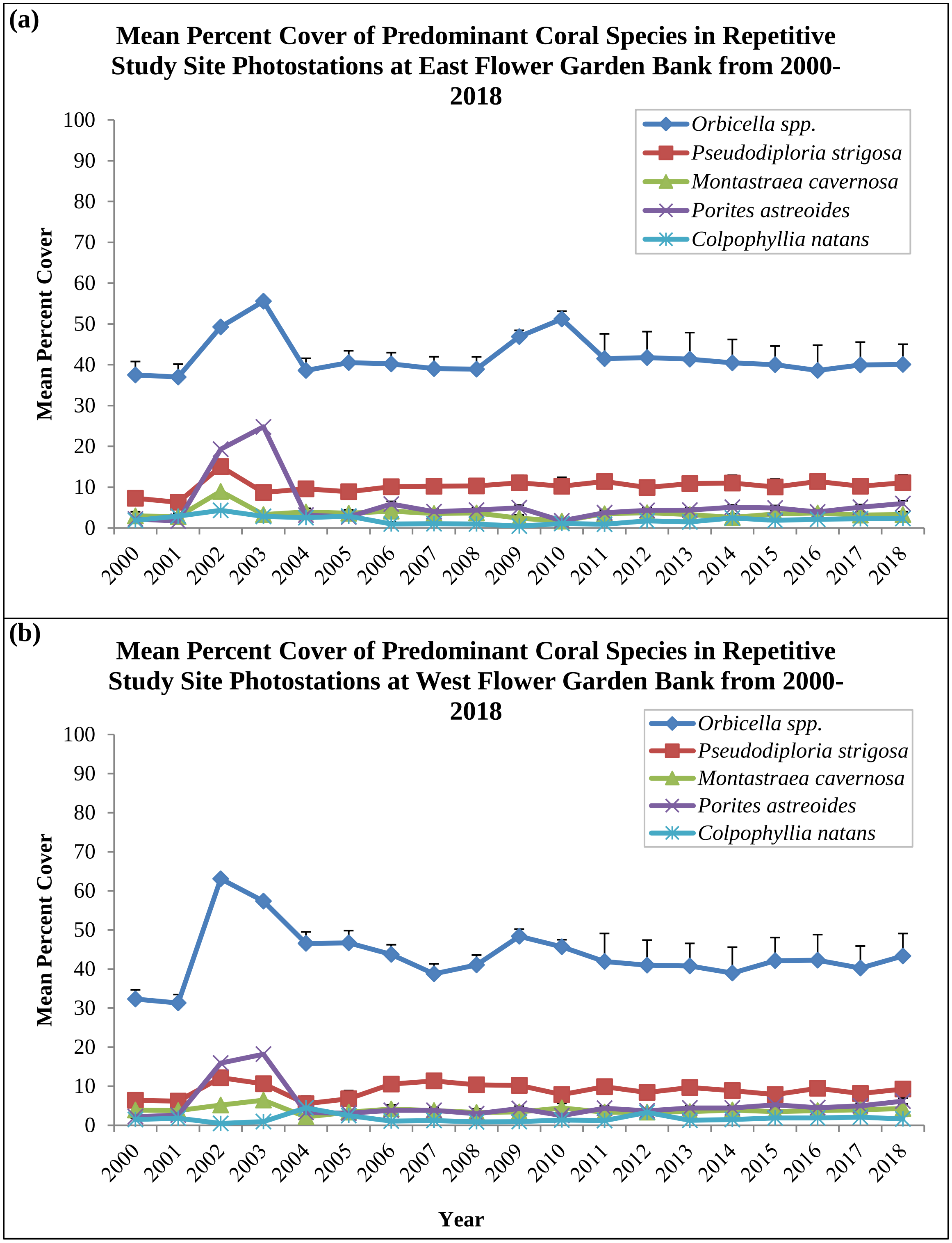

Figure 3.5. Mean percent cover of predominant coral species + SE in repetitive study site photostations at (a) EFGB and (b) WFGB from 2000 to 2018. *Orbicella* species combines *Orbicella franksi*, *Orbicella faveolata*, and *Orbicella annularis* for historical data comparison.

Data for 2000 to 2001 are from Dokken et al. (2003); 2002 to 2008 from PBS&J (Precht et al. 2006; Zimmer et al. 2010); and 2009 to 2017 from FGBNMS (Johnston et al. 2013, 2015, 2017a, 2017b, 2018b)

Sponge, macroalgae, and CTB data were not available to incorporate into the analysis until 2002. Similar to random transect data described in Chapter 2, periods of lower CTB cover generally coincided with increases in the macroalgae component (Figure 3.4). Macroalgae and CTB cover varied inversely and were significantly correlated in the EFGB photostations (τ=-7.37, p<0.001) and the WFGB photostations (τ=-8.66, p<0.001). Macroalgae significantly increased in the EFGB photostations (τ=0.65, p<0.001) and the WFGB photostations (τ=0.56, p<0.001). CTB varied in the EFGB photostations over time and significantly decreased in the EFGB photostations (τ=-0.49, p<0.001) and the WFGB photostations (τ=-0.48, p<0.001) from 2002 to 2018 (Figure 3.4), reflecting increasing overgrowth by macroalgae during this period.

For yearly mean benthic percent cover data in EFGB repetitive study site photostations (2002 to 2018), SIMPROF analysis detected four significant year clusters (A: 2002 to 2003 and 2009 to 2010; B: 2006 to 2008 and 2014; C: 2013 and 2016, and D: 2005, 2011 to 2012, and 2015 to 2018) (Figure 3.6). The year 2004 was grouped individually. Between clusters A and B, coral and CTB mean percent cover contributed to over 83% of the dissimilarity (55.50% and 28.35%, respectively), corresponding to the shift in decreased CTB cover from 2002 to 2003 and after 2010 (Figure 3.4). Macroalgae (49.44%) and CTB (49.77%) contributed to the dissimilarity between clusters B and C, due to the large increase in macroalgae and decrease in CTB. Between clusters C and D, macroalgae and CTB mean percent cover contributed to over 97% of the dissimilarity (54.27% and 42.96%, respectively) from continued increasing macroalgae and decreasing CTB through 2018 (Figure 3.4). The year 2004 was not clustered with any other year, and was dissimilar to all the other groups due to high CTB and low macroalgae cover.

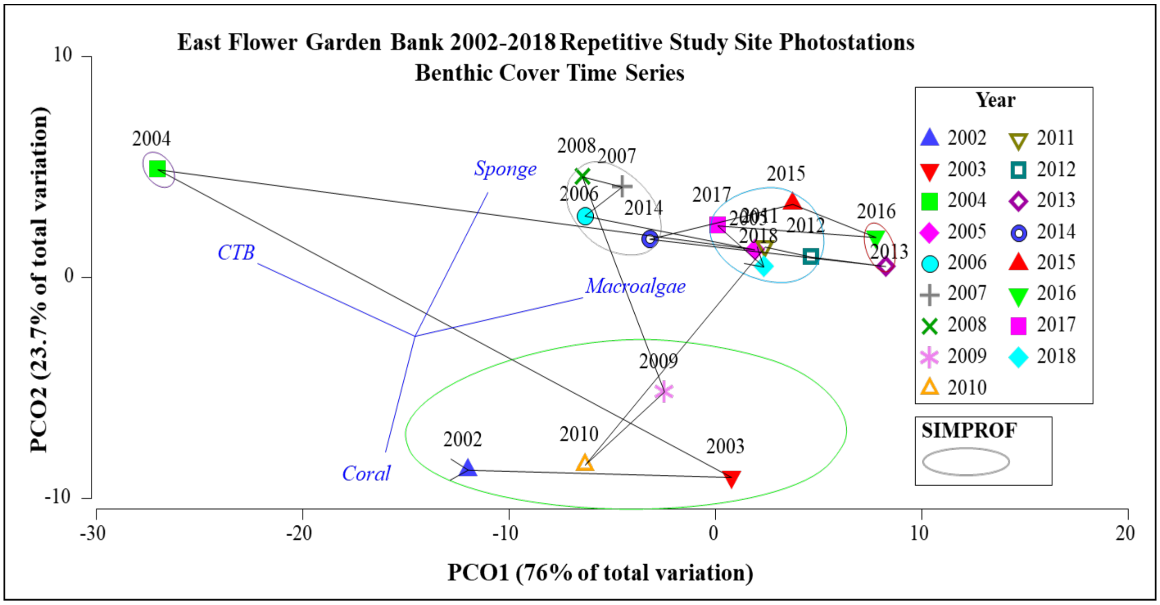

Figure 3.6. PCO for repetitive study site photostations from 2002 to 2018 at EFGB. The ovals are SIMPROF groups representing significant year clusters grouped by color. The blue vector lines represent the directions of the variable gradients for the plot.

Yearly mean benthic percent cover data in WFGB repetitive study site photostations resulted in two significant year clusters (A: 2002 to 2010 and 2018; B: 2011 and 2016) (Figure 3.7). The year 2017 was grouped individually. Between clusters A and B, macroalgae and CTB mean percent cover contributed to over 86% of the dissimilarity (65.85% and 20.40%, respectively), corresponding to the large increase in macroalgae and decrease in CTB starting in 2011, and continued elevated macroalgae cover through 2018 (Figure 3.4). The year 2017 was dissimilar to all the other groups due to increasing CTB and decreasing macroalgae cover (Figure 3.4).

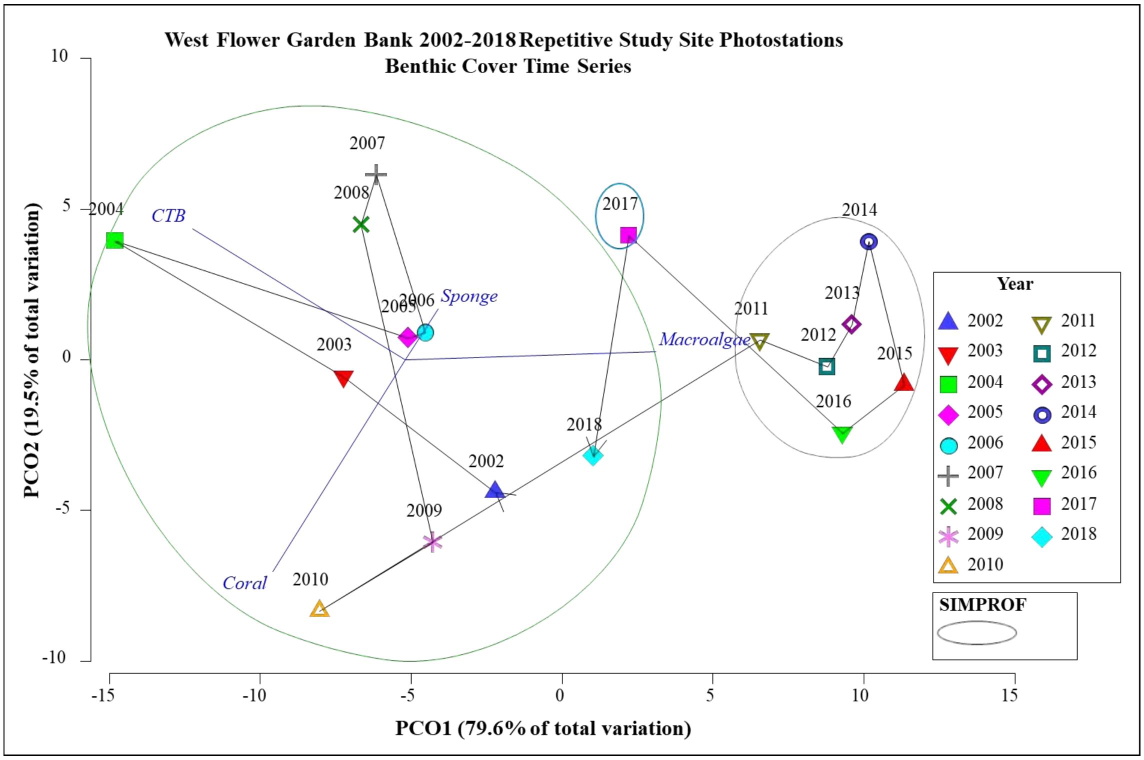

Figure 3.7. PCO for repetitive study site photostations from 2002 to 2018 at WFGB. The ovals are SIMPROF groups representing significant year clusters grouped by color. The blue vector lines represent the directions of the variable gradients for the plot.

PERMANOVA analysis comparing benthic cover in repetitive study site photostations revealed significant differences, suggesting that photostations at EFGB and WFGB were different in overall benthic community composition from 2002 to 2018 (Table 3.2). SIMPER analysis identified that for comparisons between repetitive study site photostations, the greatest contributors to the observed dissimilarity were mean macroalgae (45.34%) and CTB (31.83%) percent cover.

Table 3.2. PERMANOVA results comparing repetitive study site photostation mean percent benthic cover between EFGB and WFGB photostations from 2002 to 2018. Bold text denotes significant value.

Source	Sum of Squares	df	Pseudo-F	P (perm)
Bank Photostation Cover	375	1	4.32	**0.02**
Res	2779	32		
Total	3154	33		

Repetitive Study Site Photostation Discussion

The majority of the repetitive study site photostations (24 at EFGB and 27 at WFGB) have been in place since the beginning of the monitoring program, and display a time series from 1989 to 2018. As an example of the value of long-term repetitive photographs, EFGB repetitive photostation #102 documents increasing coral cover over time (Figure 3.8). Some colonies appeared paler in certain years due to variations in photographic equipment (e.g., 35 mm slides, 35 mm film, and digital images) and ambient conditions, and as colony health or condition changed. Furthermore, photo quality is affected by time of day, camera settings, lighting, etc. Changes over time include bare substrate colonization and overgrowth by *Pseudodiploria strigosa* and *Porites astreoides* colonies in the center of the station from 1989 to 2018 (Figure 3.8 a and h); algal colonization after tissue loss on an *Orbicella faveolata* head in the upper right corner in 1996 (affecting approximately 50% of the colony) (Figure 3.8 b); bleaching *Millepora alcicornis* that appeared in the center of the station in 2002 (Figure 3.8 c); algal colonization on a *Pseudodiploria strigosa* head in the lower left corner affecting approximately 50% of the colony after 2013 (Figure 3.8 f); and algal colonization in the center of the station in 2013, with subsequent loss of that algae after 2015 (Figure 3.8 f, g, and h).

Mean percent coral cover within the EFGB and WFGB repetitive study site photostations varied greatly from 1989 to 2018. A prominent increase in coral cover from 2001 to 2002 (Figure 3.5), specifically within the *Orbicella* species group, may be an artifact of different contracted analysts examining the repetitive photostation data, as the methods did not change between these years. The Center for Coastal Studies at Texas A&M Corpus Christi was responsible for the LTM program from 1996 to 2001 (Dokken et al. 2003), and in 2002 it was taken over by PBS&J Ecological Services, a consulting company based out of Miami, Florida (Precht et al. 2006, 2008; Zimmer et al. 2010). Additional photostations were added to both study sites in 1990 and 2003 (Gittings et al. 1992; Precht et al. 2006).

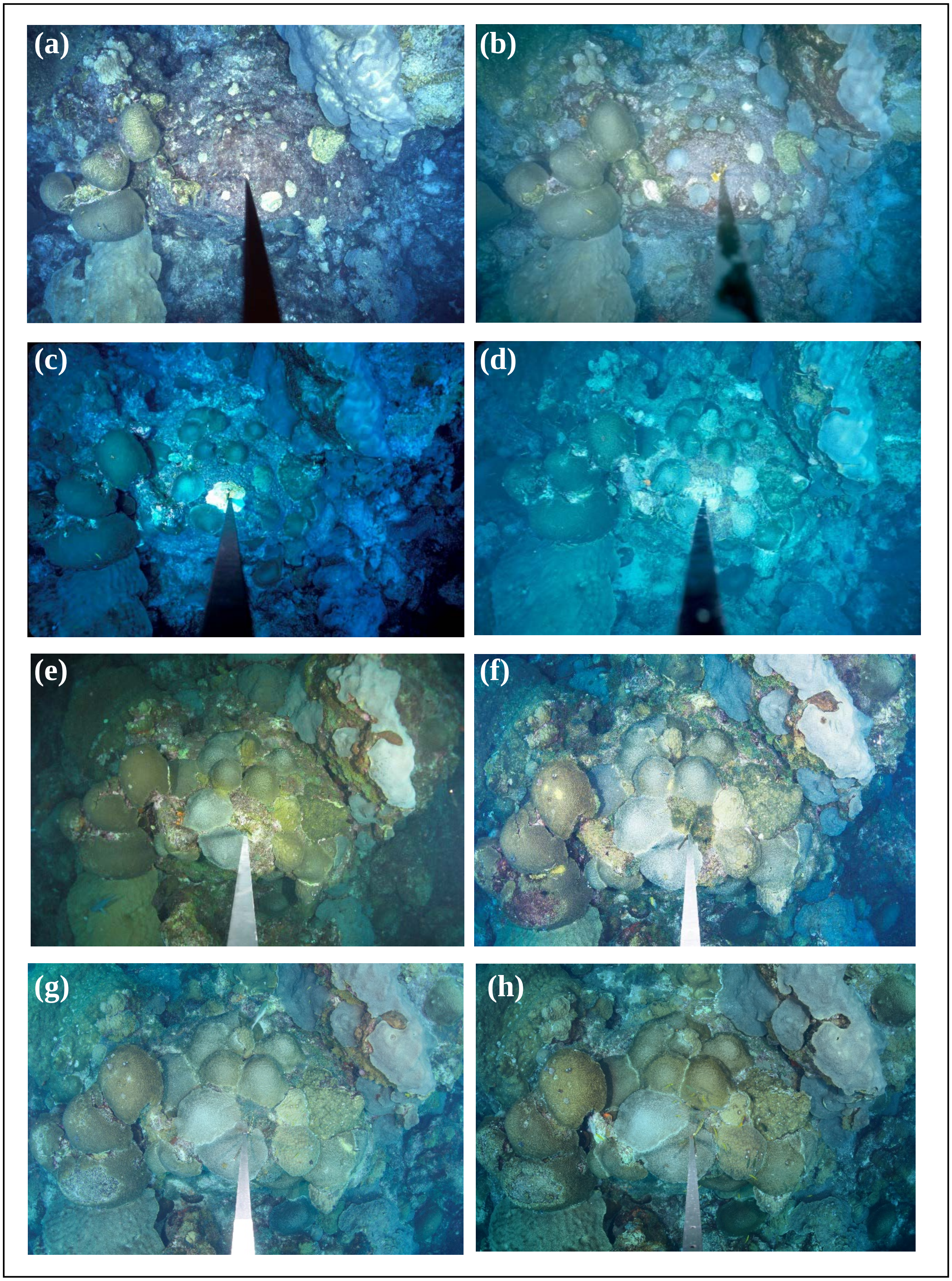

Figure 3.8. EFGB repetitive study site photostation #102 time series from (a) 1989; (b) 1996; (c) 2002; (d) 2006; (e) 2010; (f) 2013; (g) 2015; and (h) 2018. Camera mounted above aluminum t-frame. Photos: NOAA

Greater coral cover estimates were obtained from the repetitive study site photostations in comparison to the random transects (66% compared with 54%) at both EFGB and WFGB combined in 2018. It should be noted that the repetitive photostations were not intended to be representative of the coral reef community within EFGB and WFGB study sites, as they were selectively placed on habitat with either large coral colonies or coral recruits in order to monitor individual sites and species interactions over time. As described in Chapter 2, the randomly selected benthic transects are the primary mechanism for community analysis for the study sites, while the repetitive photostations provide a long-term dataset allowing for specific conclusions about sites over time.

Despite the higher coral cover in the repetitive study site photostations, these sites showed trends similar to those observed in the random transects, suggesting that monitoring these specific stations may give a representative view of the dynamics of the overall study site (e.g., the increasing trend in macroalgal cover). For FGBNMS, the long-term repetitive photostations are critical for enabling researchers to track individual sites over time, especially during extreme events, such as the 2016 bleaching event (Johnston et al. 2019), and as environmental conditions change (Heron et al. 2016; von Hooidonk et al. 2016; Hughes et al. 2017).

Chapter 4. Repetitive Deep Photostations

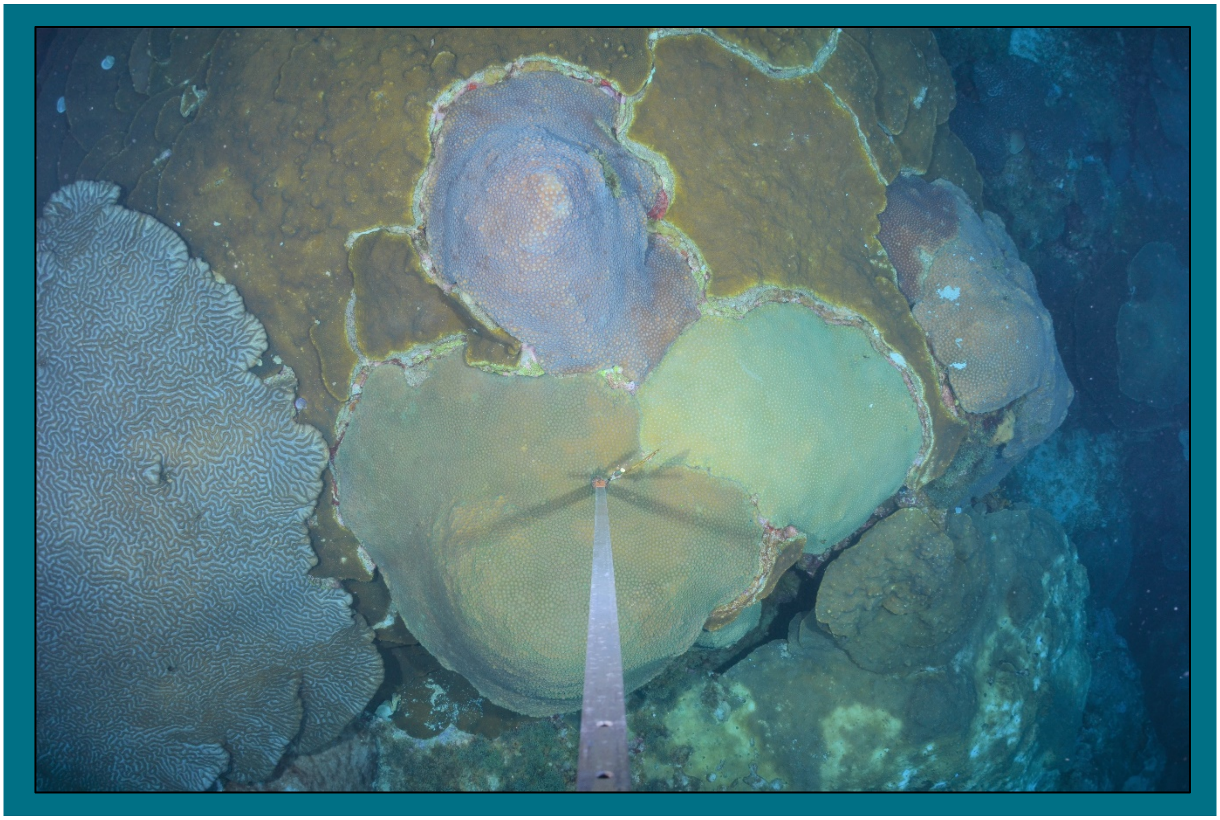

East Flower Garden Bank repetitive deep photostation #07 in 2018 with camera mounted above aluminum t-frame. Photo: G.P. Schmahl/NOAA

Repetitive Deep Photostation Introduction

Permanent repetitive deep photostations were photographed to document changes in the composition of benthic assemblages in water depths from 24–40 m, to follow specific colonies over time, and to compare to the benthic composition of the shallower repetitive study site photostations. The deep repetitive photostations were located outside the EFGB and WFGB study sites, and photographs were analyzed to measure percent benthic cover components using random-dot analysis.

Repetitive Deep Photostation Methods

Repetitive Deep Photostation Field Methods

The repetitive deep photostations, marked by permanent pins and numbered tags on the reef, were located by SCUBA divers using detailed underwater maps displaying compass headings and distances to each station. Twenty-three photostations at EFGB were located outside the study site (east of buoy #2) in depths ranging from 32–40 m (Figure 1.3). Twenty-four photostations at WFGB were located outside the study site (near buoy #2) in depths ranging from 24–38 m (Figure 1.4). After stations were located, divers photographed each station (for more detailed methods, reference Johnston et al. 2017a). All stations were located and photographed in 2018 using a Nikon® D7000® SLR camera (see Chapter 3 Methods – Repetitive Study Site Photostation Field Methods).

Nine of the 23 deep repetitive stations at EFGB were established in 2003 and 12 of the 24 deep repetitive stations at WFGB were established in 2012. Two stations were added to EFGB in 2013. Twelve additional stations were installed at each bank in 2017 at depths ranging from 30–40 m. These new sites increased the number of repetitive sites at these depths, allowing for additional comparisons of the benthic community between the deeper photostations and the shallower photostations within the study sites.

It should be noted that over the period of study, underwater camera setups used to capture benthic cover changed as technology advanced from 35 mm film (2003 to 2007) to digital still images (2008 to 2018) (Precht et al. 2006; Zimmer et al. 2010; Johnston et al. 2013, 2015, 2017a, 2017b). From 2003 to 2009, photographs for each repetitive deep photostation encompassed an 8 m^2 area, but changed to a 5 m^2 area in 2009, a 9 m^2 area in 2010, and back to a 5 m^2 area from 2011 onward due to changes in camera equipment and updated technology.

Repetitive Deep Photostation Data Processing

Mean percent benthic cover from repetitive deep photostation images was analyzed using CPCe version 4.1 (Aronson et al. 1994; Kohler and Gill 2006). A total of 100 random dots were overlaid on each photograph and benthic species lying under these points were identified and verified by QA/QC (see Chapter 2 Methods – Random Transect Data Processing). Point count analysis was conducted for all photos and mean percent cover for functional groups was determined by averaging all photostations per bank study site. Results are presented as mean percent cover ± standard error.

Repetitive Deep Photostation Statistical Analysis

All nonparametric analysis for non-normal data was carried out using Primer® version 7.0 and monotonic trends were detected using the Mann-Kendall trend test in R version 2.13.2 (see Chapter 2 Methods – Random Transect Statistical Analysis).

Repetitive Deep Photostation Results

Repetitive Deep Photostation Mean Percent Cover

EFGB repetitive deep photostation mean coral cover was 70.22 ± 2.96%, macroalgae cover was 20.26 ± 2.43%, CTB cover was 6.28 ± 0.85%, sponge cover was 2.83 ± 1.14%, and other cover was 0.41 ± 0.22% (Figure 4.1). At WFGB, mean coral cover was 74.60 ± 3.24%, macroalgae cover was 13.65 ± 2.12%, CTB cover was 7.91 ± 1.53%, sponge cover was 2.85 ± 0.74%, and other cover was 0.99 ± 0.36% (Figure 4.1). When compared for differences based on functional groups using PERMANOVA, no significant differences were found, suggesting that EFGB and WFGB repetitive deep photostations were similar to each other in overall benthic community composition. For both EFGB and WFGB repetitive deep photostations combined, mean coral cover was 72.41 ± 3.10%, macroalgae cover was 16.95 ± 2.28%, CTB cover was 7.10 ± 1.19%, sponge cover was 2.84 ± 0.94%, and other cover was 0.70 ± 0.29%.

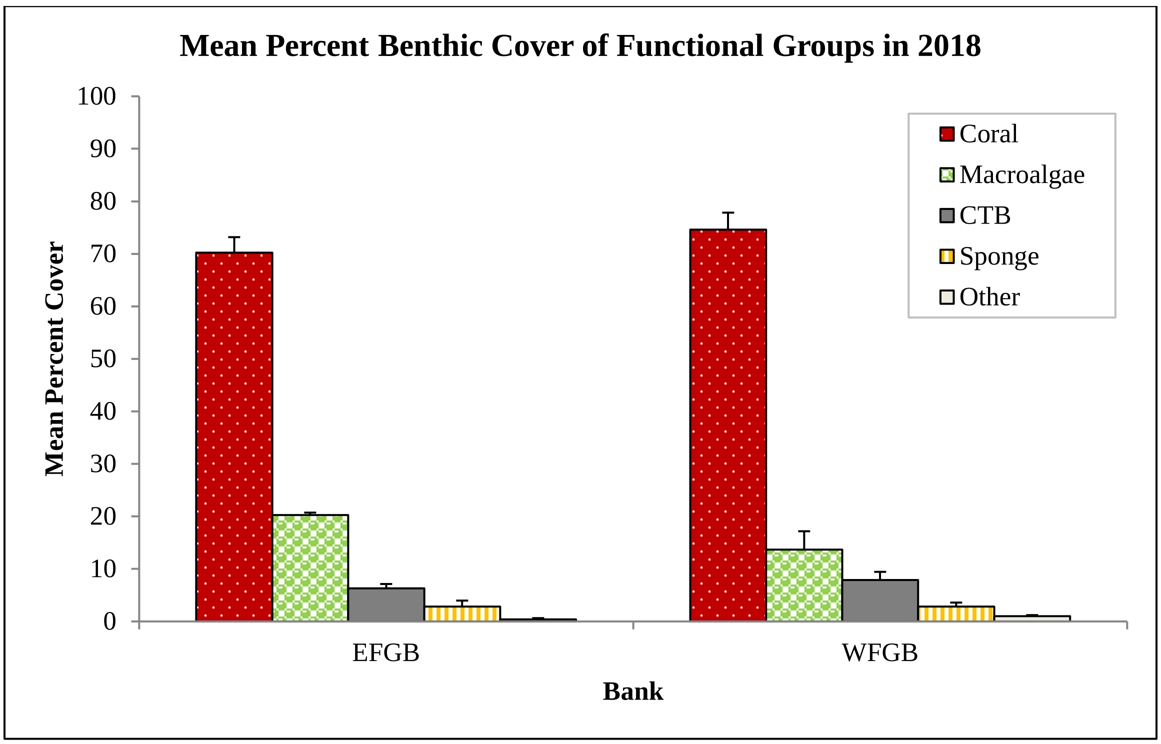

Figure 4.1. Mean percent benthic cover + SE from repetitive deep photostation functional groups at EFGB and WFGB in 2018.

Twelve species of coral were observed in the EFGB repetitive deep photostations and 13 species were observed in the WFGB repetitive deep photostations, for a total of 13 coral species for repetitive deep photostations from both banks combined (Figure 4.2). *Orbicella franksi* was the coral species with the highest percent cover in EFGB (34.17 ± 3.61%) and WFGB (40.22 ± 4.86%) deep photostations, followed by *Montastraea cavernosa* in EFGB (10.65 ± 2.55%) and WFGB (11.75 ± 2.62%) deep photostations (Figure 4.2). PERMANOVA analysis revealed no significant differences in repetitive deep photostation coral species composition between banks.

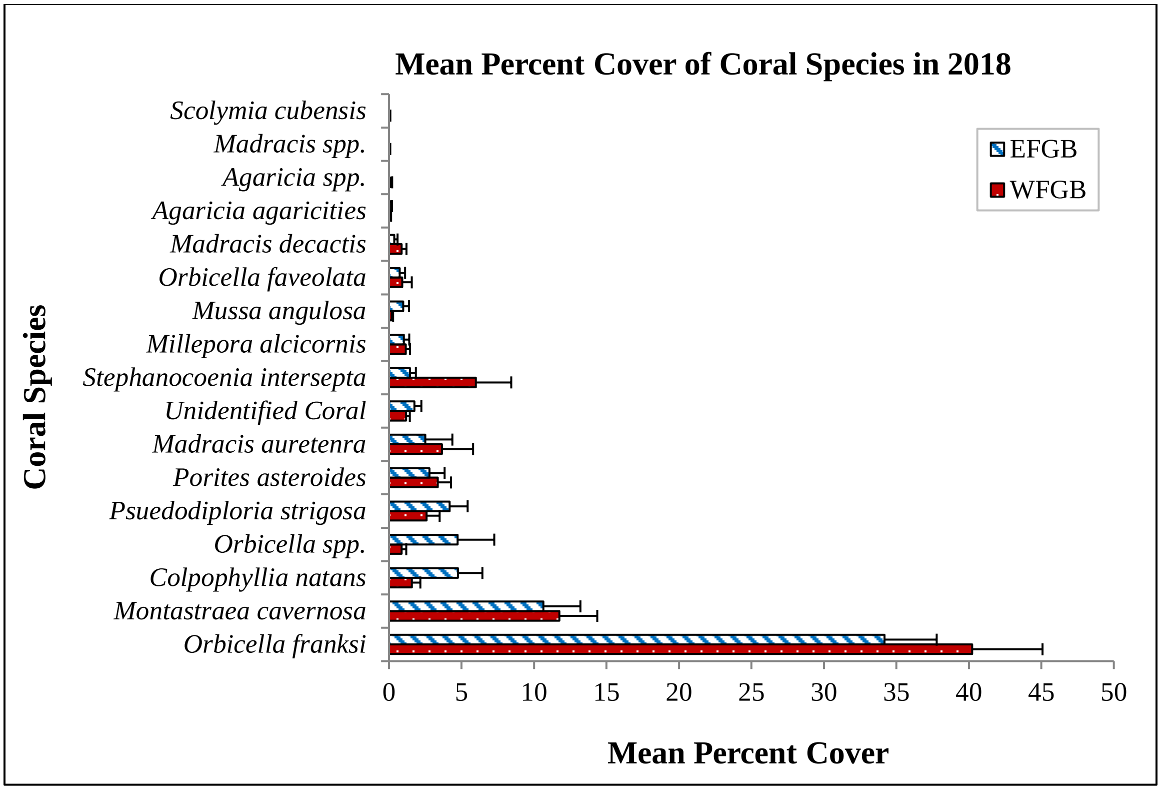

Figure 4.2. Mean percent cover + SE of observed coral species from repetitive deep photostations at EFGB and WFGB in 2018.

Less than 0.5% of the coral cover analyzed was observed to pale or bleach in the EFGB and WFGB repetitive deep photostations. In addition, less than 0.3% of corals in the repetitive deep photostations were affected by fish biting or signs of mortality.

Repetitive Deep Photostation and Repetitive Study Site Photostation Comparisons

Mean percent coral cover was higher in the repetitive deep photostations (deep stations) when compared to the shallower repetitive study site photostations (shallow stations), averaging 72.41% at the deep stations and 65.89% at the shallow stations for both banks combined. Mean macroalgae cover was 16.95% at the deep stations and 20.05% at the shallow stations. Mean percent CTB cover was 7.10% at the deep stations and 12.01% at the shallow stations. Mean percent sponge cover was 2.84% at the deep stations and 0.91% at the shallow stations, and other cover was approximately 1% at both the deep and shallow stations (Figure 4.3).

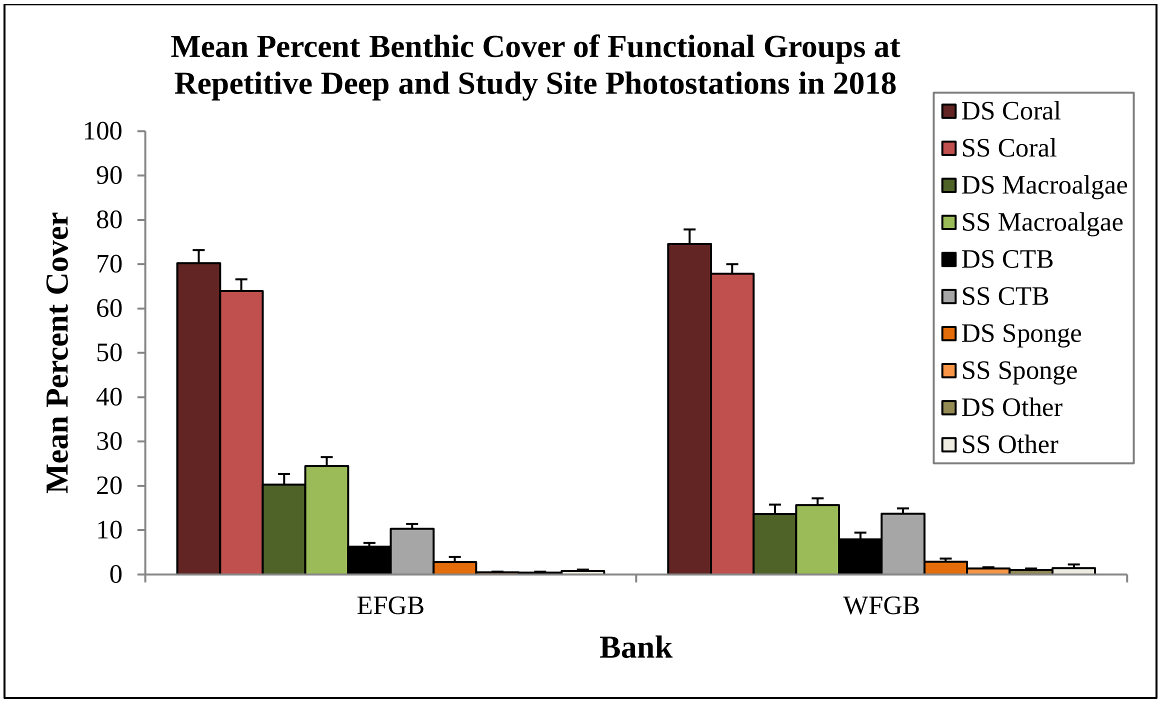

Figure 4.3. Repetitive deep station (DS) and repetitive study site shallow station (SS) functional group mean benthic percent cover + SE at EFGB and WFGB in 2018.

When compared for differences between banks and depth based on mean percent cover, PERMANOVA analysis revealed a significant difference between depths, suggesting that EFGB and WFGB deep photostations were significantly different in overall benthic cover from the shallow photostations (Table 4.1). Mean coral cover was the primary contributor (41.67%) to the observed dissimilarity based on SIMPER analysis, and was significantly higher at the deep stations.

Table 4.1. PERMANOVA results comparing repetitive deep and shallow photostation mean percent benthic cover from EFGB and WFGB in 2018. Bold text denotes significant value.

Source	Sum of Squares	df	Pseudo-F	P (perm)
Bank Photostation Cover	2437	1	38.31	0.456
Depth	2354	1	5.77	**0.013**
Bank Photostation Cover x Depth	63	1	0.16	0.831
Res	49792	122		
Total	54961	125		

To further investigate differences in coral cover between depths, species level data were analyzed. Mean *Orbicella franksi* (29.74%) and *Montastraea cavernosa* (14.21%) percent cover were the primary contributors to the observed dissimilarity between repetitive deep and shallow photostation coral species.

Repetitive Deep Photostation Long-Term Trends

The mean percent benthic cover from the repetitive deep photostations was analyzed to measure changes over time. In the EFGB repetitive deep photostations from 2003 to 2018, mean percent coral cover ranged from 72–86% (Figure 4.4). Coral species with the greatest mean percent cover over time were within the *Orbicella* species group (44.71%) (primarily *Orbicella franksi*), followed by *Montastraea cavernosa* (13.88%) (Figure 4.5). It should be noted that the change in photographic area in 2009 and 2010 due to changing camera equipment may be correlated with inflated percent coral cover estimates that resulted in these years (Figure 4.4). It should also be noted that the twelve additional stations installed in 2017 were incorporated into the long-term trend analysis.

Macroalgae and CTB cover were significantly correlated (τ=-3.652, p=0.003), with macroalgae significantly increasing over time (τ=0.524, p=0.008), coinciding with decreases in CTB cover (Figure 4.4). Overall, the most noticeable pattern was the inverse relationship between CTB and macroalgae cover (similar to benthic cover in both random transects and repetitive study site photostations), with increased macroalgae cover starting in 2005, and peaking at approximately 21% in 2012 at the EFGB repetitive deep photostations.

In 2012, deep photostations were established at WFGB. The mean percent coral cover ranged from 72–77% from 2012 to 2018 (Figure 4.4). Like the EFGB repetitive deep stations, coral species with the highest mean percent cover in the WFGB repetitive deep stations were within the *Orbicella* species group (37.24%) (primarily *Orbicella franksi*), followed by *Montastraea cavernosa* (16.37%) (Figure 4.5). Since 2012, macroalgae cover has ranged from 13–21% and CTB has ranged from 5–11%. Sponge cover was approximately 1% from 2012 to 2018. No significant increases or decreases in percent cover data were detected in the WFGB repetitive deep photostations.

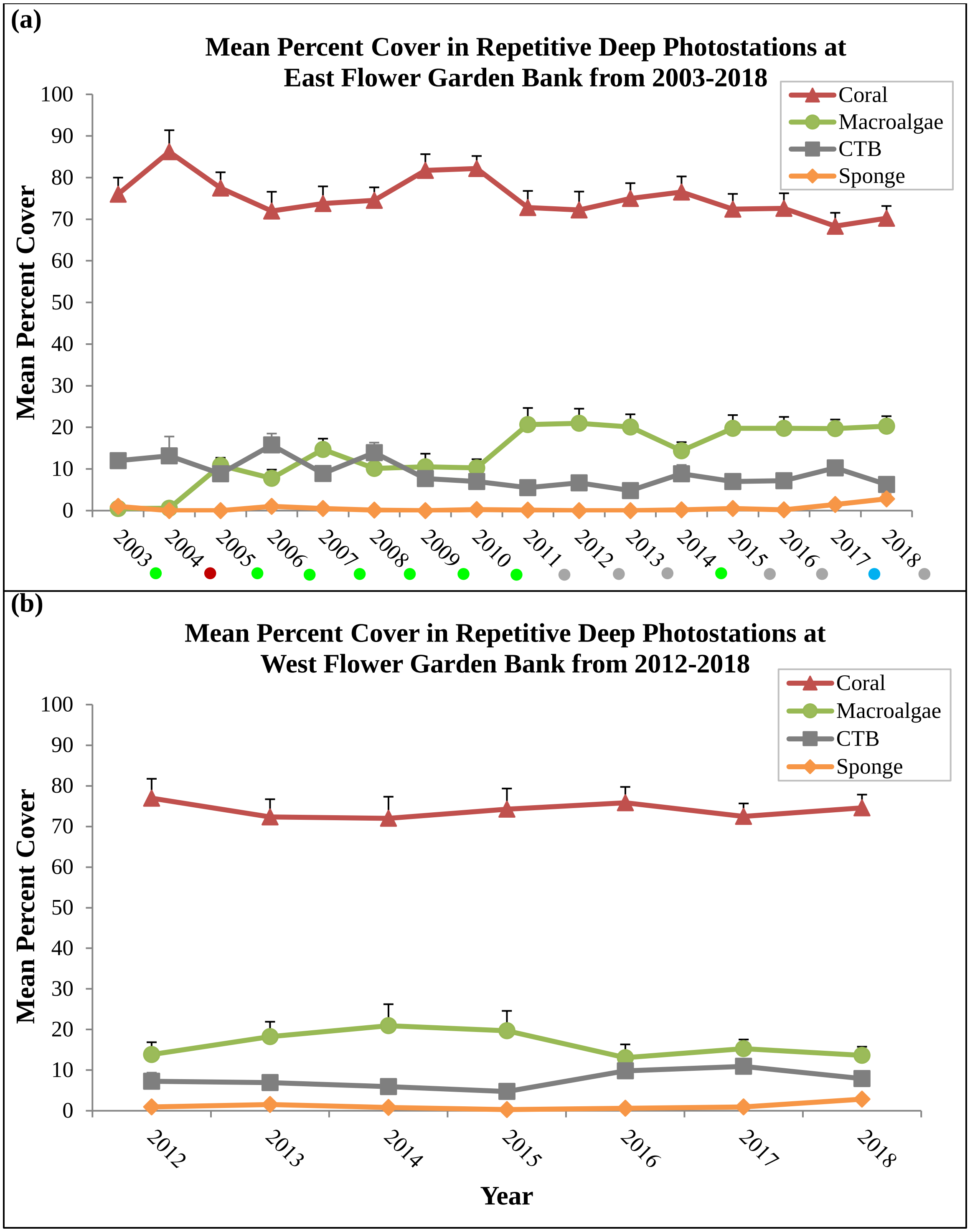

Figure 4.4. Mean percent benthic cover + SE of repetitive deep photostation functional groups at (a) EFGB from 2003 to 2018 and (b) WFGB from 2012 to 2018. Sample size increased from 11 to 23 photostations at EFGB and 12 to 24 photostations at WFGB in 2018. The colored dots represent significant year clusters corresponding to SIMPROF groups in Figure 4.6.

Data for 2003 to 2008 are from PBS&J (Precht et al. 2006; Zimmer et al. 2010) and data for 2009 to 2017 are from FGBNMS (Johnston et al. 2013, 2015, 2017a, 2017b, 2018b).

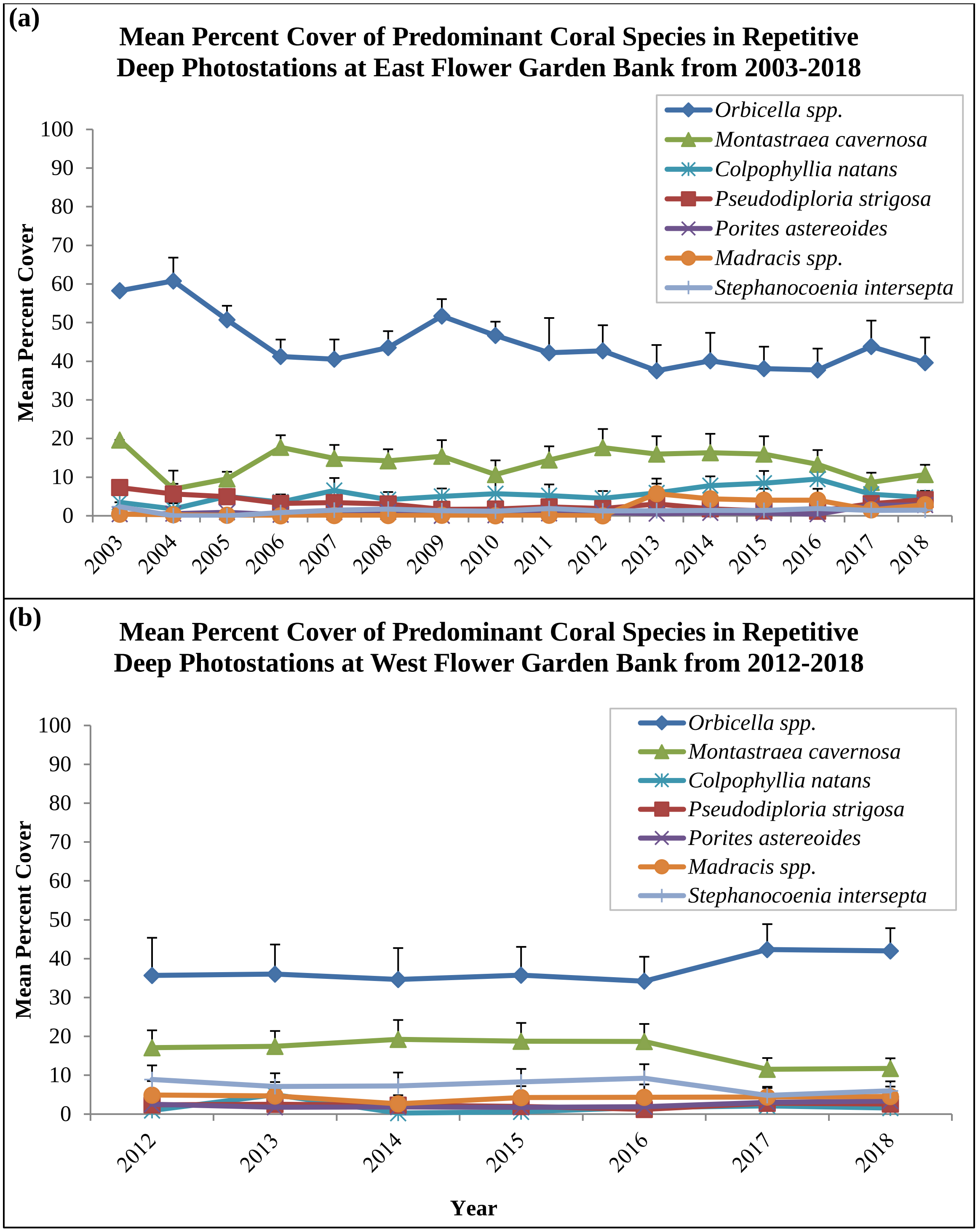

Figure 4.5. Mean percent cover + SE of predominant coral species in repetitive deep photostations at (a) EFGB from 2003 to 2018 and (b) WFGB from 2012 to 2018. Sample size increased from 11 to 23 photostations at EFGB and 12 to 24 photostations at WFGB in 2017. *Orbicella* species combines *Orbicella franksi*, *Orbicella faveolata*, and *Orbicella annularis* for historical data comparison.

Data for 2002 to 2008 are from PBS&J (Precht et al. 2006; Zimmer et al. 2010) and data for 2009 to 2017 are from FGBNMS (Johnston et al. 2013, 2015, 2017a, 2017b, 2018b).

For yearly mean benthic percent cover data in EFGB repetitive deep photostations (2003 to 2018), SIMPROF analysis detected two significant year clusters (A: 2003, 2005 to 2010, and 2014; B: 2011 to 2013, 2015 to 2016, and 2018) (Figure 4.6). The years 2004 and 2017 were grouped individually. Between clusters A and B, macroalgae and coral mean percent cover contributed to over 85% of the dissimilarity (67.98% and 17.06%, respectively) due to increasing macroalgae and slight decreases in coral cover over time (Figure 4.4). The year 2004 was not clustered with any other year, and was dissimilar to all other groups due to high CTB and low macroalgae cover. The year 2017 was not clustered with any other year, and was dissimilar to all other groups due to changes in coral cover, possibly from the addition of new photostations.

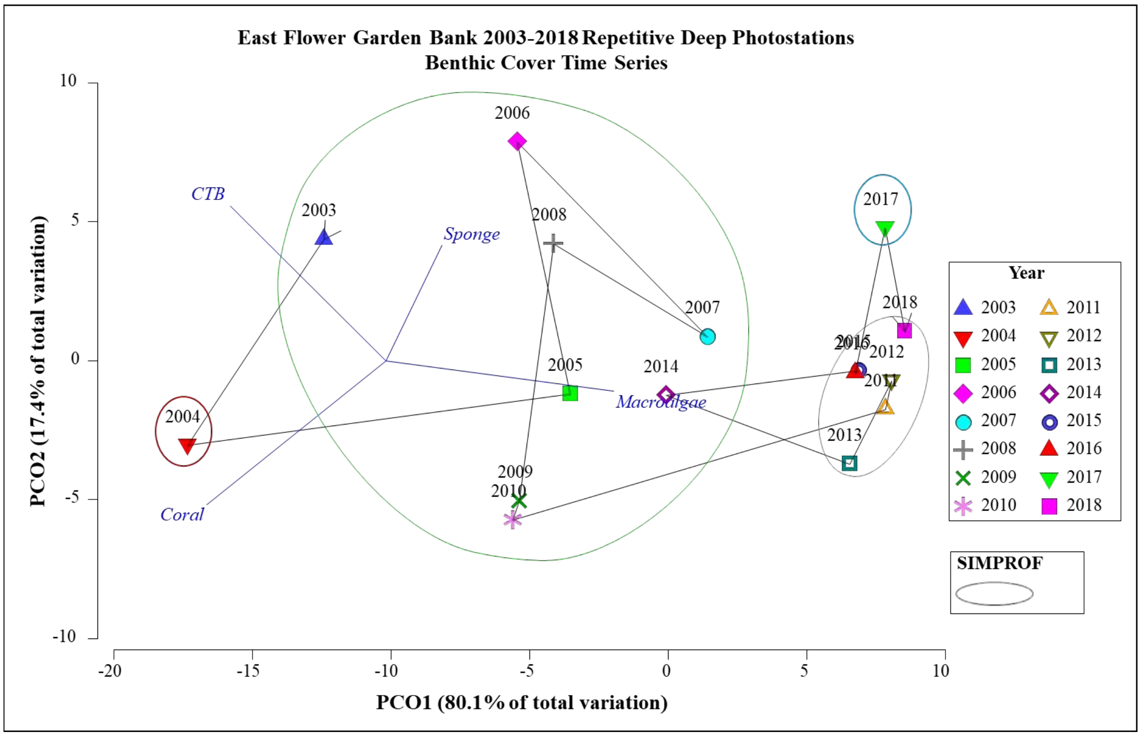

Figure 4.6. PCO for repetitive deep photostations from 2003 to 2018 at EFGB. The ovals are SIMPROF groups representing significant year clusters grouped by color. The blue vector lines represent the directions of the variable gradients for the plot.

For yearly mean benthic percent cover data in WFGB repetitive deep photostations (2012 to 2018), no significant year clusters were detected, suggesting the WFGB repetitive deep photostations were similar to each other in overall benthic community composition over time.

PERMANOVA results revealed no significant differences among deep photostation communities, suggesting that EFGB and WFGB repetitive deep photostations were similar to each other in benthic community composition over time.

Repetitive Deep Photostation Discussion

Nine repetitive deep photostations have been in place since 2003 at EFGB (with two stations added in 2013), and twelve repetitive deep photostations have been in place since 2012 at WFGB. Twelve additional stations were added to each bank in 2017. Percent coral cover within EFGB repetitive deep photostations has ranged from 68% to 86% since 2003 (Figure 4.4). Percent coral cover within WFGB repetitive deep photostations has ranged from 77% to 72% since 2012 (Figure 4.4).

In the example from EFGB repetitive deep photostation #07 (Figure 4.7), the overall coral community remained stable and in good health, showing the value of long-term repetitive photographs. Some colonies appeared paler in certain years due to variations in zooxanthellae concentrations and/or photographic equipment (e.g., 35 mm film and digital images) and ambient conditions, as all photos were subject to varying degrees of camera settings, lighting, etc., from year to year. The large *Montastraea cavernosa* colonies in the center of the station gained tissue over the years, and the margin of the *Colpophyllia natans* colony on the left side of the station grew closer to the *Montastraea cavernosa* colonies (Figure 4.9 a and j).

Significantly higher mean coral cover estimates (72%) were obtained from the repetitive deep photostations than from either the shallower repetitive photostations (66%) or the random transects (54%) at both EFGB and WFGB study sites. This has been documented in previous reports (Precht et al. 2006; Zimmer et al. 2010; Johnston et al. 2013, 2015, 2017a, 2017b, 2018b), and it is not unusual for corals on the deep slopes of coral reefs to cover more bottom area than those at shallower depths. This is due, in part, to the tendency for corals to grow flatter at deeper depths to more efficiently capture light (Bridge et al. 2011). The repetitive deep stations were dominated by *Orbicella franksi* (similar to the random transects and repetitive study site photostations); however, *Montastraea cavernosa* had the second highest cover, unlike the shallower areas in the study sites, where *Psuedodiploria strigosa* had the second highest cover. Coral colonies in the repetitive deep photostations also flatten in shape and plate out, increasing their surface area for sunlight uptake at these deeper depths.

A noticeable difference between EFGB and WFGB repetitive deep photostations and the repetitive study site photostations and random transects was the lack of *Orbicella annularis* cover at the deeper depths and decreased occurrence of *Pseudodiploria strigosa*. *Stephanocoenia intersepta* and *Madracis* species were also more abundant in the repetitive deep stations. Macroalgae cover, while lower than shallower sites, increased over time in the EFGB repetitive deep photostations, following a similar pattern to the repetitive study site photostations and random transects.

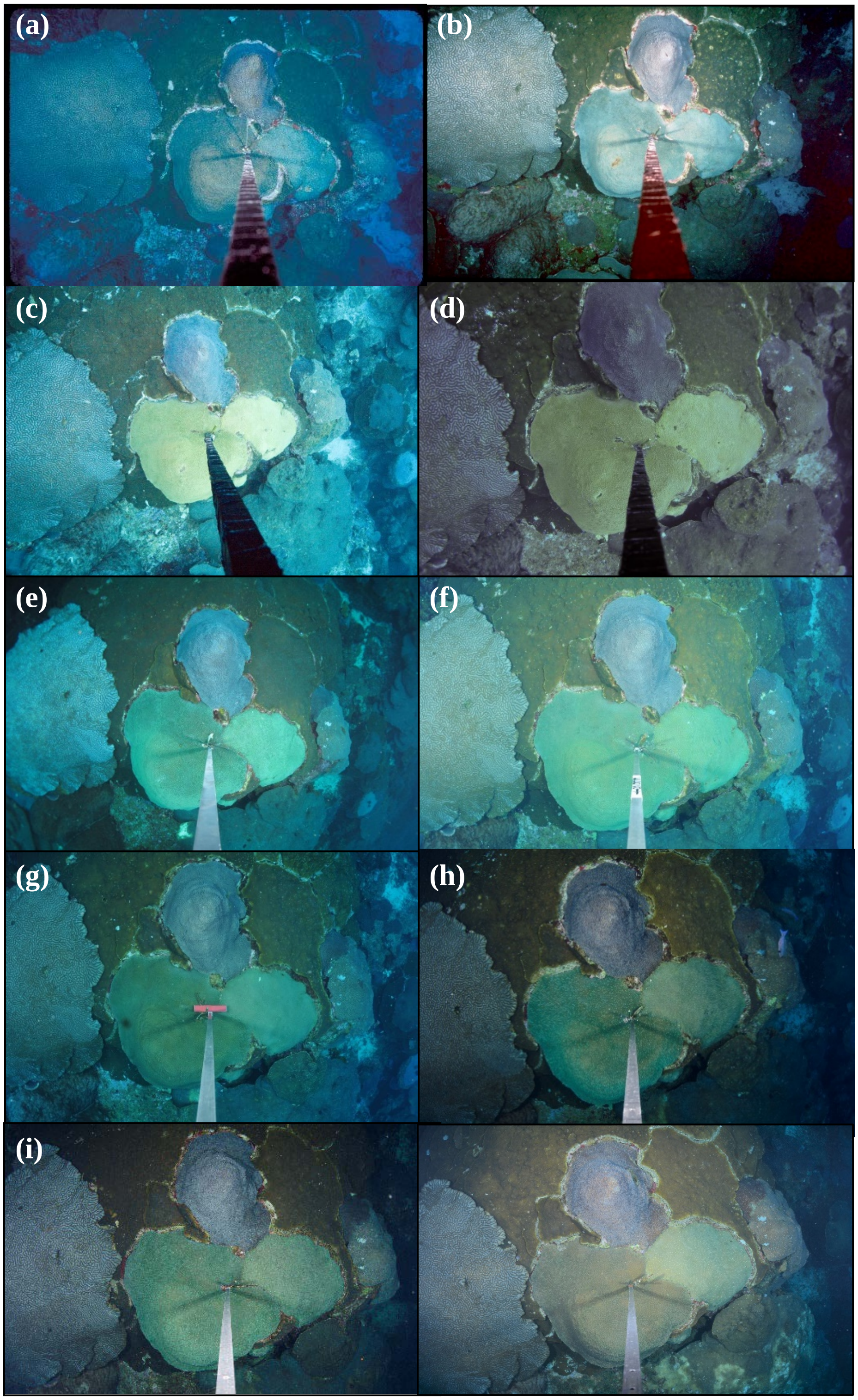

Figure 4.7. Select photos from EFGB repetitive deep photostation #07 show a time series from (a) 2005; (b) 2007; (c) 2008; (d) 2009; (e) 2010; (f) 2011; (g) 2012; (h) 2013; (i) 2016; and (j) 2018. Photos: NOAA

It should be noted that the repetitive deep photostations may not provide an accurate assessment of the predominant species within deeper habitats outside the EFGB and WFGB study sites, as these stations were selectively placed on habitat with large coral colonies to monitor individual corals. As described in Chapter 2, the randomly selected benthic transects allowed for conclusions to be made about the entire study site, while the repetitive deep photostations provided a long-term dataset, allowing for conclusions to be made about repetitive sites over time in habitat deeper than the study sites.

As with both the repetitive study site photostations and random transects on the shallower portion of the reef, periods of increased algae cover generally coincided with decreases in the CTB category. Similar to random transects, increased macroalgae cover was not concomitant with significant coral cover decline over time in repetitive deep photostations. Overall, the most noticeable patterns were: 1) inverse relationship between CTB and macroalgae cover, 2) increasing macroalgae cover within the EFGB photostations, and 3) mean coral cover above 70% over time.

Chapter 5. Coral Demographics

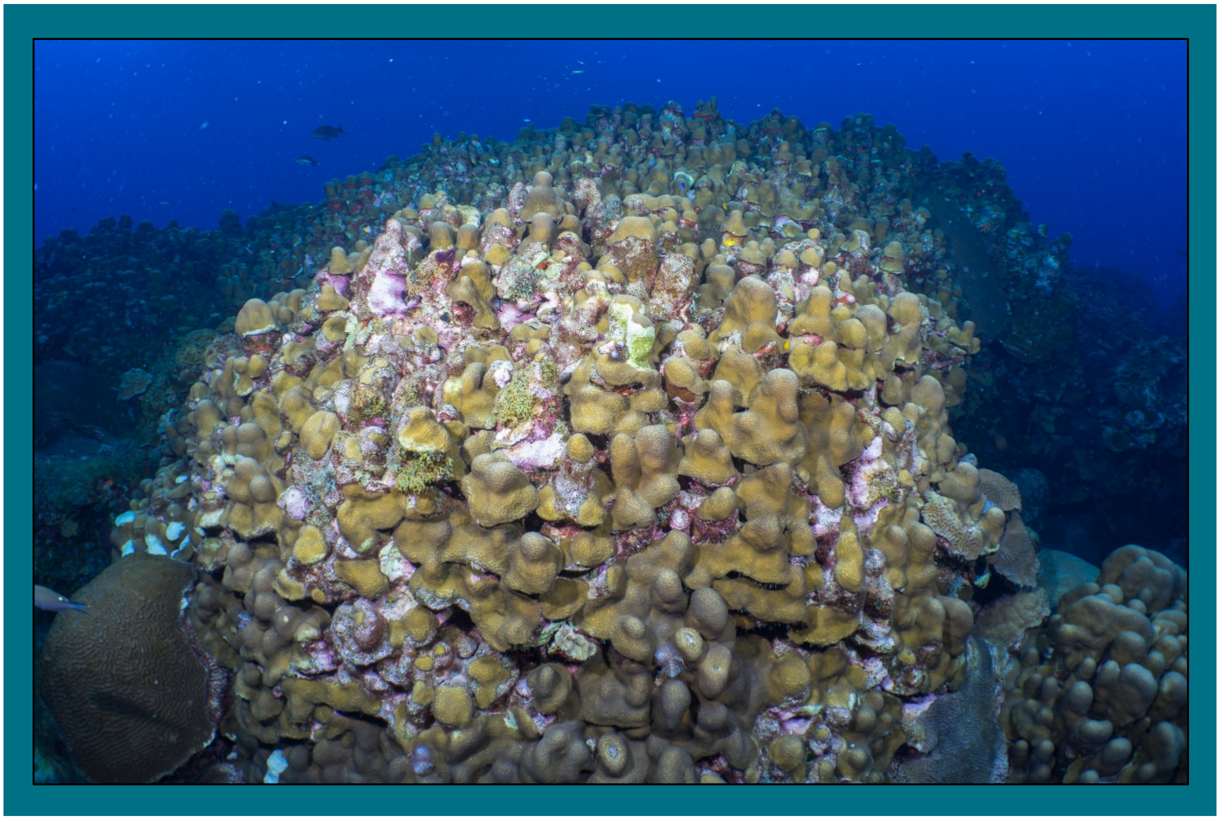

A large colony of lobed star coral (*Orbicella annularis*) at East Flower Garden Bank in 2018. Photo: G.P. Schmahl/NOAA

Coral Demographic Introduction

To document coral colony size, density, and condition, coral demographic surveys were conducted. These surveys provide species-specific insight for corals beyond percent cover alone; coral size and abundance are key metrics for describing trends in coral reef population dynamics.

Coral Demographic Methods

Coral Demographic Field Methods

Coral demographic surveys were conducted to document species richness, abundance, density, coral colony size, and condition. Due to limited time available for these surveys on the long-term monitoring cruises, coral demographic surveys were conducted by NOAA's National Coral Reef Monitoring Program with assistance from FGBNMS divers from June 11 to 15, 2018 aboard the M/V *Fling* in stratified random locations on the EFGB and WFGB coral caps. A total of 17 surveys were completed at EFGB and 20 surveys were completed at WFGB.

To document coral colony size and condition, a 10 m x 1 m belt transect survey was conducted. Each coral colony (diameter > 4 cm) was identified and measured (length x width x height (cm)) to estimate colony size (cm^3). For example, a coral colony measuring 50 cm in each dimension would equal 125,000 cm^3. The entire coral colony (skeleton and live tissue) on a planar dimension was measured, where length was the maximum diameter, width was the perpendicular diameter, and height was measured from the base of the skeletal unit to the top of the colony (Roberson et al. 2014). The survey began at marker 0 m and ended at 10 m. Divers used meter long PVC measuring poles to aid with coral size estimations (Figure 5.1). Measurements were made to the nearest centimeter. Coral condition measurements such as percent paling or bleaching and mortality (recent, old, or transitional - if any) were also estimated and recorded. Estimation of percent bleaching included the percent of a coral colony that was white with no visible zooxanthellae. Estimation of percent paling included the percent of a colony that was pale in color relative to what is considered "normal" for the species (AGRRA 2012). Estimates of various stages of mortality were made separately. Recent mortality was an estimate of the percentage of a colony with an exposed bare skeleton and little to no algae growth such that coral species could still be determined. Transitional mortality was an estimate of the percentage of a colony with an exposed bare skeleton colonized by filamentous algae. Old mortality was an estimate of the percentage of old dead, tissue-free skeleton on the colony (e.g. no distinct corallites visible with colonization by macroalgae and other encrusting species). Datasheets included additional information to be collected by surveyors, such as survey depth and seawater temperature.

The belt transect survey, which was closely based on surveys used for the Atlantic and Gulf Rapid Reef Assessment (AGRRA) program in the Caribbean region, is used by

NOAA's National Coral Reef Monitoring Program (AGRRA 2012; Roberson et al. 2014). The surveys were time-intensive due to the abundance of corals.

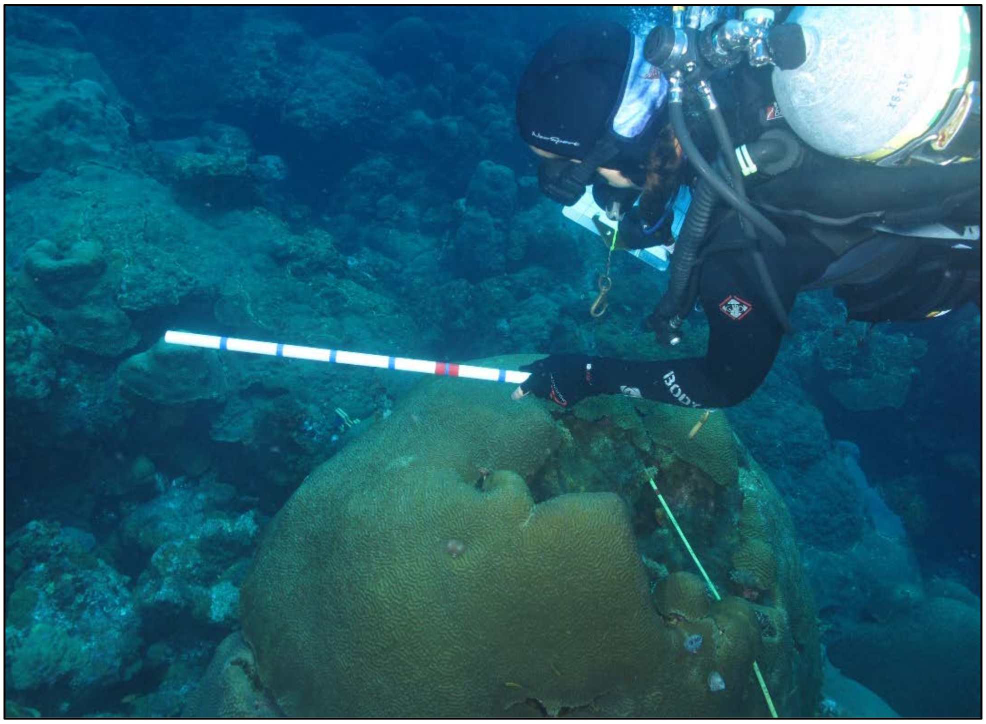

Figure 5.1. A PVC measuring stick aids in estimating the width of a colony on a coral demographic survey at EFGB. Photo: G.P. Schmahl/NOAA

Consistency of survey methods was maintained through the use of scientific divers trained to identify coral species found at FGBNMS. Divers were experienced in the survey technique, and equipment checklists were provided in the field to ensure divers had all equipment and were confident with tasks assigned. Surveyors reviewed and entered coral demographic data in a Microsoft® Excel® database on the same date the survey took place. All datasheets were reviewed and compared to data entered in the database during field operations to check for entry errors, and mistakes were corrected before data analysis was completed.

Coral Demographic Data Analysis

Coral density was expressed as the number of individual coral colonies per m^2 ± standard error. Estimates of coral colony size were obtained by multiplying the length, width, and height of colonies measured in the field. Colony size calculations were not adjusted to account for partial mortality. Statistical analyses were conducted on square root transformed coral colony size data using non-parametric distance-based analyses with Primer® version 7.0 (Anderson et al. 2008; Clarke et al. 2014). A Euclidian distance similarity matrix was calculated and PERMANOVA was used to test for differences in colony sizes among species and bank study sites.

Coral Demographic Results

For the coral demographic survey data collected in 2018, the average survey depth was 21 m at EFGB and 24 m at WFGB. Species richness included 16 coral species in surveys at EFGB and 18 at WFGB (Table 5.1). Overall mean coral density (corals/m^2 ± standard error) was 4.86 ± 0.36 at EFGB and 5.04 ± 0.41 at WFGB. The most abundant species in the surveys was *Porites astreoides*, followed by *Orbicella franksi* (Table 5.1). While *Porites astreoides* was the most abundant species observed, these small corals covered much less area than larger coral species.

Orbicella franksi colonies occupied the most area on surveys at both EFGB and WFGB; however, *Orbicella annularis* colonies were the largest colonies in EFGB surveys (120 cm mean maximum diameter), followed by *Orbicella franksi* (102 cm mean maximum diameter) (Table 5.1). *Siderastrea siderea* colonies were the largest in WFGB surveys (208 cm mean maximum diameter), followed by *Orbicella annularis* (188 cm mean maximum diameter) (Table 5.1). Within all surveys, no coral disease was documented.

Table 5.1. Total number of colonies, total colony mean maximum diameter (cm), and mean colony size (cm^3) from 2018 coral demographic EFGB surveys (n=17) and WFGB surveys (n=20).

Coral Species	EFGB Surveys			WFGB Surveys		
	Total Colonies	Mean Max Diameter (cm)	Mean Size (cm^3)	Total Colonies	Mean Max Diameter (cm)	Mean Size (cm^3)
Porites astreoides	301	26	8979	476	19	3924
Orbicella franksi	120	102	783990	114	106	728142
Pseudodiploria strigosa	109	66	390949	88	72	407596
Orbicella faveolata	53	76	339045	50	129	1597871
Montastraea cavernosa	48	47	86944	60	56	232213
Agaricia agaricites	44	11	408	65	9	1309
Colpophyllia natans	44	69	368787	28	81	1264887
Stephanocoenia intersepta	38	29	16124	51	33	23570
Orbicella annularis	28	120	1657790	4	188	5228975
Madracis auretenra	11	97	332526	2	36	21978
Madracis decactis	11	37	150638	19	40	269256
Siderastrea siderea	6	24	11718	5	208	13481775
Mussa angulosa	5	25	3851	4	26	8651
Porites furcata	5	25	3576	14	58	33651
Scolymia cubensis	3	6	30	12	6	78
Agaricia spp.	1	23	299	0	0	0
Agaricia fragilis	0	0	0	9	12	438
Helioseris cucullata	0	0	0	2	34	5719
Colpophyllia spp.	0	0	0	1	18	306
Madracis spp.	0	0	0	1	12	960
Porites spp.	0	0	0	1	8	112
Scolymia spp.	0	0	0	1	4	32

PERMANOVA results revealed significant differences among species and colony size from surveys between banks. The bank colony size by species interaction was also significant (Table 5.2).

Table 5.2. PERMANOVA results comparing colony size (cm^3) by coral species and bank from EFGB and WFGB coral demographic surveys in 2018. Bold text denotes significant value.

Source	Sum of Squares	df	Pseudo-F	P (perm)
Colony Size by Bank	5162100	1	26.81	**0.001**
Colony Size by Species	104430000	21	25.82	**0.001**
Colony Size Bank x Species	23626000	14	8.76	**0.001**
Res	346050000	1797		
Total	474580000	1833		

Coral Demographic Discussion

Coral size and abundance are important metrics for describing trends in coral reef population dynamics. Although the corals of the *Orbicella* species group are the predominant reef building corals at EFGB and WFGB in terms of percent cover, *Porites astreoides* was the most abundant species, despite the smaller area covered by these colonies. Though the coral community in the study sites has remained relatively stable throughout the monitoring program from 1989 to 2018, coral communities are rapidly changing worldwide (Jackson et al. 2014; Johnston et al. 2016b). The overall loss of coral cover in the Caribbean region due to disease, hurricane damage, anthropogenic impacts, and thermal stress has resulted in shifts in species composition in certain reef areas (Alvarez-Filip et al. 2013; Jackson et al. 2014).

On many reefs in the Caribbean region, dominant reef-building corals, such as those found at EFGB and WFGB, have declined, allowing “weedy,” opportunistic coral species to increase in abundance (Green et al. 2008; Alvarez-Filip et al. 2013). This decreases reef functionality and complexity, and threatens the stability of coral reef biodiversity (Alvarez-Filip et al. 2013; Graham and Nash 2013). Continued monitoring of the coral community in the study sites will document changes in the community compared to the historical baseline. These data enable resource managers to make decisions that facilitate the survival of keystone reef-building species rather than focusing only on actions that emphasize maintaining high percentages of coral cover.

Chapter 6. Lateral Growth of Coral Margins

A NOAA diver with camera and strobe mounted on a short aluminum t-frame takes a photograph of a symmetrical brain coral (*Pseudodiploria strigosa*) colony margin within the EFGB study site. Photo: G.P. Schmahl/NOAA

Lateral Growth Introduction

To document growth or regression of coral edges, lateral margins of selected *Pseudodiploria strigosa* colonies were photographed annually. *Pseudodiploria strigosa* was more suitable for marginal comparisons than other coral species because of the conspicuous patterns and grooves that could be matched when repetitive annual photographs are overlaid. Despite the improved methods for collecting comparable lateral photos, problematic methodologies have not allowed for repeatable images throughout the program; therefore, NOAA will no longer be collecting lateral growth data after 2018.

Lateral Growth Methods

Lateral Growth Field Methods

At the beginning of the LTM program in 1989, sixty lateral growth photostations, located on the margins of select colonies, were established to assess coral margin growth rates within the study sites (Gittings et al. 1992). Problematic methodologies did not allow for repeatable photography throughout the years of the monitoring program; therefore, modifications in the lateral growth methodology were made in 2013 and 2014, consisting of a "key and keyhole" repetitive photostation design as a last effort for this type of data collection (Chapter 6 cover photo). A thick plastic plate bolted to bare substrate acted as a keyhole next to a *Pseudodiploria strigosa* margin. A mini t-frame "key" pole inserted into holes in the plate allowed for precise and consistent camera orientation for photographic repeatability (Figure 6.1). The key holes were plugged with rubber stoppers during the year to prevent biofouling once the camera pole was removed from the plate.

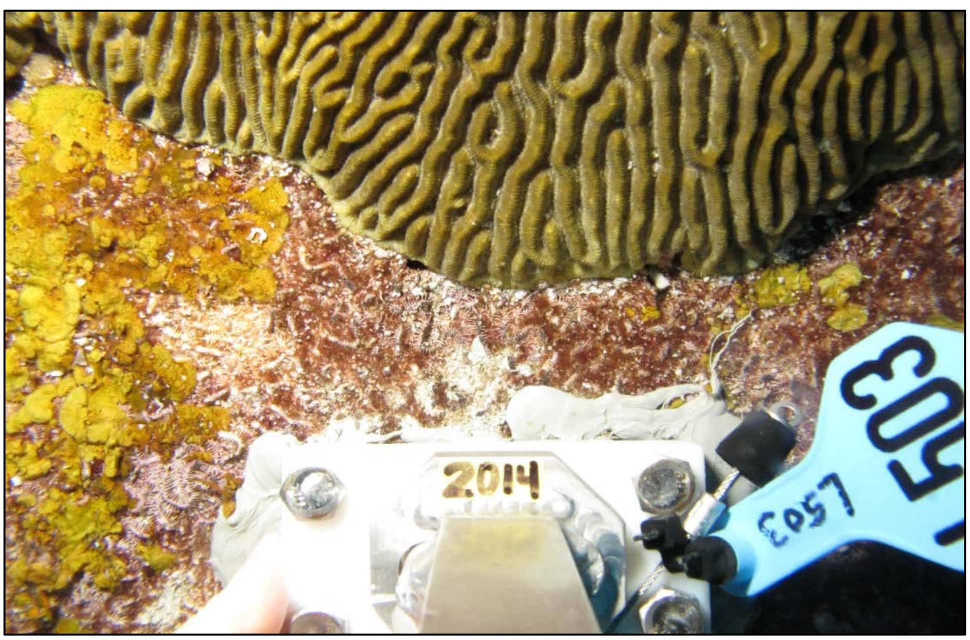

Figure 6.1. *Pseudodiploria strigosa* lateral growth photostation with mini t-frame inserted into the station base plate next to the coral colony. Photo: NOAA

Thirty lateral growth photostations per study site, marked with numbered tags on the reef, were located by SCUBA divers using detailed underwater maps displaying compass headings and distances to each station within the study sites (Figure 1.5 and 1.6). After each station was located, divers photographed each one. Lateral growth photostations were photographed using a Canon Power Shot G11® camera (set in macro mode) in a Fisheye FIX® housing with a standard flatport and two Inon® strobes mounted to the top of a mini t- frame pole (Figure 6.1) (for more detailed methods, reference Johnston et al. 2017a).

Lateral Growth Data Analysis

Images corresponding to a specific lateral growth photostation were compared from 2014 to 2018. Lateral differences in the margins of the *Pseudodiploria strigosa* colonies were evaluated by overlaying the pairs of photographs with Adobe Photoshop® using separate layers to trace coral margins (Figure 6.2). A scale bar was created for each photo using the known length of the base plate to ensure marginal growth calculations were accurate. Using ImageJ®, the scale was set and marginal distances of growth and/or retreat were measured using the wand tool, allowing area to be measured inside irregular shapes (Figure 6.2). These values were then combined to obtain an overall area in cm^2 of growth and retreat for each image. Successive photographs of a given colony were aligned using the colony's ridge patterns.

Net change (positive=growth, negative=retreat) was calculated for the 2014 and 2018 comparable image margins to determine overall growth, retreat, or stability of *Pseudodiploria strigosa* colony margins. Change was calculated by subtracting the area (cm^2) of the first year from the second year to determine growth or loss of marginal tissue area. Areas of the image that were out of focus or shadowed during analysis were not included in the total percentage. Results were presented as change in area ± standard error.

Nonparametric analysis for non-normal data was used for tissue change comparisons. The Mann-Whitney-Wilcoxon two sample rank sum test was performed in R version 2.13.2 to identify differences in net change of coral margins between EFGB and WFGB study sites from 2014 to 2018 (Yau 2016). Comparisons were based on group distributions (W) with a 95% confidence interval (CI) to identify significant differences (α=0.05).

Consistency for lateral growth photostation methods was ensured by multiple scientific divers all trained on the same camera systems for correct camera operation. Camera settings and equipment were standardized so that consistent repetitive images were taken annually and equipment checklists were provided in the field to ensure divers had all equipment and were confident with tasks assigned. Lateral photographs were reviewed promptly after images were taken to ensure the quality was sufficient for analysis. During analysis for QA/QC, a scale bar was created for each photo to ensure marginal growth calculations were accurate.

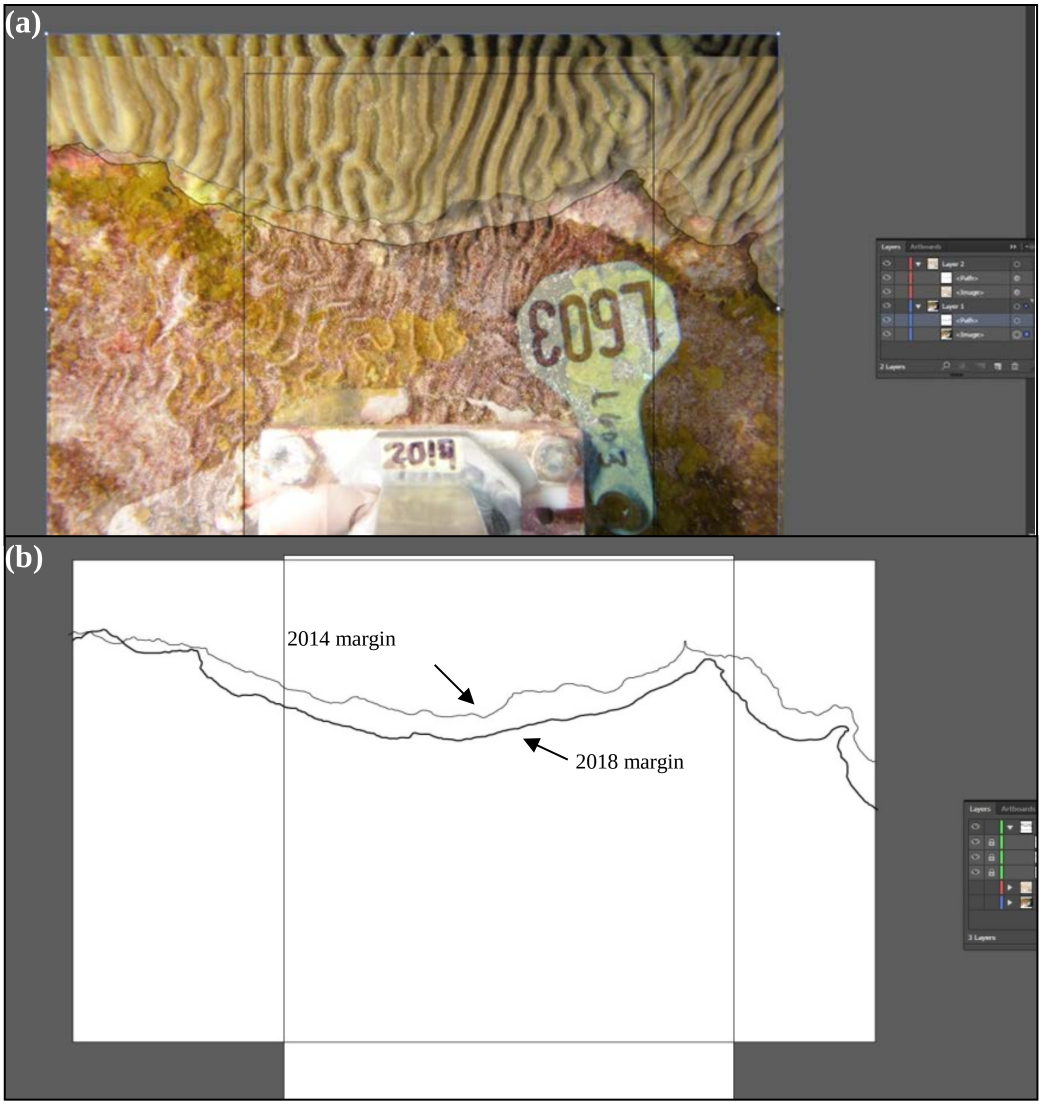

Figure 6.2. (a) A *Pseudodiploria strigosa* lateral growth photostation image from 2014 layered on top of the 2018 photograph, and (b) the outlined 2014 margin (thin grey line) layered on top of the 2018 margin (bold black line). Photo: NOAA

Lateral Growth Results

Overall, coral margins from *Pseudodiploria strigosa* lateral growth photostation colonies selected for analysis increased in area within EFGB and WFGB study sites (Figure 6.3). Net marginal change from 2014 to 2018 was positive in both EFGB (2047.30 ± 5.63 cm^2) and WFGB (1884.11 ± 5.18 cm^2) photostations (Figure 6.3). Results of the Mann-Whitney-Wilcoxon test indicated that net marginal change from 2014 to 2018 was not significantly different between the EFGB and WFGB photostations.

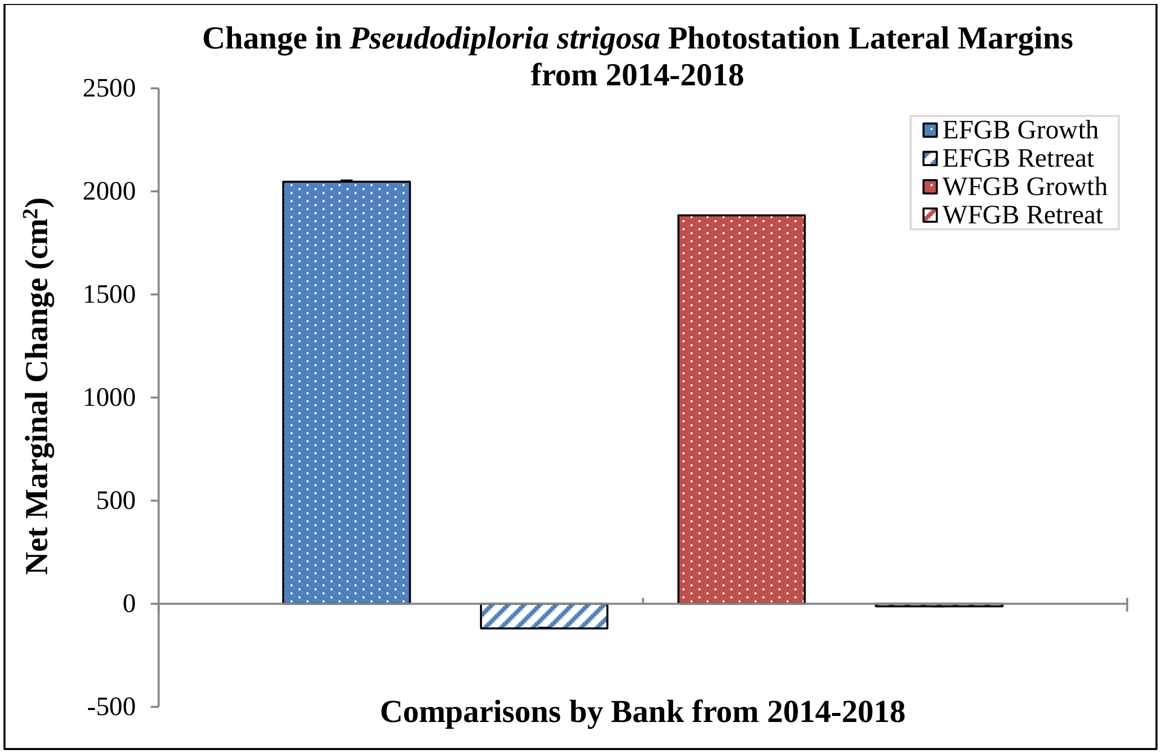

Figure 6.3. Net change (cm^2) + SE in *Pseudodiploria strigosa* colony margins from 2014 to 2018 in EFGB and WFGB lateral growth photostations.

Lateral Growth Discussion

This method is not common among coral reef monitoring programs and has been proven to be extremely problematic throughout the long-term monitoring program (Johnston et al. 2017a). Many factors have affected the quality of lateral growth data for many years. The photostations have a short useful life span since the colonies can overgrow the small area within the station in a short period of time (e.g., 5 to 10 years). Throughout the monitoring program, researchers have encountered problems with locating overgrown lateral growth photostations and photographing the stations in a consistent way (e.g., at the same angle every time), which resulted in a different orientation from one year to the next. The updated lateral growth method implemented in 2013 using the key and keyhole design proved to be precise and allowed for consistent photographic repeatability.

Despite the improved methods for collecting comparable data from lateral stations, it should be noted that these stations will still have a short lifespan as the colony margins overgrow the area between the margin and the photostation plate. The plates of these photostations also become covered with biofouling organisms quickly, and must be thoroughly cleaned annually. As the second largest contributor to coral cover at EFGB and WFGB after *Orbicella franksi, Pseudodiploria strigosa* colonies have been used for much of the long-term monitoring history as an indicator of coral health by monitoring marginal growth and retreat (Bright et al. 1985; Dokken et al. 2003; Gittings et al. 1992;

Precht et al. 2006; Precht et al. 2008; Zimmer et al. 2010; Johnston et al. 2017a). However, this is not a common method and does not allow for comparison to other coral reef monitoring programs in the region or around the globe.

BOEM and NOAA have reviewed the methods employed and conclude that lateral growth data will no longer be collected after 2018.

Chapter 7. Sea Urchin and Lobster Surveys

A long-spined sea urchin (*Diadema antillarum*) on the reef at EFGB. Photo: G.P. Schmahl/ NOAA

Sea Urchin and Lobster Surveys Introduction

The long-spined sea urchin (*Diadema antillarum*) was an important herbivore on coral reefs throughout the Caribbean until 1983, when an unknown pathogen decimated populations throughout the region, including FGBNMS (Gittings and Bright 1987). This invertebrate is a significant marine herbivore and can substantially control macroalgae cover on coral reefs. Additionally, lobsters are commercially important species throughout much of the Caribbean and Gulf of Mexico; however, population dynamics of Caribbean spiny lobster (*Panulirus argus*) and spotted spiny lobster (*Panulirus guttatus*) at EFGB and WFGB are not well understood. Therefore, sea urchin and lobster surveys help document the abundance of these species within the study sites.

Sea Urchin and Lobster Surveys Methods

Sea Urchin and Lobster Surveys Field Methods

Due to the nocturnal nature of these species, visual surveys were conducted at night, a minimum of 1.5 hours after sunset. Surveys for *Diadema antillarum*, *Panulirus argus*, and *Panulirus guttatus* were conducted along all study site perimeter lines and crosshairs. A 2 m wide belt transect was surveyed along each of the six 100 m perimeter lines at each study site, thus totaling 1,200 m^2 per bank. The first diver began on the right side of the line and the second diver on the left. Divers swam slowly along the boundary line, recording sea urchins and lobsters within a 1 m swath on their side of the line. Divers used flashlights to look into and under reef crevices and, if a sea urchin or lobster was seen, observations were recorded on a datasheet including bank, boundary line, and the number of sea urchins or lobsters observed. In 2018, all lines were surveyed within the EFGB and WFGB study sites.

Consistency for the survey method was ensured by multiple scientific divers trained to identify sea urchin and lobster species located at FGBNMS. Divers were experienced in the survey technique used, and equipment checklists were provided to ensure divers had equipment for assigned tasks. QA/QC procedures ensured surveyors reviewed and entered species count data in a Microsoft® Excel® database on the same date the survey took place. All datasheets were reviewed and compared to data entered in the database during field operations to check for entry errors, and mistakes were corrected before data analysis was completed.

Sea Urchin and Lobster Surveys Analysis

Density was calculated as number of individuals per 100 m^2 for each species ± standard error. Statistical analyses were conducted on square root transformed density data using non-parametric distance-based analyses with Primer® version 7.0 (Anderson et al. 2008; Clarke et al. 2014). PERMANOVA examined differences in density between year and bank study sites with a similarity matrix using the Euclidean distance measure.

Sea Urchin and Lobster Surveys Results

Density of *Diadema antillarum* was 1.58 ± 0.10 individuals/100 m² within the EFGB study site and 15.08 ± 0.38 individuals/100 m² within the WFGB study site in 2018 (Table 7.1). No *Panulirus guttatus* or *Panulirus argus* were observed (Figure 7.1).

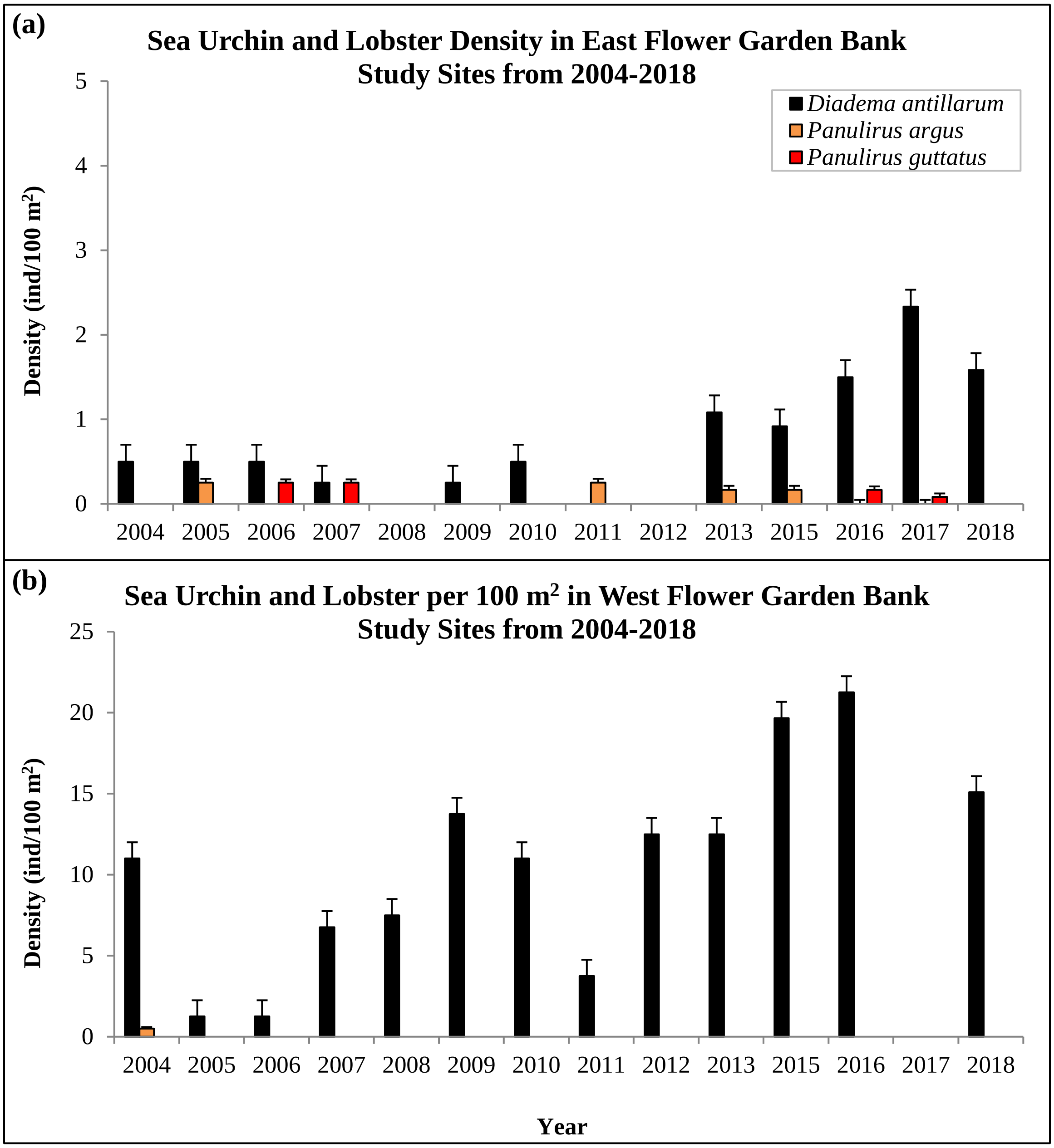

Figure 7.1. Sea urchin and lobster density (individuals/100 m^2) + SE within EFGB and WFGB study sites from 2004 to 2018.

No data are available for either bank for 2014 and at WFGB for 2017. Data for 2004 to 2008 are from PBS&J (Precht et al. 2006; Zimmer et al. 2010) and from 2009 to 2017 are from FGBNMS (Johnston et al. 2013, 2015, 2017a, 2017b, 2018b).

Since 2004, *Diadema antillarum* densities have ranged from 0–2.3 individuals/100 m^2 within the EFGB study site and 1.25–21.25 individuals/100 m^2 within the WFGB study site. Higher numbers of *Diadema antillarum* have been observed during surveys at the WFGB study site throughout the monitoring program (Figure 7.1). Since 2004, lobster densities have ranged from 0–0.25 individuals/100 m^2 within the EFGB and WFGB study sites combined.

When compared for differences between bank study sites and years based on *Diadema antillarum* density, PERMANOVA analysis revealed a significant difference (Table 7.1), suggesting that sea urchin density was significantly greater within the WFGB study site.

Table 7.1. PERMANOVA results comparing sea urchin densities between EFGB and WFGB study sites and years 2004 to 2018. Bold text denotes significant value.

Source	Sum of Squares	df	Pseudo-F	P (perm)
Bank Study Site	38	1	73.21	**0.001**
Year	11	13	1.74	0.175
Res	6	12		
Total	55	26		

Sea Urchin and Lobster Surveys Discussion

Diadema antillarum are important herbivores on coral reefs, helping to reduce macroalgae through grazing, which makes room for coral growth and new recruits (Edmunds and Carpenter 2001; Carpenter and Edmunds 2006). After the mass die off in 1983, *Diadema antillarum* populations have not recovered to pre-1983 levels (Gittings 1998), which were at least 140 individuals/100 m^2 at EFGB and 50 individuals/100 m^2 at WFGB (Gittings unpublished data). Post-1983 *Diadema antillarum* densities dropped to near zero (Gittings and Bright 1987). Since then, patchy but limited recovery has been documented in the Caribbean region (Edmunds and Carpenter 2001; Kramer 2003; Carpenter and Edmunds 2006). *Diadema antillarum* densities at nearby Stetson Bank have also increased in recent years, averaging 170 individuals/100 m^2 in 2016 (Nuttall et al. 2018). No estimates of sea urchin abundance were made at Stetson Bank prior to the die off.

Diadema antillarum populations within the EFGB study site remained low during the 2018 monitoring period and were similar to those reported in previous studies (Zimmer et al. 2010; Johnston et al. 2017a, 2017b, 2018b). Populations within the WFGB study site have been consistently higher than EFGB. The previous fluctuations in annual density estimates suggest caution in declaring a recovering *Diadema antillarum* population at FGBNMS; continued monitoring will be required to track and compare temporal changes at both bank study sites.

Lobster densities within EFGB and WFGB study sites have been historically low throughout the monitoring program. Lobsters are, however, occasionally observed by divers at other times, occurring on the banks in low abundance.

Chapter 8. Fish Surveys

A school of horse-eye jack (*Caranx latus*) swim over the reef at East Flower Garden Bank in 2018. Photo: NOAA

Fish Surveys Introduction

Divers conducted stationary reef fish visual census surveys in EFGB and WFGB study sites to examine fish community composition and changes over time. The surveys were used to characterize and compare fish assemblages between bank study sites and years.

Fish Surveys Methods

Fish Surveys Field Methods

Fishes were assessed by divers using modified stationary reef fish visual census surveys based on methods originally described by Bohnsack and Bannerot (1986). Twenty-four randomly located surveys were conducted within study sites at EFGB and WFGB. Each survey represented one sample. Observations of fishes were restricted to an imaginary cylinder with a 7.5 m radius, extending from the substrate to the surface (for more detailed methods, reference Johnston et al. 2017a) (Figure 8.1).

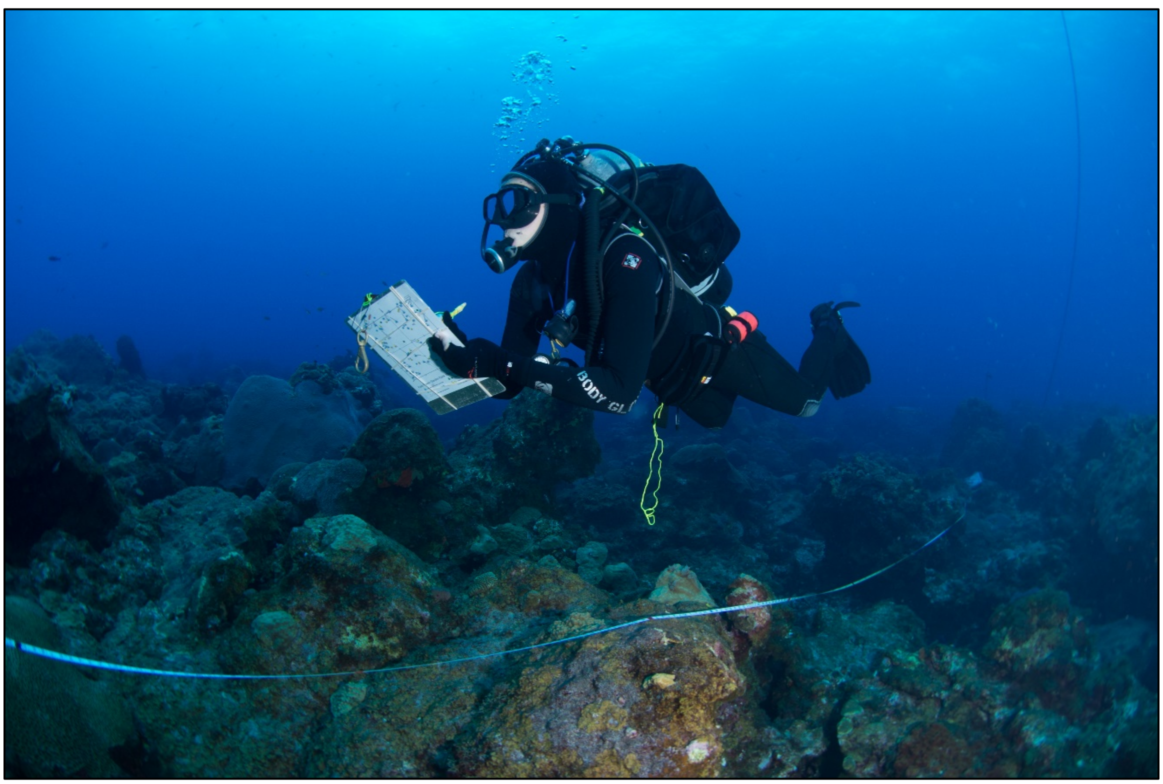

Figure 8.1. NOAA diver conducting a fish survey within the EFGB study site. Photo: G.P. Schmahl/NOAA

All fish species observed within the first five minutes of the survey were recorded while the diver slowly rotated in place in the imaginary survey cylinder. Immediately following this five-minute observation period, one rotation was conducted for each species noted in the original five-minute period to record abundance (number of individuals per species) and fork length (within size bins). Size for each individual was estimated and binned into one of eight groups: <5 cm, ≥5 to <10 cm, ≥10 to <15 cm, ≥15 to <20 cm, ≥20 to <25 cm, ≥25 to <30 cm, ≥30 to <35 cm, and ≥35 cm. If fishes were greater than 35 cm in length, divers estimated size to the nearest cm. Each survey required approximately 15 to 20 minutes to complete. Transitory or schooling species were counted and measured at the time the individuals moved through the cylinder during the initial five-minute period. After the initial five-minute period, additional species were recorded but marked as observed after the official survey period. These observations were excluded from the analysis, unless otherwise stated. Fish surveys began in the early morning (after 0700 CDT), and were repeated throughout the day until dusk (1900 CDT).

Consistency in the survey method was maintained with the use of scientific divers trained to identify fish species located at FGBNMS. Divers were experienced in the survey technique used, equipment checklists were provided in the field to ensure divers had equipment for assigned tasks, and all fish survey divers carried a pre-marked PVC measuring stick to provide a size reference.

Fish Surveys Data Processing

Surveyors reviewed and entered fish survey data in a Microsoft® Excel® database on the same date the survey took place. Fish survey datasheets were retained and reviewed after fieldwork was completed for QA/QC. All datasheets were reviewed and compared to data entered in the database to check for entry errors, and any mistakes were corrected prior to data processing. For each entry, fish family, trophic guild, and biomass were automatically recorded in the database (Bohnsack and Harper 1988; Froese and Pauly 2018). Species were classified into four major trophic guild categories: herbivores (H), piscivores (P), invertivores (I), and planktivores (PL).

Fish Surveys Statistical Analysis

Summary statistics of fish census data included abundance, density, sighting frequency, and species richness. Total abundance was calculated as the number of individuals per sample, and percent relative abundance was the total number of individuals for one species divided by the total of all species and multiplied by 100. Density was expressed as the number of individual fish per 100 m^2 ± standard error, and calculated as the total number of individuals per sample by the area of the survey cylinder (176.7 m^2) and multiplied by 100. Sighting frequency for each species was expressed as the percentage of the total number of samples in which the species was recorded. Mean species richness was the average number of species represented per sample ± standard error.

Fish biomass was expressed as grams per 100 m^2 ± standard error and computed by converting length data to weights using the allometric length-weight conversion formula (Bohnsack and Harper 1988) based on information provided by FishBase (Froese and Pauly 2018). As sizes less than 35 cm were binned, the median size in each size bin was used to calculate biomass (for example, fish in the ≥5 to <10 cm size bin were assigned the fork length of 7.5 cm). Observations of manta rays and stingrays were removed from biomass analyses only, due to their rare nature and large size.

For family analysis, percent coefficient of variation (CV%) was calculated to determine the power of the analyses. CV% was calculated using the following formula:

$$CV\% = SE/\bar{\bar{X}}$$

where SE = standard error and $\bar{\bar{X}}$ = population mean. A CV% of 20% or lower is optimal, as it would be able to statistically detect a minimum change of 40% in the population within the survey period.

Statistical analyses were conducted on square root transformed density and biomass data (reducing the influence of large schooling species on analyses) using distance-based Bray-Curtis similarity matrices with Primer® version 7.0 (Anderson et al. 2008; Clarke et al. 2014). Significant differences in the fish community based on species level resemblance matrices were investigated using PERMANOVA (Anderson et al. 2008). If significant differences were found, species contributing to observed differences were examined using SIMPER to assess the percent contribution of species to dissimilarity between study sites (Clarke et al. 2014). Differences at the family level for key species were compared for significant dissimilarities using ANOSIM. For long-term density and biomass trends for which data were available (2011 to 2018), the distance between centroids was calculated from Bray-Curtis similarity matrices and visualized using metric multi-dimensional scaling (MDS) plots with a time series trajectory overlay split between locations (Anderson et al. 2008).

Dominance plots were generated based on species abundance and biomass with Primer® version 7.0 (Anderson et al. 2008; Clarke et al. 2014). W-values (difference between the biomass and abundance curves) were calculated for each survey (Clarke 1990). W-values range between $-1<w>1$, where w=1 indicates that the population is dominated by a few large species, w=-1 indicates that the population is dominated by numerous small species, and w=0 indicates that accumulated biomass is evenly distributed between large and small species. Significant dissimilarities in w-values between bank study sites was tested using ANOSIM on untransformed data with Euclidean distance similarity matrices (Clarke et al. 2014).

Fish Surveys Results

A total of 29 families and 70 species (66 at EFGB and 58 at WFGB) were recorded in 2018 for all samples combined from EFGB and WFGB study sites. Mean species richness was 21.75 ± 0.65 per survey within the EFGB study site and 22.75 ± 0.57 per survey within the WFGB study site. Bonnetmouth (*Emmelichthyops atlanticus*) had the highest relative abundance of all species (72%) within the EFGB study site, followed by bluehead (*Thalassoma bifasciatum)* (7%), creole wrasse (*Clepticus parrae*) (4%), and brown chromis (*Chromis multilineata*) (3%) (Figure 8.2). It should be noted that bonnetmouth are an ephemeral species, but large transient schools have been documented in surveys at both banks in recent years (Johnston et al. 2017b, 2018b).

Within the WFGB study site, bonnetmouth had the highest relative abundance of all species (74%), followed by bluehead (10%), creole wrasse (3%), and brown chromis (3%) (Figure 8.2).

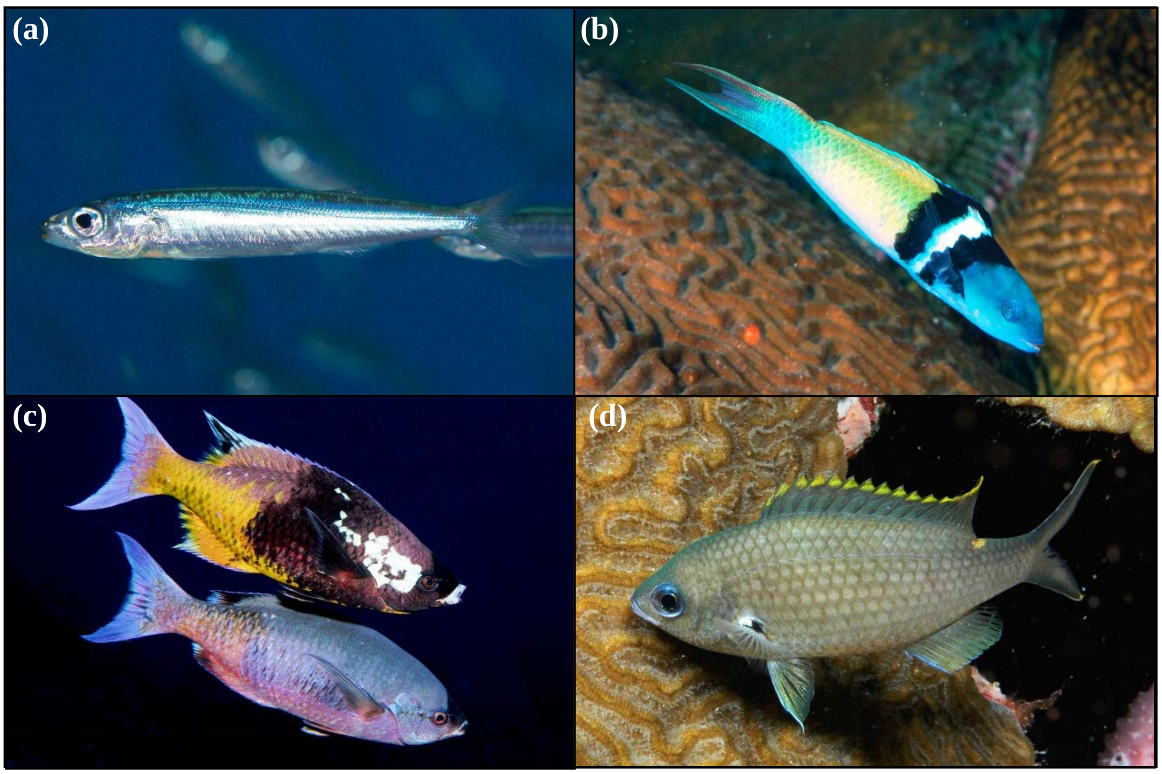

Figure 8.2. Most abundant fish species observed within EFGB and WFGB study sites in 2018: (a) bonnetmouth, (b) bluehead, (c) creole wrasse, and (d) brown chromis. Photos: (a) Carlos Estapé; (b, c, and d) G.P. Schmahl/NOAA

Sighting Frequency and Occurrence

The most frequently sighted species within study sites at both banks was bluehead, observed in 96% of surveys at EFGB and 100% of surveys at WFGB. Other frequently sighted species included blue tang (*Acanthurus coeruleus*), sharpnose puffer (*Canthigaster rostrate*), and bicolor damselfish (*Stegastes partitus*) (Table 8.1). Most shark and ray species are considered “rare,” typically occurring in <20% of all surveys (REEF 2014); however, no shark species or manta rays (*Manta* spp.) were observed in surveys.

Table 8.1. Top 15 most frequently sighted species within surveys in EFGB and WFGB study sites, including sighting frequency for all surveys combined in 2018.

Family Name: Species Name (Common Name)	EFGB	WFGB	All Surveys
Labridae: *Thalassoma bifasciatum* (bluehead)	95.83	100.00	97.92
Acanthuridae: *Acanthurus coeruleus* (blue tang)	79.17	91.67	85.42
Tetraodontidae: *Canthigaster rostrata* (sharpnose puffer)	79.17	91.67	85.42
Pomacentridae: *Stegastes partitus* (bicolor damselfish)	75.00	91.67	83.33
Labridae: *Bodianus rufus* (Spanish hogfish)	75.00	91.67	83.33
Pomacentridae*: Chromis multilineata* (brown chromis)	75.00	87.50	81.25
Pomacentridae*: Chromis cyanea* (blue chromis)	75.00	79.17	77.08
Labridae: *Sparisoma viride* (stoplight parrotfish)	75.00	79.17	77.08
Balistidae: *Melichthys niger* (black durgon)	75.00	70.83	72.92
Labridae: *Clepticus parrae* (creole wrasse)	70.83	75.00	72.92
Labridae: *Scarus vetula* (queen parrotfish)	45.83	91.67	68.75
Pomacentridae*: Stegastes planifrons* (threespot damselfish)	50.00	87.50	68.75
Pomacentridae*: Stegastes variabilis* (cocoa damselfish)	54.17	75.00	64.58
Epinephelidae: *Cephalopholis cruentata* (graysby)	58.33	70.83	64.58
Epinephelidae: *Paranthias furcifer* (Atlantic creolefish)	75.00	45.83	60.42

Density

Mean fish density (individuals/100 m²) ± standard error was 564.68 ± 126.94 within the EFGB study site and 471.87 ± 146.38 within the WFGB study site. PERMANOVA analysis revealed fish density was significantly greater within the EFGB study site (Table 8.2). SIMPER analysis identified the main contributors resulting in differences between study sites was due to a greater abundance of bonnetmouth (25.81%) at EFGB (Table 8.3).

Table 8.2. PERMANOVA results comparing mean fish density between EFGB and WFGB study sites from 2018. Bold text denotes significant value.

Source	Sum of Squares	df	Pseudo-F	P (perm)
Bank Study Site	5460	1	3.95	**0.001**
Res	63604	46		
Total	69065	47		

Table 8.3. Mean density (individuals/100 m^2) ± SE of the top 15 highest density species from EFGB and WFGB study site surveys, and all surveys combined, in 2018.

Family Name: Species Name (Common Name)	EFGB	WFGB	All Surveys
Haemulidae: *Emmelichthyops atlanticus* (bonnetmouth)	405.75 ± 120.78	349.46 ± 146.75	377.61 ± 94.11
Labridae: *Thalassoma bifasciatum* (bluehead)	39.45 ± 11.88	45.30 ± 4.30	42.37 ± 6.26
Labridae: *Clepticus parrae* (creole wrasse)	24.55 ± 9.30	16.51 ± 3.62	20.53 ± 4.97
Pomacentridae: *Chromis multilineata* (brown chromis)	22.43 ± 4.86	16.36 ± 3.39	19.39 ± 2.96
Epinephelidae: *Paranthias furcifer* (Atlantic creolefish)	13.30 ± 4.18	0.99 ± 0.59	7.14 ± 2.27
Pomacentridae: *Chromis cyanea* (blue chromis)	6.27 ± 1.44	7.50 ± 1.33	6.89 ± 0.97
Pomacentridae: *Stegastes partitus* (bicolor damselfish)	5.59 ± 1.26	3.77 ± 0.52	4.68 ± 0.68
Tetraodontidae: *Canthigaster rostrata* (sharpnose puffer)	4.03 ± 1.98	2.92 ± 0.30	3.48 ± 1.00
Pomacentridae: *Stegastes planifrons* (threespot damselfish)	2.00 ± 0.56	4.62 ± 0.58	3.31 ± 0.44
Labridae: *Scarus taeniopterus* (princess parrotfish)	6.06 ± 2.28	0.52 ± 0.21	3.29 ± 1.20
Labridae: *Bodianus rufus* (Spanish hogfish)	3.25 ± 1.19	1.86 ± 0.23	2.56 ± 0.61
Kyphosidae: *Kyphosus saltatrix/incisor* (Bermuda chub)	4.39 ± 3.28	0.54 ± 0.18	2.46 ± 1.65
Pomacentridae: *Stegastes variabilis* (cocoa damselfish)	2.38 ± 1.03	1.74 ± 0.27	2.06 ± 0.53
Labridae: *Sparisoma viride* (stoplight parrotfish)	2.38 ± 0.69	1.65 ± 0.27	2.02 ± 0.37
Labridae: *Scarus vetula* (queen parrotfish)	1.70 ± 0.61	1.96 ± 0.21	1.83 ± 0.32

Trophic Guild Analysis

Species were grouped by trophic guild into four major categories, as defined by NOAA's Center for Coastal Monitoring and Assessment Biogeography Branch fish trophic level database: herbivores, piscivores, invertivores, and planktivores (Caldow et al. 2009). Size-frequency distributions using relative abundance were graphed for each trophic guild (Figure 8.3).

Piscivore was the predominant trophic guild within the EFGB study site. Piscivores were primarily either small (<5 to <15 cm) or large individuals (≥35 cm). Herbivore size distribution was variable within the EFGB study site, with a slight trend toward larger individuals (≥20 to <35 cm). Invertivores were primarily smaller individuals (<5 cm to <15 cm). The majority of planktivores were of moderate size (≥15 to <35 cm) within the EFGB study site (Figure 8.3).

Piscivore was the predominant trophic guild within the WFGB study site. Piscivores were primarily either small (<5) or large individuals (>30 cm). Planktivore size distribution was variable within the WFGB study site, with a trend toward moderate to smaller individuals (<5 to <25 cm). Invertivores were primarily small to medium size individuals (<5 cm to <30 cm). Herbivore size distribution was variable within the WFGB study site, with a slight trend toward small to moderate size individuals (≥5 to <35 cm) (Figure 8.3).

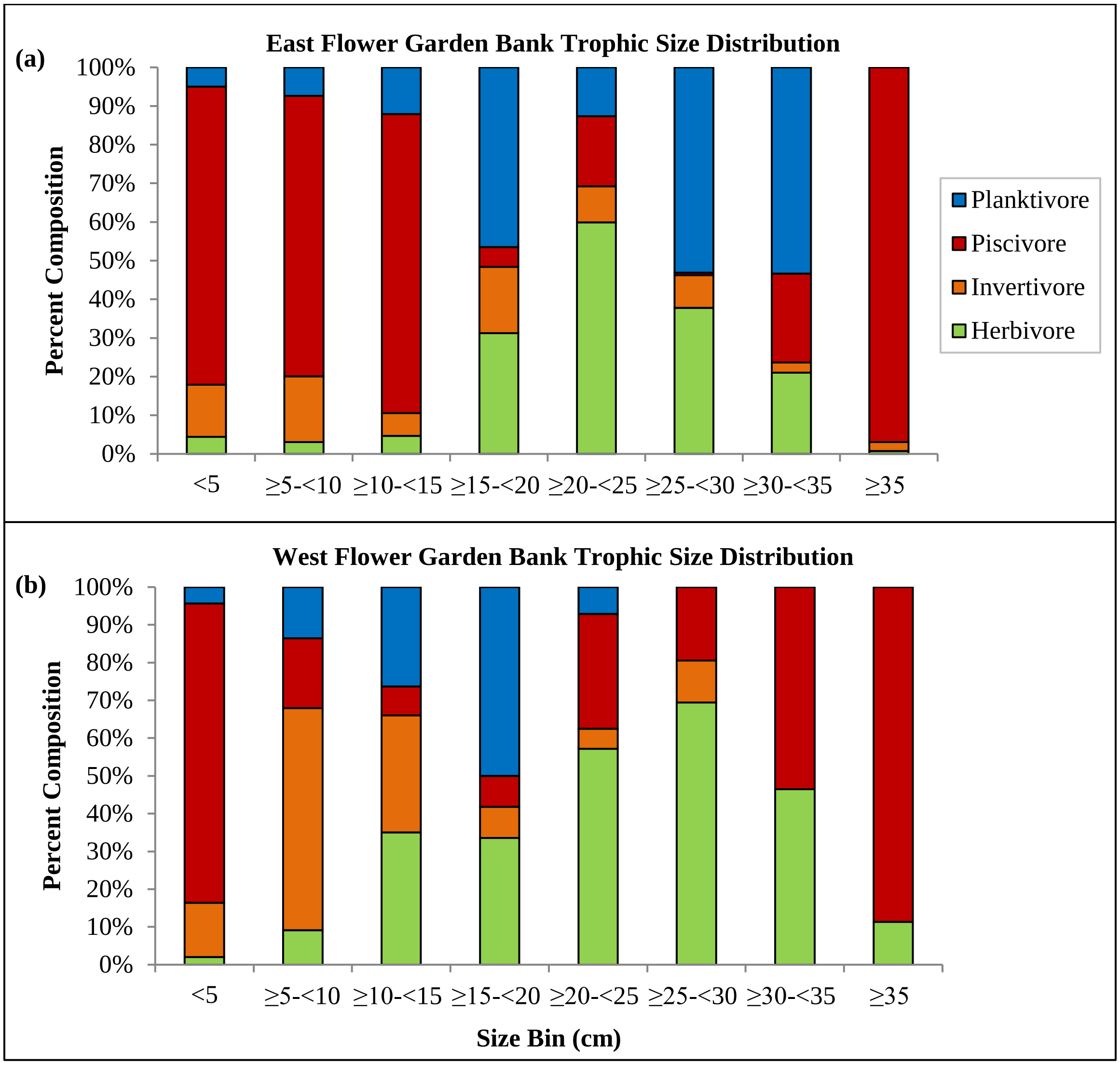

Figure 8.3. Fish survey size distribution by trophic guild within (a) EFGB and (b) WFGB study sites in 2018.

Biomass

Mean biomass (g/100 m^2) ± standard error was 60,160.96 ± 45,822.84 within the EFGB study site and 7,104.07 ± 1,508.24 within the WFGB study site in 2018. PERMANOVA analysis revealed that fish biomass was significantly greater within the EFGB study site (Table 8.4). SIMPER analysis identified the main contributors resulting in higher fish biomass within the EFGB study site was greater local abundance of great barracuda (*Sphyraena barracuda*) (11.32%) and horse-eye jack (*Caranx latus*) (9.98%).

Table 8.4. PERMANOVA results comparing mean fish biomass between EFGB and WFGB study sites from 2018. Bold text denotes significant value.

Source	Sum of Squares	df	Pseudo-F	P (perm)
Bank Study Site	9237	1	4.06	**0.001**
Res	104710	46		
Total	113950	47		

When classified by trophic guild, piscivores had the highest mean biomass and invertivores had the lowest mean biomass across all surveys (Table 8.5). PERMANOVA analysis revealed significant differences in trophic guilds between study sites (Table 8.6). SIMPER analysis identified the main difference as greater local abundance of piscivores (46.97%) in the EFGB study site (Table 8.5).

Table 8.5. Mean biomass (g/100 m^2) ± SE for each trophic guild from EFGB and WFGB study site surveys, and all surveys combined in 2018.

Trophic Group	EFGB	WFGB	All Surveys
Herbivore	3,592.25 ± 733.26	1,704.34 ± 347.90	2,648.29 ± 540.58
Invertivore	931.35 ± 190.11	293.09 ± 59.83	612.22 ± 124.97
Planktivore	3,667.20 ± 748.56	334.83 ± 68.35	2,001.02 ± 408.46
Piscivore	51,970.17 ± 10608.37	4,771.81 ± 974.04	28,370.99 ± 5791.20

Table 8.6. PERMANOVA results comparing trophic guild biomass between EFGB and WFGB study sites from 2018. Bold text denotes significant value.

Source	Sum of Squares	df	Pseudo-F	P (perm)
Bank Study Site	2747	1	2.96	**0.03**
Res	42684	46		
Total	45431	47		

Overall, piscivores at the study sites represented approximately 84% of biomass, followed by herbivores (8%), planktivores (6%) and invertivores (2%) for both study sites combined.

Within each trophic guild, mean biomass for each species was calculated (Table 8.7). For the herbivore guild, 33% of the biomass was contributed by Bermuda chub (*Kyphosus saltatrix/incisor*). For the invertivore guild, the greatest contribution was from Spanish hogfish (*Bodianus rufus*) (16% of guild biomass). For the piscivore guild, horse-eye jack contributed the greatest biomass to all surveys, at 85%. For the planktivore guild, the greatest contribution was from Atlantic creolefish (*Paranthias furcifer*) (74% of guild biomass).

Table 8.7. Biomass (g/100 m^2) ± SE of each species, grouped by trophic guild from EFGB and WFGB study site surveys, and all surveys combined, in 2018.

	Family Name: Species Name - Common Name	**EFGB**	**WFGB**	**All Surveys**
Herbivore	Kyphosidae: *Kyphosus saltatrix/incisor* (Bermuda chub)	1699.13 ± 1204.00	92.59 ± 41.16	895.86 ± 607.32
	Labridae: *Sparisoma viride* (stoplight parrotfish)	339.62 ± 141.70	623.36 ± 147.68	481.49 ± 103.33
	Balistidae: *Melichthys niger* (black durgon)	592.68 ± 200.66	293.34 ± 79.08	443.01 ± 108.90
	Labridae: *Scarus vetula* (queen parrotfish)	173.47 ± 69.99	353.25 ± 61.79	263.36 ± 48.01
	Labridae: *Scarus taeniopterus* (princess parrotfish)	391.31 ± 192.74	49.98 ± 24.86	220.65 ± 99.30
	Acanthuridae: *Acanthurus coeruleus* (blue tang)	181.43 ± 58.48	129.27 ± 19.31	155.35 ± 30.70
	Labridae: *Sparisoma aurofrenatum* (redband parrotfish)	53.33 ± 21.77	93.29 ± 29.03	73.31 ± 18.19
	Labridae: *Scarus iseri* (striped parrotfish)	79.75 ± 79.75	0.11 ± 0.05	39.93 ± 39.87
	Acanthuridae: *Acanthurus chirurgus* (doctorfish)	11.13 ± 6.56	45.17 ± 15.78	28.15 ± 8.81
	Acanthuridae: *Acanthurus tractus* (ocean surgeonfish)	33.72 ± 16.42	4.31 ± 2.54	19.01 ± 8.49
	Pomacentridae: *Microspathodon chrysurus* (yellowtail damselfish)	15.81 ± 5.93	10.94 ± 3.09	13.37 ± 3.32
	Pomacentridae: *Stegastes variabilis* (cocoa damselfish)	9.15 ± 3.93	2.75 ± 1.05	5.95 ± 2.07
	Pomacentridae: *Stegastes partitus* (bicolor damselfish)	8.97 ± 4.37	1.95 ± 0.81	5.46 ± 2.26
	Pomacentridae: *Stegastes adustus* (dusky damselfish)	0.50 ± 0.35	3.96 ± 1.61	2.23 ± 0.85
	Pomacentridae: *Stegastes diencaeus* (longfin damselfish)	1.22 ± 1.22	0.00	0.61 ± 0.61
	Blenniidae: *Ophioblennius macclurei* (redlip blenny)	0.56 ± 0.25	0.06 ± 0.03	0.31 ± 0.13
	Labridae: *Sparisoma atomarium* (greenblotch parrotfish)	0.44 ± 0.22	0.00	0.22 ± 0.11
	Gobiidae: *Gnatholepis thompsoni* (goldspot goby)	0.03 ± 0.01	0.01 ± 0.01	0.02 ± 0.01
Invertivore	Labridae: *Bodianus rufus* (Spanish hogfish)	141.44 ± 57.40	51.49 ± 12.60	96.46 ± 29.80
	Mullidae: *Mulloidichthys martinicus* (yellow goatfish)	162.42 ± 126.72	23.80 ± 10.93	93.11 ± 63.72
	Labridae: *Thalassoma bifasciatum* (bluehead)	113.22 ± 63.72	15.92 ± 4.56	64.57 ± 32.39
	Lutjanidae: *Lutjanus griseus* (gray snapper)	99.55 ± 80.11	0.00	49.77 ± 40.29
	Balistidae: *Canthidermis sufflamen* (ocean triggerfish)	65.50 ± 65.50	31.93 ± 23.38	48.71 ± 34.49

Invertivore	Pomacanthidae: *Holacanthus ciliaris* (queen angelfish)	57.29 ± 28.71	13.26 ± 13.26	35.27 ± 15.97
	Balistidae: *Balistes vetula* (queen triggerfish)	58.78 ± 58.78	0.00	29.39 ± 29.39
	Pomacanthidae: *Holacanthus tricolor* (rock beauty)	23.33 ± 11.85	31.17 ± 9.43	27.25 ± 7.51
	Pomacentridae: *Stegastes planifrons* (threespot damselfish)	9.42 ± 3.63	37.67 ± 7.50	23.55 ± 4.61
	Chaetodontidae: *Chaetodon sedentarius* (reef butterflyfish)	21.22 ± 6.16	23.57 ± 7.11	22.39 ± 4.66
	Epinephelidae: *Epinephelus adscensionis* (rock hind)	38.69 ± 21.02	0.00	19.35 ± 10.78
	Chaetodontidae: *Chaetodon ocellatus* (spotfin butterflyfish)	29.42 ± 15.03	5.63 ± 3.89	17.52 ± 7.87
	Ostraciidae: *Lactophrys triqueter* (smooth trunkfish)	18.97 ± 7.71	13.31 ± 6.08	16.14 ± 4.87
	Pomacentridae: *Abudefduf saxatilis* (sergeant major)	26.12 ± 14.73	2.35 ± 1.23	14.24 ± 7.52
	Pomacentridae: *Chromis multilineata* (brown chromis)	13.10 ± 4.04	12.00 ± 3.17	12.55 ± 2.54
	Labridae: *Halichoeres garnoti* (yellowhead wrasse)	6.91 ± 3.04	12.22 ± 4.33	9.57 ± 2.64
	Pomacanthidae: *Holacanthus bermudensis* (blue angelfish)	11.20 ± 11.20	0.00	5.60 ± 5.60
	Epinephelidae: *Cephalopholis fulva* (coney)	8.71 ± 8.53	0.00	4.35 ± 4.27
	Epinephelidae: *Epinephelus guttatus* (red hind)	8.07 ± 6.17	0.00	4.03 ± 3.11
	Chaetodontidae: *Prognathodes aculeatus* (longsnout butterflyfish)	4.86 ± 3.08	0.68 ± 0.61	2.77 ± 1.58
	Diodontidae: *Diodon holocanthus* (balloonfish)	2.77 ± 2.77	2.77 ± 2.77	2.77 ± 1.94
	Labridae: *Halichoeres maculipinna* (clown wrasse)	3.31 ± 1.93	1.53 ± 1.09	2.42 ± 1.11
	Holocentridae: *Holocentrus adscensionis* (squirrelfish)	1.92 ± 1.92	2.63 ± 2.63	2.27 ± 1.61
	Ostraciidae: *Lactophrys bicaudalis* (spotted trunkfish)	0.00	3.72 ± 3.72	1.86 ± 1.86
	Tetraodontidae: *Canthigaster rostrata* (sharpnose puffer)	1.63 ± 0.64	1.31 ± 0.29	1.47 ± 0.35
	Labridae: *Halichoeres radiatus* (puddingwife)	0.67 ± 0.66	2.14 ± 1.99	1.40 ± 1.04
	Chaetodontidae: *Chaetodon striatus* (banded butterflyfish)	0.00	2.68 ± 2.24	1.34 ± 1.12
	Monacanthidae: *Cantherhines macrocerus* (whitespotted filefish)	2.43 ± 1.50	0.00	1.21 ± 0.76
	Monacanthidae: *Cantherhines pullus* (orangespotted filefish)	0.00	1.32 ± 1.07	0.66 ± 0.54
	Pomacentridae: *Stegastes leucostictus* (beaugregory)	0.27 ± 0.24	0.00	0.14 ± 0.12
	Gobiidae: *Elacatinus oceanops* (neon goby)	0.09 ± 0.02	0.00 ± 0.00	0.05 ± 0.01

	Cirrhitidae: *Amblycirrhitus pinos* (redspotted hawkfish)	0.06 ± 0.06	0.00	0.03 ± 0.03
	Sciaenidae: *Equetus punctatus* (spotted drum)	0.00	0.00 ± 0.00	0.00 ± 0.00
Piscivore	Carangidae: *Caranx latus* (horse-eye jack)	45977.08 ± 45784.99	2361.49 ± 1507.95	24169.28 ± 22882.11
	Sphyraenidae: *Sphyraena barracuda* (great barracuda)	2648.99 ± 1087.32	1617.84 ± 498.41	2133.42 ± 596.42
	Haemulidae: *Emmelichthyops atlanticus* (bonnetmouth)	1799.23 ± 1127.84	85.06 ± 29.87	942.15 ± 571.92
	Carangidae: *Caranx lugubris* (black jack)	1041.58 ± 906.62	11.34 ± 11.34	526.46 ± 454.75
	Lutjanidae: *Lutjanus jocu* (dog snapper)	39.11 ± 39.11	483.61 ± 286.27	261.36 ± 146.55
	Carangidae: *Caranx ruber* (bar jack)	232.35 ± 120.00	15.83 ± 6.28	124.09 ± 61.50
	Epinephelidae: *Cephalopholis cruentata* (graysby)	46.03 ± 15.49	92.32 ± 18.88	69.17 ± 12.54
	Epinephelidae: *Mycteroperca interstitialis* (yellowmouth grouper)	93.11 ± 47.27	0.33 ± 0.23	46.72 ± 24.34
	Serranidae: *Mycteroperca tigris* (tiger grouper)	7.34 ± 5.07	81.74 ± 62.70	44.54 ± 31.59
	Scorpaenidae: *Pterois volitans* (lionfish)	60.52 ± 30.86	20.23 ± 12.71	40.37 ± 16.77
	Muraenidae: *Gymnothorax moringa* (spotted moray)	24.13 ± 24.13	0.00	12.06 ± 12.06
	Aulostomidae: *Aulostomus maculatus* (Atlantic trumpetfish)	0.71 ± 0.71	2.03 ± 2.03	1.37 ± 1.07
Planktivore	Epinephelidae: *Paranthias furcifer* (Atlantic creolefish)	2879.75 ± 1569.87	73.62 ± 48.56	1476.68 ± 803.42
	Labridae: *Clepticus parrae* (creole wrasse)	782.86 ± 362.50	257.61 ± 104.39	520.24 ± 190.49
	Pomacentridae: *Chromis cyanea* (blue chromis)	4.14 ± 2.84	2.52 ± 0.73	3.33 ± 1.45
	Pomacentridae: *Chromis insolata* (sunshinefish)	0.01 ± 0.01	0.71 ± 0.45	0.36 ± 0.23
	Opistognathidae: *Opistognathus aurifrons* (yellowhead jawfish)	0.27 ± 0.27	0.27 ± 0.20	0.27 ± 0.17
	Pomacentridae: *Chromis scotti* (purple reeffish)	0.09 ± 0.07	0.04 ± 0.02	0.07 ± 0.04
	Pomacentridae: *Neopomacentrus cyanomos* (regal demoiselle)	0.06 ± 0.04	0.05 ± 0.03	0.06 ± 0.02

Abundance-Biomass Curves

Mean w-values for the EFGB study site were 0.04 ± 0.01 and mean w-values for the WFGB study site were 0.06 ± 0.01. For all samples within each study site, mean w-values remained close to 0, indicating a balanced community where biomass was spread uniformly between large and small species (Figure 8.4). ANOSIM comparisons of w-values between bank study sites revealed no significant dissimilarities between the dominance plot w-values.

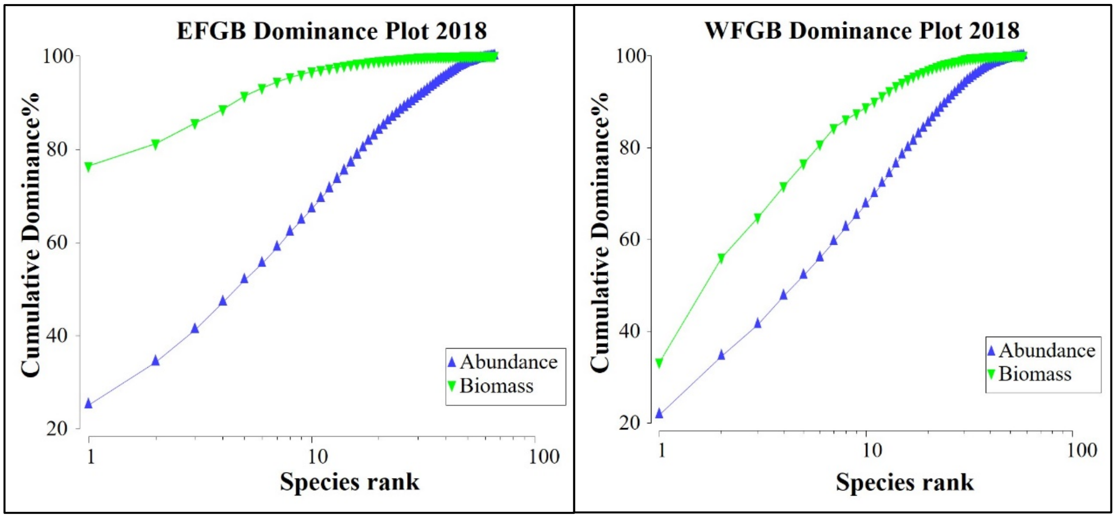

Figure 8.4. Abundance-Biomass curves for EFGB and WFGB study sites in 2018.

Family Level Analysis

Due to particular interest in grouper and snapper families related to fishing and parrotfish due to their role as important herbivores, additional analyses were conducted on these fish families to determine size frequency distributions from 2018 surveys. Further analyses were also conducted for invasive species, including lionfish (*Pterois volitans*) and regal demoiselle (*Neopomacentrus cyanomos*).

Grouper species documented at EFGB and WFGB include nine species from the *Mycteroperca*, *Cephalopholis* and *Epinephelus* genera: graysby (*Cephalopholis cruentata*), coney (*Cephalopholis fulva*), rock hind (*Epinephelus adscensionis*), red hind (*Epinephelus guttatus*), black grouper (*Mycteroperca bonaci*), yellowmouth grouper (*Mycteroperca interstitialis*), yellowfin grouper (*Mycteroperca venenosa*), scamp (*Mycteroperca phenax*), and tiger grouper (*Mycteroperca tigris*). In 2018, six species were observed in all surveys combined: coney, graysby, red hind, rock hind, tiger grouper, and yellowmouth grouper. It should be noted that coefficient of variation percentages (12.89% for density, 22.90% for biomass) indicated that the density and biomass data collected in 2018 had relatively good power to detect population changes.

ANOSIM results indicated significant spatial variation in grouper community composition between EFGB and WFGB study sites based on density (*Global R*=0.05, *p*=0.025) and biomass (*Global R*=0.06, *p*=0.018). The observed dissimilarity between study sites was mainly attributable to graysby for density (55.61%) and biomass (52.83%), as the WFGB study site had greater overall density and biomass of graysby. Mean biomass of small-bodied grouper, including coney, graysby, red hind, and rock hind was 101.50 ± 34.89 in the EFGB study site and 92.32 ± 18.88 in the WFGB study site. Mean biomass of large-bodied grouper, including tiger grouper and yellowmouth grouper was 100.45 ± 48.07 within the EFGB study site and 82.07 ± 62.85 within the WFGB study site. Size distributions of observed grouper in 2018 varied by species (Figure 8.5).

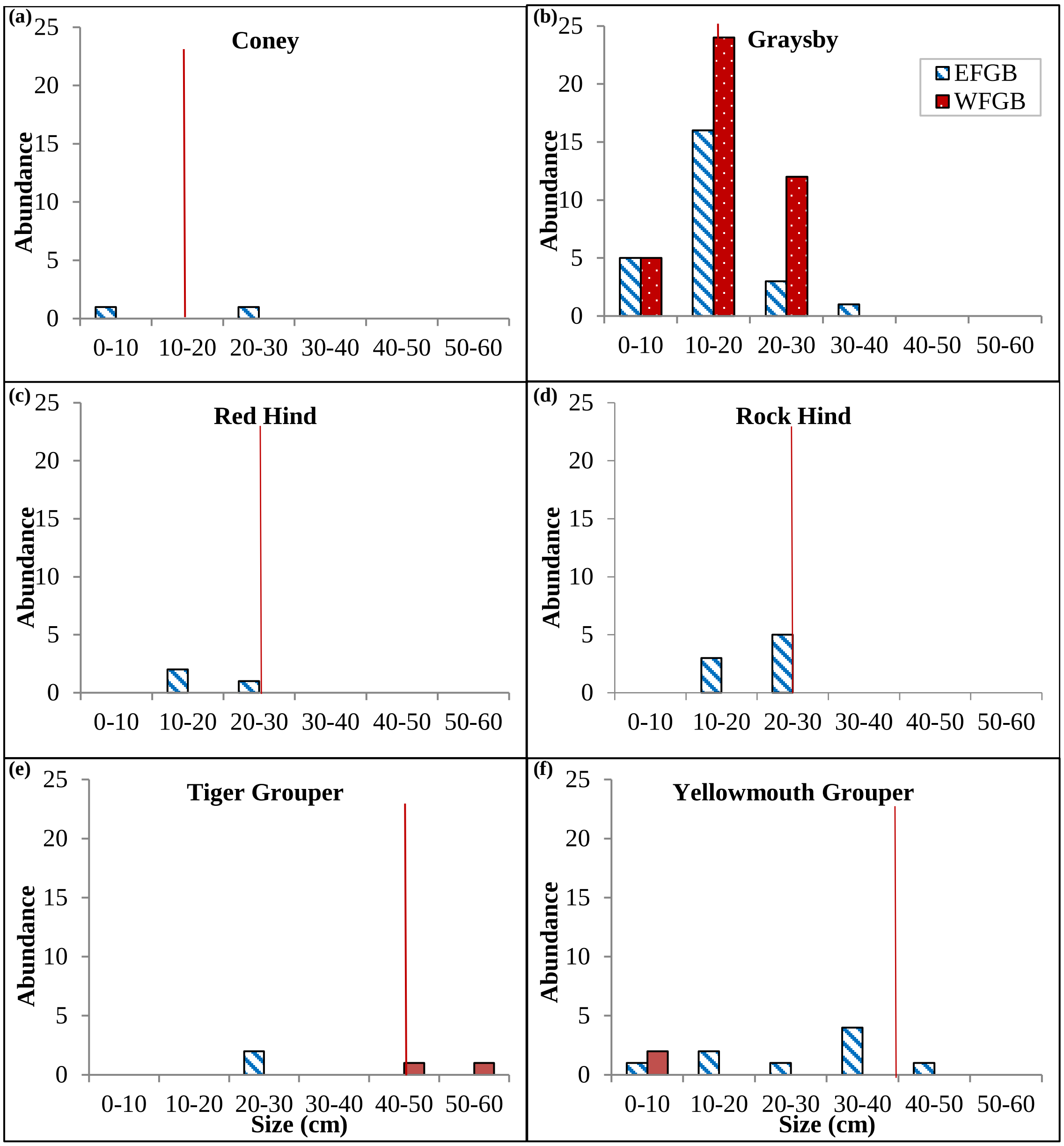

Figure 8.5. Size frequency of grouper species within EFGB and WFGB study site surveys in 2018: (a) coney, (b) graysby, (c) red hind, (d) rock hind, (e) tiger grouper, and (e) yellowmouth grouper. Vertical solid red lines represent estimated size of female maturity (Froese and Pauly 2018).

The snapper family comprised two species from the *Lutjanidae* genus: gray snapper (*Lutjanus griseus*) and dog snapper (*Lutjanus jocu*). Coefficient of variation percentages (44.96% for density, 48.26% for biomass) indicated that the data collected in 2018 had poor power to detect population differences due to the low number of snapper observed. Mean snapper biomass was 138.65 ± 87.23 within the EFGB study site and 483.61 ± 286.27 within the WFGB study site. Dog snapper size distributions were dominated by larger individuals that were reproductively mature, while gray snapper were all reproductively immature individuals (Figure 8.6). No statistical analysis was completed on snapper biomass or density due to the low number of snapper observed in surveys.

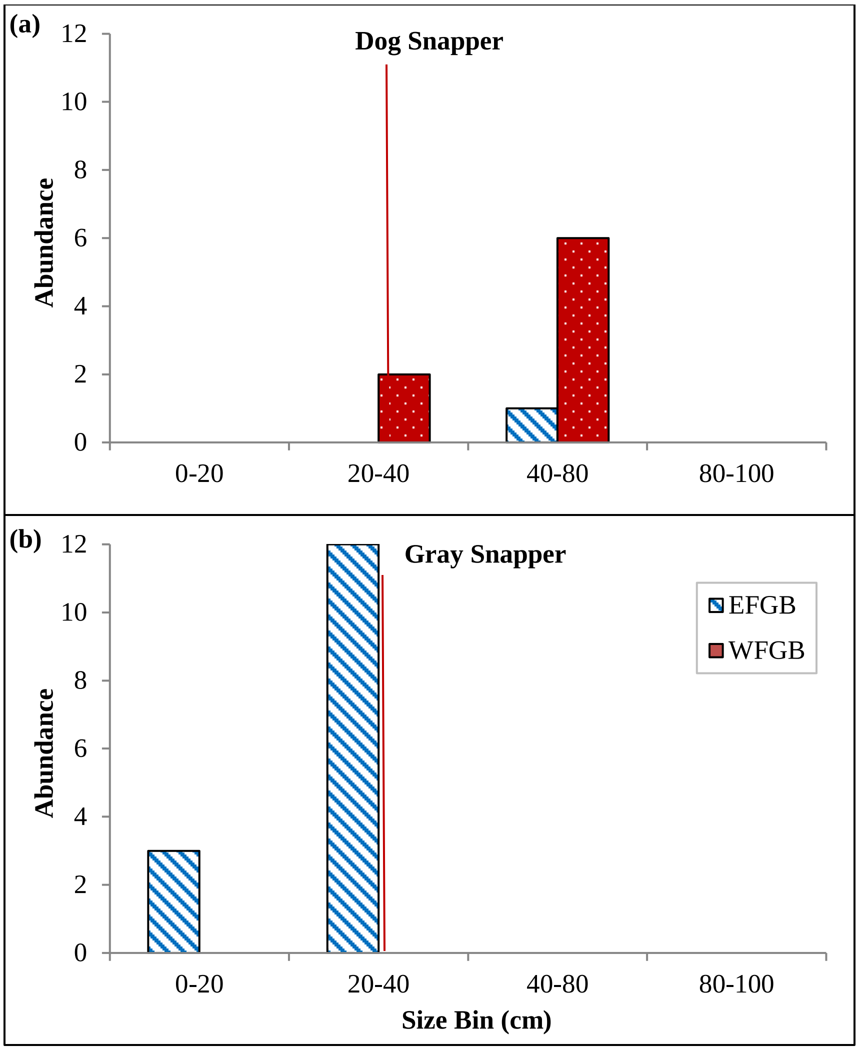

Figure 8.6. Size frequency of snapper species observed within EFGB and WFGB study site surveys in 2018: (a) gray snapper and (b) dog snapper. Vertical solid red lines represent estimated size of female maturity (Froese and Pauly 2018).

Parrotfishes are important herbivores on coral reefs because they are effective grazers (Jackson et al. 2014). Common parrotfish found at the EFGB and WFGB included six species: striped parrotfish (*Scarus iseri*), princess parrotfish (*Scarus taeniopterus*), queen parrotfish (*Scarus vetula*), greenblotch parrotfish (*Sparisoma atomarium*), redband parrotfish (*Sparisoma aurofrenatum*), and stoplight parrotfish (*Sparisoma viride*). Coefficient of variation percentages (18.86% for density and 14.41% for biomass) indicated that the data had good power to detect population differences.

Mean biomass of parrotfishes was 1,037.92 ± 258.06 within the EFGB study site and 1,120.00 ± 178.12 within the WFGB study site. The parrotfish population at both EFGB and WFGB study sites had wide size distributions, but were dominated by smaller individuals (<20 cm) (Figure 8.7). ANOSIM results indicated significant spatial variation in parrotfish community composition between EFGB and WFGB study sites based on density (*Global R*=0.29, *p*=0.001) and biomass (*Global R*=0.17, *p*=0.001). The observed dissimilarity in density between study sites was mainly attributable to princess parrotfish (26.69%), as the EFGB study site had greater overall density of princess parrotfish. The observed dissimilarity in biomass between study sites was mainly attributable to stoplight parrotfish (32.42%), as stoplight parrotfish biomass was greater at EFGB.

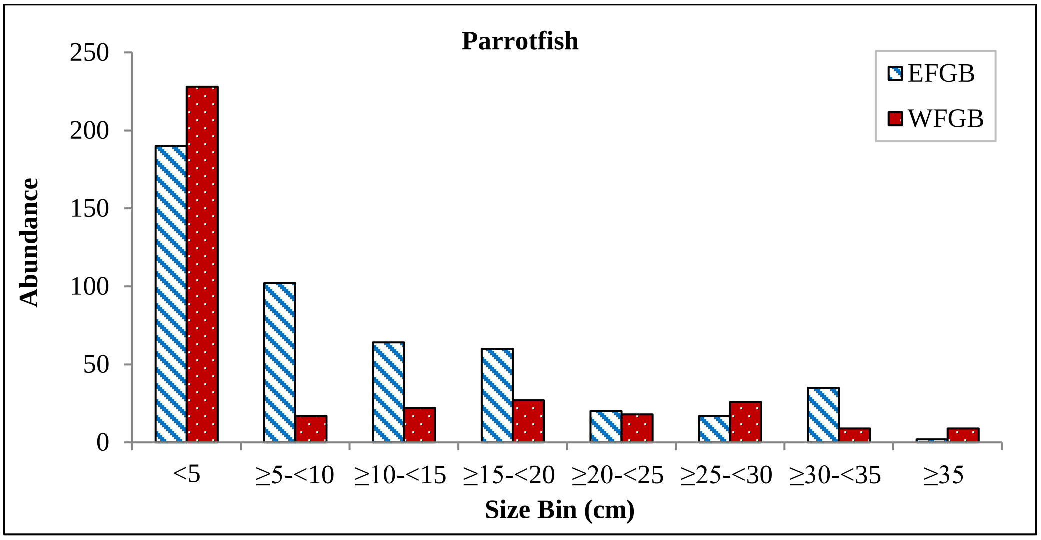

Figure 8.7. Size frequency of parrotfishes within EFGB and WFGB study site surveys in 2018.

Lionfish

This reporting year marks the sixth consecutive documentation of lionfish (*Pterois volitans*), an invasive species native to the Indo-Pacific, in long-term monitoring study site surveys. Total abundance was 11 individual lionfish within the EFGB study site surveys and seven lionfish in the WFGB study site surveys (sighting frequency 25% and 17%, respectively). Since the initial documentation of lionfish in the long-term monitoring dataset, overall abundance increased from 2013 to 2014, but decreased in

2016 and 2017, and then increased in 2018 (Figure 8.8). Lionfish size distributions were dominated by moderate and large sized individuals (15 to 35cm) (Figure 8.9).

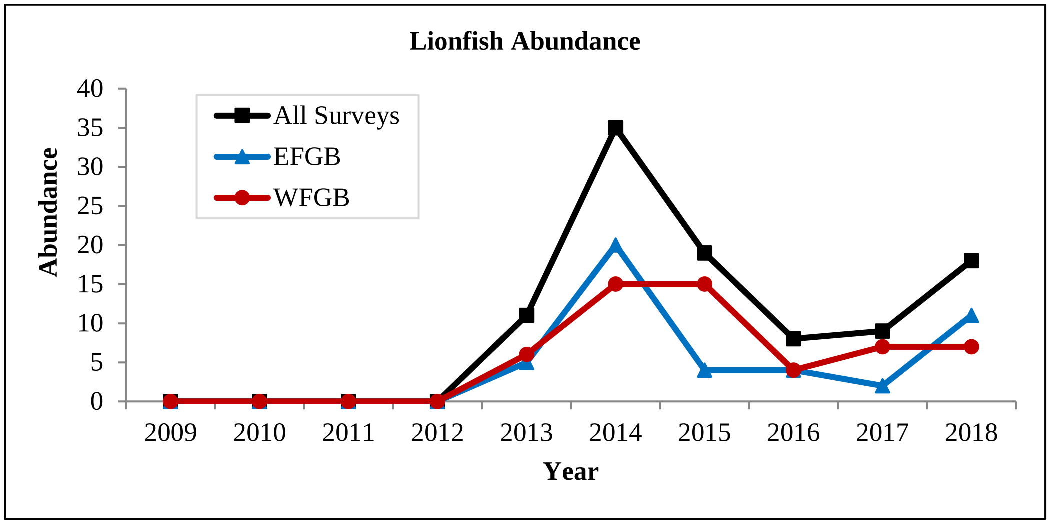

Figure 8.8. Lionfish abundance within EFGB and WFGB study site surveys from 2012 to 2018.

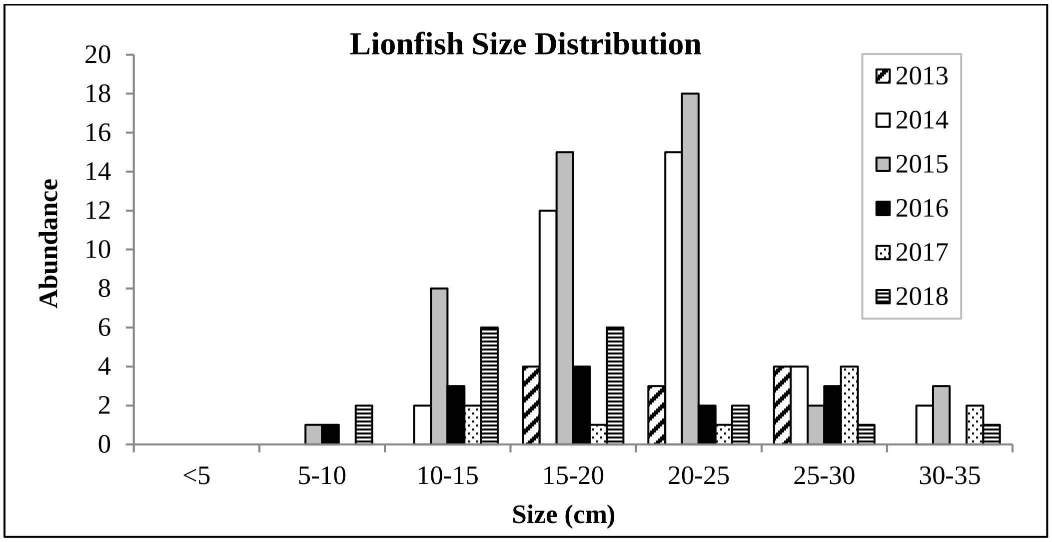

Figure 8.9. Lionfish size distribution within EFGB and WFGB study site surveys from 2013 to 2018.

Coefficient of variation percentages (35.17% for density and 41.54% for biomass) indicated that the data had poor power to detect population differences due to the low number of lionfish observed. Mean density for all surveys was 0.21 ± 0.07 and mean biomass was 60.52 ± 30.86 for the EFGB study site and 20.23 ± 12.71 for the WFGB study site. Due to the low number of lionfish observed and poor coefficient of variation percentage score, ANOSIM statistics were not calculated.

Regal Demoiselle

The first sighting of regal demoiselle (*Neopomacentrus cyanomos*) within FGBNMS occurred at Stetson Bank on June 27, 2018 at multiple buoyed locations across the bank at approximately 24 m depth. After the completion of the long-term monitoring cruises in August 2018, sightings of regal demoiselle (5-10 cm in total length), observed schooling with other reef fish, were also confirmed within study site surveys. The regal demoiselle is a non-native species from the Indo-Pacific region. Mean density for all surveys was 0.26 ± 0.10 and mean biomass for all surveys was 0.06 ± 0.02.

Figure 8.10. A regal demoiselle, a non-native species now present within FGBNMS. Photo: G.P. Schmahl/NOAA

Fish Surveys Long-Term Trends

Since 2002, mean fish density ranged from 52.70 to 564.68 individuals/100 m^2 within EFGB study sites, and 64.80 to 471.87 individuals/100 m^2 within WFGB study sites (Figure 8.11).

Fish community density was compared among years and bank study sites when complete survey data was available (2011 to 2018). PERMANOVA analysis revealed significant differences between bank study sites and years, and the year x bank study site interaction was also significant (Table 8.8), demonstrating fish density was highly variable between year and EFGB and WFGB study sites from 2011 to 2018, with shifts in the fish communities over time (Figure 8.12). The observed dissimilarity in density between study sites from 2011 to 2018 was mainly attributable to bonnetmouth (10.23%), brown chromis (8.82%), and creole wrasse (6.03%).

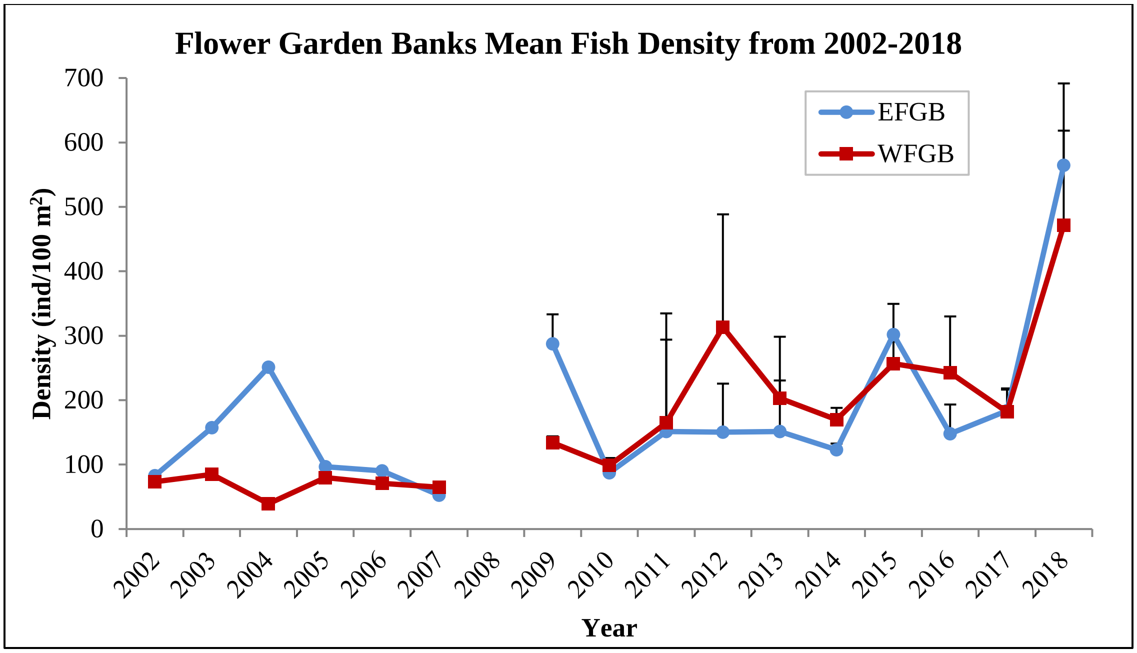

Figure 8.11. Mean fish density (individuals/100 m^2) + SE within EFGB and WFGB study sites from 2002 to 2018. No data were collected in 2008 and SE was not available before 2009. Data for 2002 to 2008 are from PBS&J (Precht et al. 2006; Zimmer et al. 2010) and data from 2009 to 2017 are from FGBNMS (Johnston et al. 2013, 2015, 2017a, 2017b, 2018b).

Table 8.8. PERMANOVA results comparing mean fish density within EFGB and WFGB study sites from 2011 to 2018. Bold text denotes significant value.

Source	Sum of Squares	df	Pseudo-F	P (perm)
Year	87539	7	3.11	**0.001**
Bank Study Site	9736	1	7.82	**0.001**
Year*Bank Study Site	28134	7	3.23	**0.001**
Res	473220	380		
Total	598530	395		

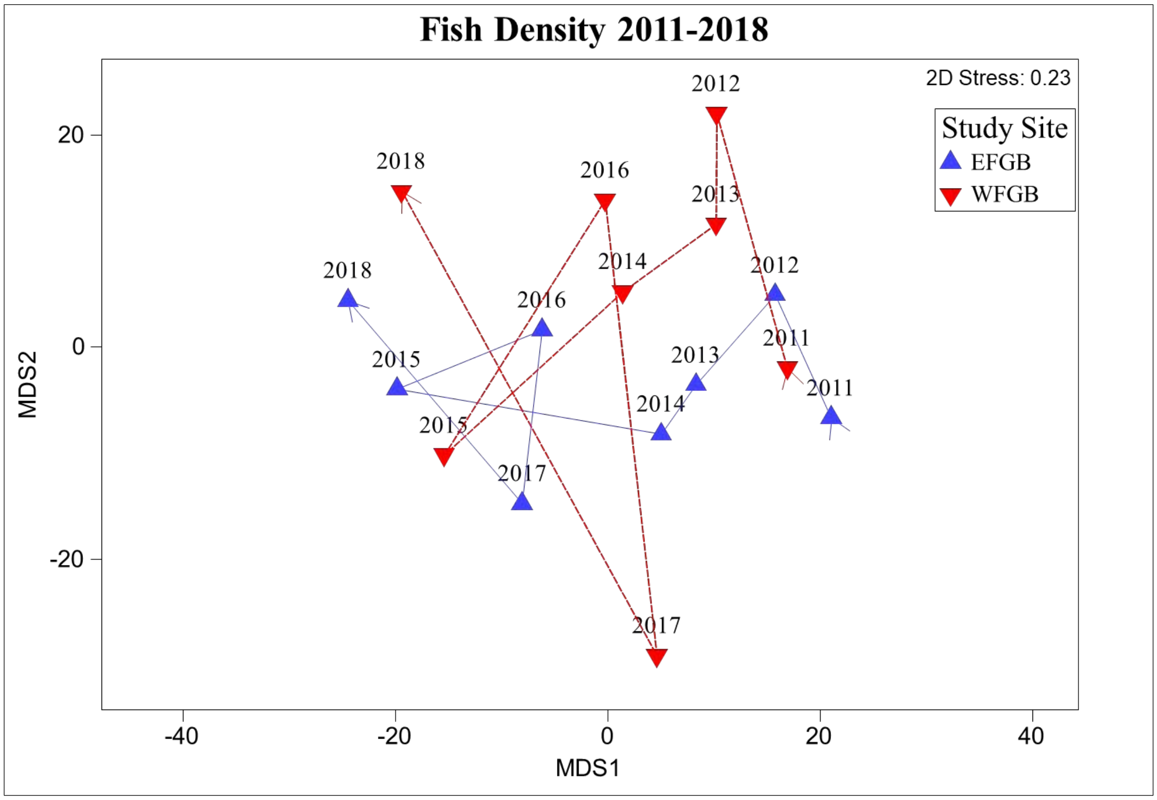

Figure 8.12. Two-dimensional MDS plot based on Bray-Curtis similarities showing shifts in the fish community due to changes in density within EFGB and WFGB study sites from 2011 to 2018.

Biomass data were first collected in 2006, and ranged from 4,547.24 to 60,160.96 g/100 m^2 within the EFGB study site and 2,458.47 to 27,226.00 g/100 m^2 within the WFGB study site from 2006 to 2018 (Figure 8.13).

Biomass was highly variable in EFGB and WFGB study sites from 2011 to 2018 (Figure 8.13). When compared among years and locations from 2011 to 2018, PERMANOVA analysis revealed significant differences between bank study sites and years, and the year x bank study site interaction was also significant (Table 8.9). Although differences occurred between banks, the MDS plot displayed similar shifts in the fish communities over time (Figure 8.14). The observed dissimilarity in biomass between study sites from 2011 to 2018 was mainly attributable to great barracuda (10.90%), Atlantic creolefish (7.98%), and Bermuda chub (7.48%).

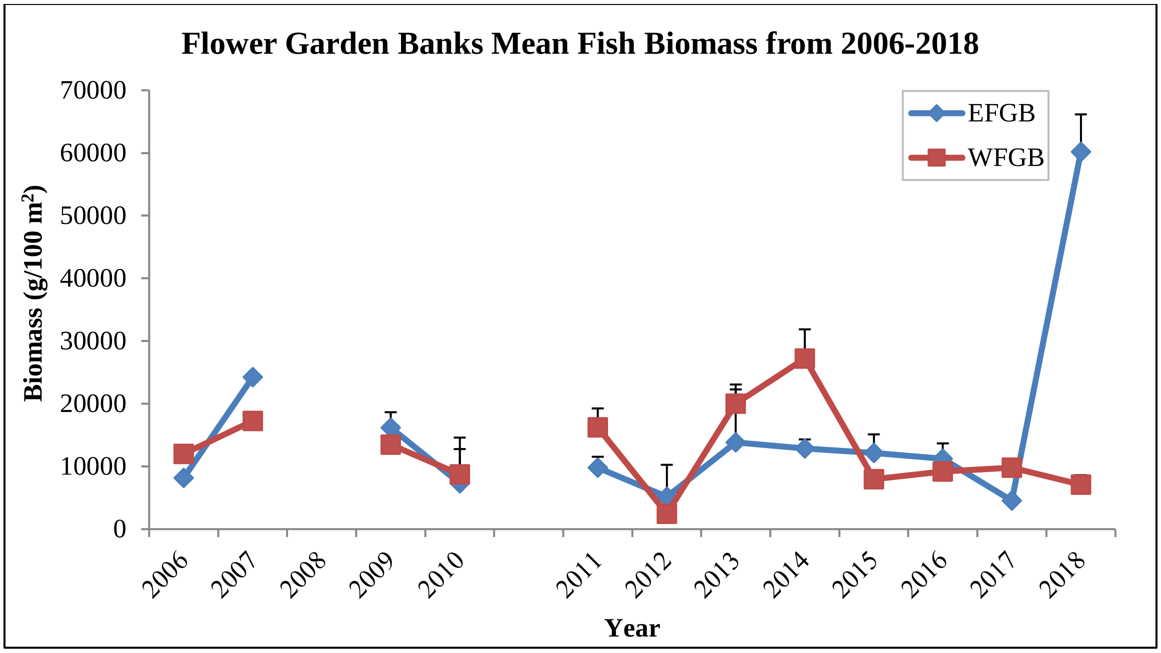

Figure 8.13. Mean fish biomass (g/100 m^2) + SE within EFGB and WFGB study sites from 2006 to 2018. No data were collected in 2008 and SE was not available before 2009. Data for 2002 to 2008 are from PBS&J (Precht et al. 2006; Zimmer et al. 2010) and data from 2009 to 2017 are from FGBNMS (Johnston et al. 2013, 2015, 2017a, 2017b, 2018b).

Table 8.9. PERMANOVA results comparing mean fish biomass within EFGB and WFGB study sites from 2011 to 2018. Bold text denotes significant values.

Source	Sum of Squares	df	Pseudo-F	P (perm)
Year	398290	7	9.82	**0.001**
Bank Study Site	7833	1	3.75	**0.001**
Year*Bank Study Site	40530	7	2.77	**0.001**
Res	793220	380		
Total	1239900	395		

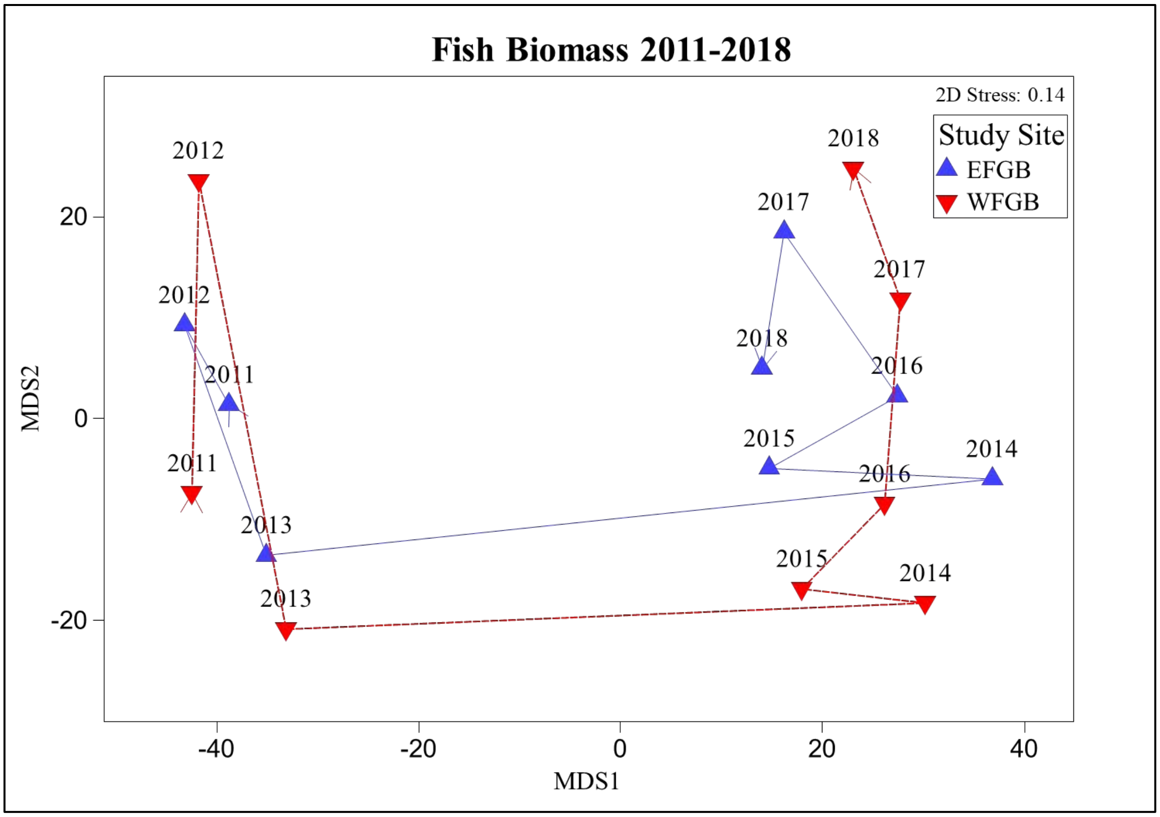

Figure 8.14. Two-dimensional MDS plot based on Bray-Curtis similarities showing shifts in the fish community due to changes in biomass within EFGB and WFGB study sites from 2011 to 2018.

To investigate trends in recreationally and commercially important species within EFGB and WFGB study sites, including grouper and snapper, additional analyses were conducted to examine density over time when complete survey data were available (2011 to 2018). The predominant grouper species within both EFGB and WFGB study sites were graysby and yellowmouth grouper. Tiger grouper, scamp, coney, red hind, and rock hind were denser in EFGB study site surveys, and black grouper were denser in WFGB study site surveys (Figure 8.15).

Grouper community density was compared among years and bank study sites from 2011 to 2018. PERMANOVA analysis revealed a significant difference between bank study sites (Table 8.10), suggesting that grouper density was higher within the EFGB study site than the WFGB study site. The observed dissimilarity in density between study sites from 2011 to 2018 was mainly attributable to graysby (44.40%), yellowmouth grouper (21.79%), and rock hind (10.80%).

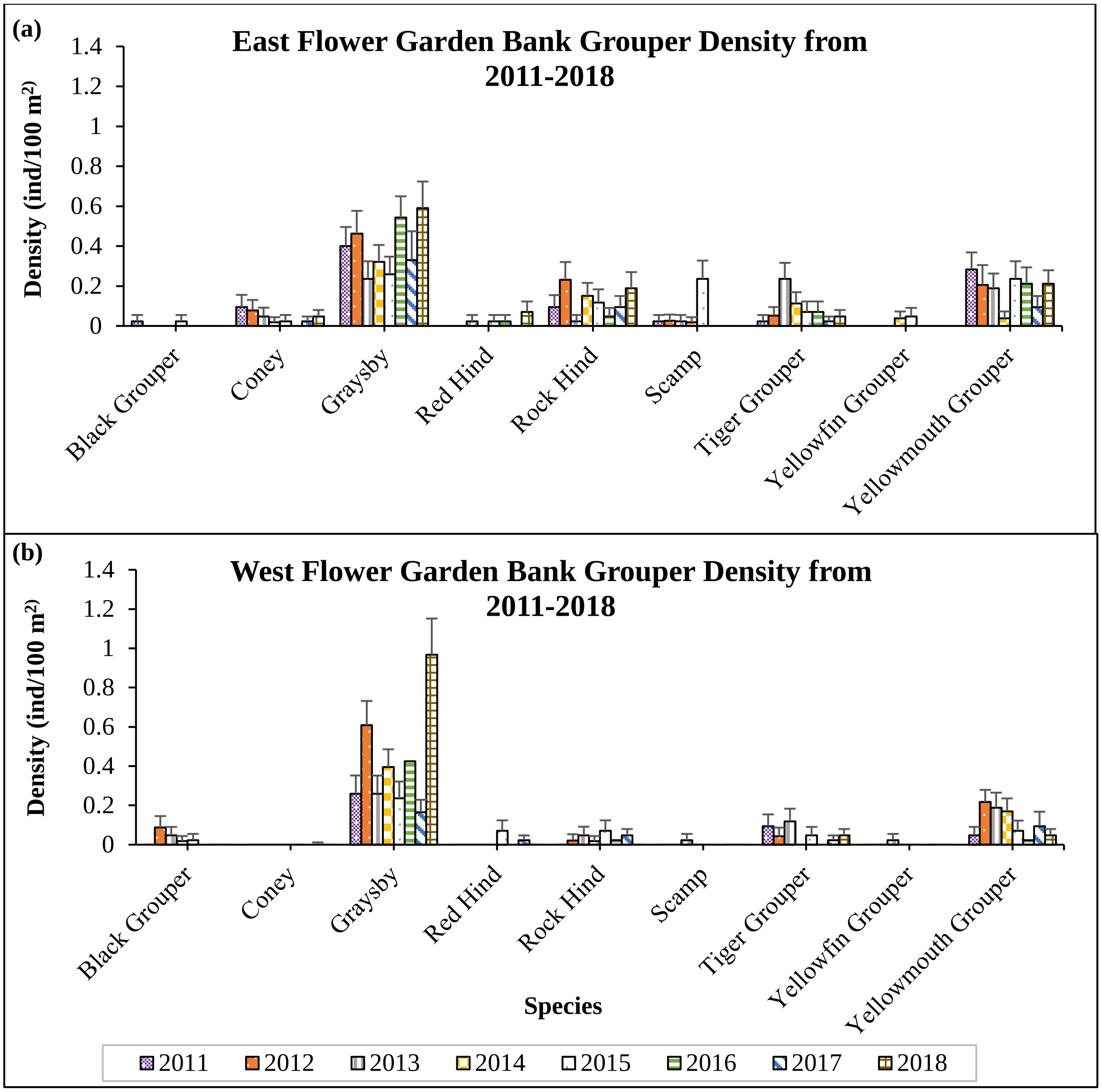

Figure 8.15. Mean density (individuals/100 m^2) + SE of grouper species within (a) EFGB and (b) WFGB study sites from 2011 to 2018. Data for 2011 to 2017 are from FGBNMS (Johnston et al. 2015, 2017a, 2017b, 2018b).

Table 8.10. PERMANOVA results comparing mean grouper density within EFGB and WFGB study sites from 2011 to 2018. Bold text denotes significant value.

Source	Sum of Squares	df	Pseudo-F	P (perm)
Year	10	7	1.85	0.070
Bank Study Site	3	1	5.27	**0.001**
Year*Bank Study Site	6	7	1.46	0.061
Res	206	380		
Total	224	395		

From 2011 to 2018, dog snapper and gray snapper were denser in WFGB study site surveys than EFGB study site surveys (Figure 8.16). Snapper community density was compared among years and bank study sites from 2011 to 2018. PERMANOVA analysis revealed a significant difference between bank study sites (Table 8.11), suggesting that snapper density was higher within the WFGB study site than the EFGB study site. The observed dissimilarity in density was mainly attributable to dog snapper (64.23%).

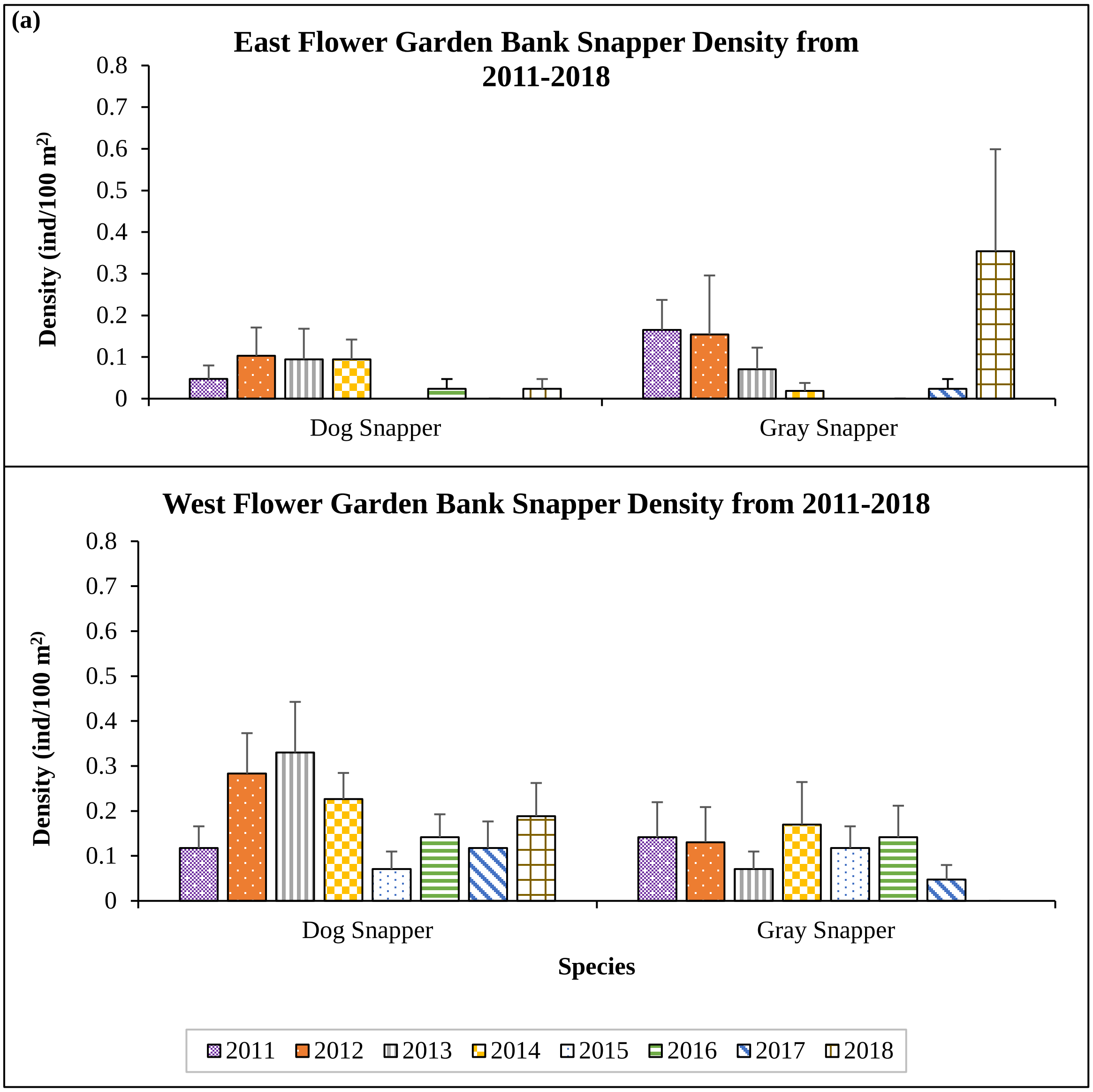

Figure 8.16. Mean density (individuals/100 m^2) + SE of snapper species within (a) EFGB and (b) WFGB study sites from 2011 to 2018. Data for 2011 to 2017 are from FGBNMS (Johnston et al. 2015, 2017a, 2017b, 2018b).

Table 8.11. PERMANOVA results comparing mean snapper density within EFGB and WFGB study sites from 2011 to 2018. Bold text denotes significant values.

Source	Sum of Squares	df	Pseudo-F	P (perm)
Year	2	7	1.35	0.298
Bank Study Site	3	1	14.39	**0.001**
Year*Bank Study Site	1	7	1.06	0.364
Res	70	380		
Total	76	395		

Fish Surveys Discussion

Fish communities are indicators of ecosystem health (Sale 1991) and are therefore an important component of long-term monitoring programs. Monitoring fish communities over time is valuable for detecting changes from normal variations that exist within the community. Historically, the fish communities at EFGB and WFGB have been considered to be low in species diversity but high in biomass (Zimmer et al. 2010). The fish assemblages of EFGB and WFGB occur near the northern latitudinal limit of coral reefs, are remote from other tropical reefs, and possess significantly different fish assemblages than reef systems in the Caribbean, including limited presence of lutjanids (snappers) and haemulids (grunts) (Rooker et al. 1997; Precht et al. 2006; Johnston et al. 2017a). Approximately 150 reef fish species have been documented on the EFGB and WFGB reef caps (Pattengill 1998; Pattengill-Semmens and Semmens 1998). Comparable studies conducted in Puerto Rico, the U.S. Virgin Islands, and FGBNMS by NOAA's National Centers for Coastal Ocean Science (Biogeography Branch) suggest that both mean biomass and mean richness is greater at EFGB and WFGB in comparison to those Caribbean reefs (Table 8.12).

Table 8.12. Comparison of other Caribbean reef biomass (g/100 m^2 ± SE) and species richness (species/100 m^2 ± SE) to EFGB and WFGB.

Region	Mean Biomass (g/100 m^2)	Mean Richness (species/100 m^2)
Puerto Rico (Caldow et al. 2015; Bauer et al. 2015a; Bauer et al. 2015b)	3,830.25 ± 188.51	18.19 ± 0.19
US Virgin Islands (Roberson et al. 2015; Pittman et al. 2015; Clark et al. 2015b; Bauer et al. 2015c)	6,355.38 ± 172.60	20.70 ± 0.12
East and West Flower Garden Banks Study Site Surveys Combined (this report)	33,632.51 ± 3,006.40	22.25 ± 0.46
East and West Flower Garden Bank Stratified Random Reef Wide Surveys Combined (Clark et al. 2015a)	34,570.87 ± 3,517.95	24.60 ± 0.36

The EFGB and WFGB have lower overall abundance of herbivorous fishes than other Caribbean reefs (Dennis and Bright 1988). Historically, low macroalgae cover was reported in annual monitoring surveys (Gittings et al. 1992), while recent data suggest a significant increase in mean macroalgae cover over time (Johnston et al. 2018b). During the 2018 study period, the herbivore guild possessed the second greatest mean biomass, contributing to 8% of the total biomass within study sites. Within the herbivore guild, 34% of the total biomass was attributed to Bermuda chub. The piscivore guild had the greatest mean biomass, contributing approximately 84% of the total biomass within study sites. Within the piscivore guild, horse-eye jack contributed over 85% of the total biomass, followed by great barracuda (8%). The contribution of great barracuda may be overinflated, as they are likely attracted to the presence of the R/V *Manta* and often congregate under the vessel within the study sites during sampling.

Piscivore-dominated biomass indicated that the ecosystem maintained an inverted biomass pyramid (Table 8.5). The inverted biomass pyramid has been documented in reef ecosystems, where piscivore dominance is associated with minimal human pressures, particularly from fishing (Friedlander and DeMartini 2002; DeMartini et al. 2008; Knowlton and Jackson 2008; Sandin et al. 2008; Singh et al. 2012). Typically, inverted biomass pyramids are associated with healthy reef systems with high coral cover that have high availability of refuges, rapid turnover rates of prey items, high energy transfer efficiencies, long predator life spans, and potential food subsidies from the surrounding pelagic environment (Odum and Odum 1971; DeMartini et al. 2008; Wang et al. 2009).

Abundance-biomass curves have historically been used to ascertain community health on shallow-water coral reefs; a community dominated by few large species is considered “healthy” and a community dominated by many small species is considered “impacted” (DeMartini et al. 2008; SOKI Wiki 2014). At EFGB and WFGB, results indicated that fish communities within study sites were evenly distributed (w-values close to 0). The dominance plot for EFGB surveys was representative of a healthy population, and the WFGB survey plot was representative of a somewhat disturbed population, with suppressed density of large fishes.

Commercially and recreationally important grouper and snapper density was higher within the EFGB study site. Observed coney, graysby, tiger grouper, and yellowmouth grouper consisted of immature and mature individuals, while all red hind and rock hind observed were immature individuals. In contrast to the grouper population, mature individuals dominated the dog snapper population, while all gray snapper observed were immature individuals. It should be noted that typical recruitment/nursery habitat for snappers (mangroves and seagrasses) are not present at EFGB and WFGB, and the mechanism for recruitment of this family to the area remains unknown (Mumby et al. 2004; Clark et al. 2014).

Parrotfishes are important herbivores on coral reefs because they are effective algal grazers (Jackson et al. 2014). Parrotfish have been identified as key reef species, and their abundance and biomass have been positively correlated with coral cover (Jackson et al. 2014). The mean biomass of parrotfish within the study sites was considered low and similar to other Caribbean reefs (Jackson et al. 2014) (Table 8.13). However, low parrotfish biomass can be associated with high fishing pressure and low coral cover, neither of which have been documented at EFGB or WFGB.

Table 8.13. Mean biomass (g/100 m^2) for parrotfish at EFGB, WFGB, and other Caribbean reefs. All data, with the exception of EFGB and WFGB data, are from AGRRA 2012.

Location	Biomass (g/100 m^2)
Mexico	1,710
Belize	1,200
East and West Flower Garden Banks Study Site Surveys Combined (this report)	1,079
Guatemala	670
Honduras	440

Lionfish were recorded in surveys for the sixth consecutive year in 2018, but have been observed by divers consistently on the reefs since 2011. Since their first observation, numbers rapidly increased through 2014, and then declined after 2015 (Johnston et al. 2016a) and rose again in 2018. It should be noted that lionfish are commonly seen during crepuscular feeding periods at dawn and dusk, and while fish surveys are spread throughout the day, surveys outside of this period may not accurately capture lionfish densities during the peak hours of their activity. However, mean lionfish densities at EFGB and WFGB (approximately 4–40 lionfish ha^{-1}) (Johnston et al. 2016a) have yet to reach levels recorded elsewhere in the southeast U.S. and Caribbean region, such as North Carolina (150 lionfish ha^{-1}) (Morris and Whitfield 2009) and the Bahamas (100–390 lionfish ha^{-1}) (Green and Côté 2009; Darling et al. 2011), as well as on artificial reefs in the northern Gulf of Mexico (10–100 lionfish ha^{-1}) (Dahl and Patterson 2014).

It should be noted that since 2015, permitted lionfish removal cruises have taken place during summer months on the recreational dive vessel M/V *Fling*, in attempts to suppress potential impacts to the native fish community from predation-induced declines; however, divers are limited to the upper portion of the reef crest (< 40 m) (Green et al. 2014; Johnston et al. 2016a). Within the long-term monitoring study sites, removals do not take place during LTM field operations, ensuring sighting frequency, density, and biomass data are not affected. However, because lionfish are removed by permitted divers at nearby moorings throughout the rest of the year, their abundance is likely lower than it would be if lionfish were not removed from the reef caps.

The regal demoiselle, a non-native species from the Indo-Pacific region, was observed in study site surveys at EFGB and WFGB for the first time in 2018. The primary hypothesis is that this species was brought to the Gulf of Mexico by the inter-ocean transfer of oil rigs (Robertson et al. 2018), and that they have the potential to displace native reef fish, such as the brown chromis (Robertson et al. 2016). Sightings from EFGB and WFGB fish surveys were reported to the United States Geological Survey (USGS) invasive species sightings database, and FGBNMS will continue to monitor this species in the future.

Chapter 9. Water Quality

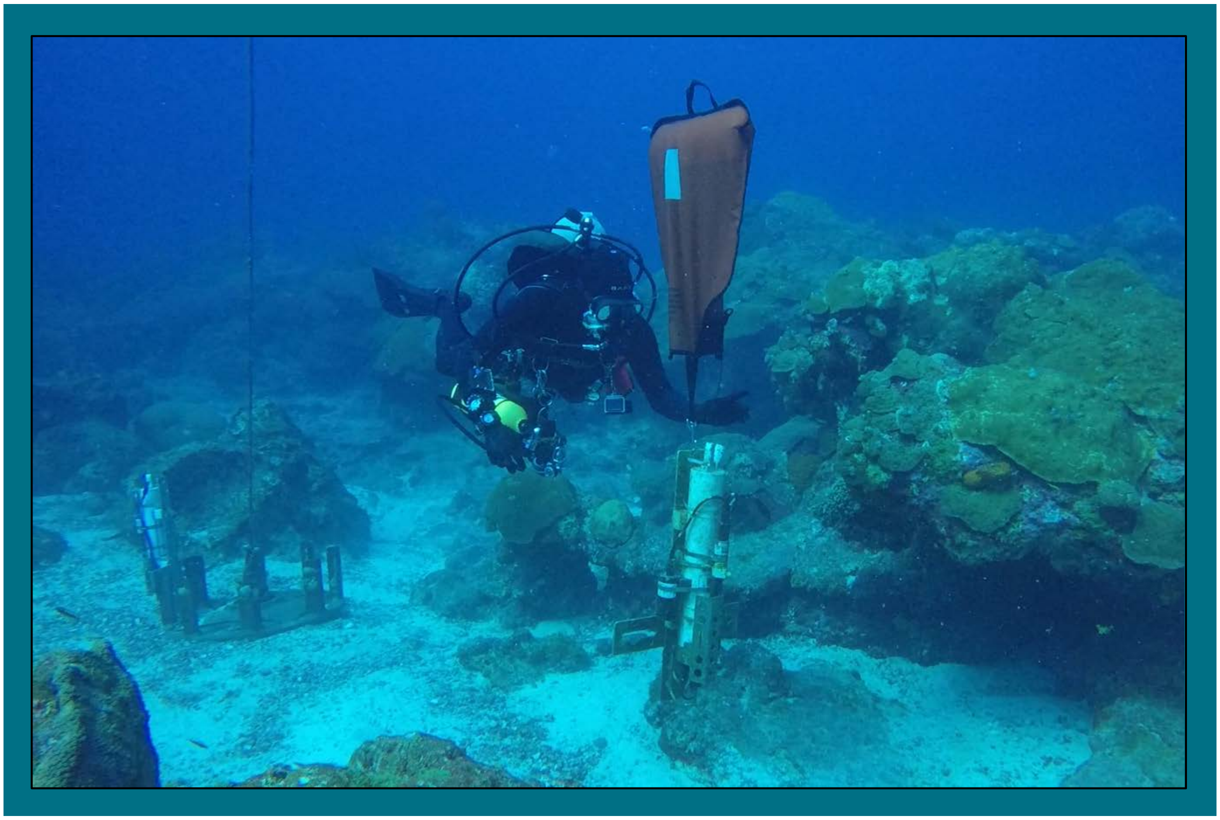

NOAA diver exchanges water quality instrument in the EFGB study site in 2018. Photo: Emma Hickerson/NOAA

Water Quality Introduction

Several water quality parameters were continuously or periodically recorded at EFGB and WFGB. At a minimum, salinity, turbidity, and temperature were recorded every hour by data loggers installed in or near the study sites at depths of approximately 24 m. Additionally, temperature loggers collected hourly readings at depths of 24 m, 30 m, and 40 m at each bank.

Water samples were collected quarterly throughout the year at three different depths and analyzed by an Environmental Protection Agency (EPA) certified laboratory for select nutrient levels. Water samples were also collected for ocean carbonate measurements. In conjunction with the quarterly water sample collections, water column profiles were also acquired. This chapter presents data from instruments and water samples collected in 2018.

Water Quality Methods

Water Quality Field Methods

Temperature and Salinity Loggers

The primary instrument used at each bank for recording temperature, salinity, and turbidity was a Sea-Bird Electronics *16plus* V2 CTD (conductivity, temperature, and depth) (SBE *16plus*) equipped with a WET Labs ECO NTUturbidity meter at an approximate depth of 24 m. Loggers were secured to railroad wheels and located in sand flats at each bank (see Chapter 1, Figures 1.3 and 1.4). These instruments recorded temperature, salinity, and turbidity on an hourly basis. Instruments were exchanged by divers for downloading and maintenance in June, August, and October 2018. They were immediately exchanged with an identical instrument to avoid any gaps in the data collection. Prior to re-installation, all previous data were removed from the instrument and battery life was checked. Maintenance and factory service of each instrument was performed annually.

Onset® Computer Corporation HOBO® Pro v2 U22-001 (HOBO) thermograph loggers were used to record temperature on an hourly basis. These loggers provided a highly reliable temperature backup for the primary SBE *16plus* logging instruments located at the 24 m stations at EFGB and WFGB. HOBO loggers were also deployed at 30 m and 40 m stations at EFGB and WFGB to record temperature hourly at deeper depths. The loggers were downloaded, maintained, and replaced on a quarterly basis. The instruments were attached directly to either the primary SBE *16plus* instrument at the 24 m station or to permanent repetitive deep photostation markers at the 30 m and 40 m depths. Prior to re-installation, all previous data were removed from the instrument and battery levels were verified.

Water Column Profiles

Water column profiles were conducted twice in 2018 with a Sea-Bird Electronics *19plus* V2 CTD that recorded temperature, salinity, pH, turbidity, fluorescence, and dissolved oxygen (DO) every ¼ second to distinguish differences between three main depth gradients: the reef cap (~20 m), mid-water column (~10 m), and the surface (~1 m). Data were recorded upon ascent following an initial two-minute soaking period after deployment. The CTD was brought to the surface at a rate <1 m/sec. In 2018, water column profiles were attained on August 17th and October 30th. Quarterly sampling did not occur in February due to unfavorable weather or in May due to vessel maintenance.

Water Samples

In conjunction with water column profiles, water samples were collected using a sampling carousel equipped with a Sea-Bird Electronics *19plus* V2 CTD and a circular rosette of twelve OceanTest Corporation 2.5 L Niskin bottles. The carousel was attached to the R/V *Manta* with a scientific winch cable, thereby allowing the operator to activate the bottles to sample at specific depths. Six samples were collected in April, August, and October of 2018. Two 2.5 L water samples were collected near the reef cap on the seafloor (~20 m depth), midwater (~10 m depth), and near the surface (~1 m depth) for transfer to laboratory collection bottles.

Water samples were analyzed for chlorophyll *a* (chl *a*) and nutrients including ammonia, nitrate, nitrite, soluble reactive phosphorous (ortho phospohate), and total Kjeldahl nitrogen (TKN) (Table 9.1). Water samples for chl *a* analyses were collected in 1000 ml glass containers with no preservatives. Samples for soluble reactive phosphorous were placed in 250 ml bottles with no preservatives. Ammonia, nitrate, nitrite, and total nitrogen samples were collected in 1000 ml bottles with a sulfuric acid preservative. An additional blind duplicate water sample was taken at one of the sampling depths for each sampling period. Within minutes of sampling, labeled sample containers were stored on ice at 4°C and a chain of custody was initiated for processing at an EPA certified laboratory. The samples were transported and delivered to A&B Laboratories in Houston, TX, within twenty-four hours of collection for analysis.

Table 9.1. Standard EPA methods used to analyze water samples collected at EFGB and WFGB.

Parameter	Test Method	Detection Limit
Chlorophyll *a*	SM 10200H	0.003-mg/l
Ammonia	SM 4500NH3D	0.10–mg/l
Nitrate	SM 4500NO3E	0.04–mg/l
Nitrite	SM 4500NO2B	0.02–mg/l
Soluble reactive phosphorous	SM 4500 P-E	0.02–mg/l
Total Kjeldahl nitrogen (TKN)	SM 4500NH3D	0.50–mg/l

Water samples for ocean carbonate measurements were collected following methods provided by the Carbon Cycle Laboratory (CCL) at Texas A&M University – Corpus

Christi (TAMU-CC). Samples were collected in Pyrex® 250 ml borosilicate bottles with polypropylene caps. Two replicates were collected at each depth. Sample bottles were filled using a 30 cm plastic tube that connected from the spout of the Niskin bottles. Sample bottles were rinsed three times using the sample water, filled carefully to reduce bubble formation, and overflowed by at least 200 ml. $HgCl_2$ (100 µl) was added to each sample bottle before inverting vigorously. Samples were then stored at 4°C. Samples and CTD profile data were sent to CCL at TAMU-CC. Samples were obtained on April 24, August 17, and October 30, 2018.

Water Quality Data Processing and Analysis

Hourly sea surface temperature (SST) and salinity data for 2018 were downloaded from the Texas Automated Buoy System (TABS) database from Buoy V, located within EFGB sanctuary boundaries (27° 53.796' N, 93° 35.838' W) (1.4 km from the EFGB reef cap). TABS Buoy N, located near WFGB, was removed on January 04, 2017 due to funding limitations; therefore, no surface buoy readings were available for analysis. In lieu of in situ surface data for WFGB, SST and sea surface salinity (SSS) satellite derived data for 2018 were downloaded from the NOAA ERDDAP data server and used for analysis for WFGB. The SST dataset used was "GHRSST Level 4 MUR Global Foundation Sea Surface Temperature Analysis (v4.1)" and the SSS dataset used was "Sea Surface Salinity, Near Real Time, Miras SMOS 3-Day Mean (smosSSS3Scan3DayAggLoM), CoastWatch v6.62, 0.25°, 2010-present" (JPL MUR MEaSUREs Project 2015; Simons 2019).

Temperature, salinity, and turbidity data recorded on SBE *16plus* instruments and HOBO loggers were downloaded and processed in August and October of 2018. QA/QC procedures consisted of a review of all files to ensure data accuracy, and instruments were serviced annually based on manufacturer recommendations. The twenty-four hourly readings obtained each day were averaged into one daily value and recorded in duplicate databases. Each calendar day was assigned a value in the database. Separate databases were maintained for each type of logger.

Due to vessel maintenance preventing full offshore operations through the first two quarters of 2018, SBE *16plus* instruments and HOBO loggers were exchanged in June and during long-term monitoring cruises in August. SBE *16plus* instrumentation and attached backup HOBO loggers were exchanged on schedule in October 2018 and again in February 2019; however, the 30 m and 40 m WFGB deep station HOBO loggers were not exchanged during these cruises due to unfavorable diving conditions at these deeper depths. Therefore, data are not available from mid-August through the end of 2018 for these particular loggers at WFGB since they were not yet exchanged at the time this report was written. TABS Buoy V data were available semi-hourly from February 16, 2018 through December 21, 2018. Satellite derived one-day mean SST data utilized for WFGB in 2018 were available as a level 4 global 0.01 degree grid produced at the NASA

Jet Propulsion Laboratory Physical Oceanography Distributed Active Archive Center with support from the NASA MEaSUREs program. Satellite derived SSS data utilized for WFGB in 2018 were available as a level 3 gridded three-day mean dataset from MIRAS satellite observations over the global ocean.

For seawater temperature, salinity, and turbidity data, EFGB and WFGB SBE *16plus* daily mean 2018 data were compared using a paired t-test in R version 2.13.2. In addition, daily mean seawater temperature data from a 25-year baseline (1990 to 2015) at depth (24 m) were used for comparison to 2018 EFGB and WFGB data with a paired t-test. For salinity data, daily mean salinity from an eight-year baseline (2008 to 2015) at depth (24 m) was used for comparison. Monotonic trends over the course of the long-term datasets were detected using the Seasonal-Kendall trend test in a Microsoft® Windows® program developed by USGS for water resource data (Hipel and McLeod 1994; Helsel and Hirsch 2002; Helsel et al. 2006). The Seasonal-Kendall trend test performed the Mann-Kendall trend test for each month and evaluated changes among the same months from different years over time, accounting for serial correlation in repeating seasonal patterns.

Chlorophyll *a* and nutrient analysis results were obtained quarterly from A&B Laboratories and compiled into an Excel® table. Ocean carbonate analysis results were compiled and received as an annual report from the CCL at TAMU-CC.

Water Quality Results

Temperature

Surface seawater temperatures recorded by TABS Buoy V within the EFGB sanctuary boundaries ranged from a minimum of 19.13°C on December 17, 2018 to a maximum of 30.42°C on July 30, 2018 (Figure 9.1). At the EFGB 24 m SBE *16plus* location, the minimum temperature logged was 20.12°C, recorded on February 01, 2018. The maximum temperature, recorded on September 30, 2018, was 29.81°C (Figure 9.1).

At the deeper 30 m and 40 m EFGB stations, slightly cooler temperatures were recorded by the HOBO loggers. At the 30 m station, the minimum temperature logged was 20.01°C, recorded on February 01, 2018. The maximum temperature, recorded on October 13, 2018 was 29.83°C (Figure 9.1). At the 40 m station, the minimum temperature logged was 20.04°C, recorded on February 03, 2018. The maximum temperature, recorded on August 03, 2018, was 29.74°C (Figure 9.1). At EFGB, the average temperature difference between the 24 m and 30 m stations was -0.47°C and the greatest temperature difference was -3.01°C on September 1, 2018. The average temperature difference between the 24 m and 40 m stations was 1.16°C and the greatest difference in temperature recorded was -4.85°C on June 14, 2018. Throughout this study period, no water temperatures exceeding 30°C were recorded by any instruments at depth at EFGB.

Satellite derived SST at WFGB ranged from a minimum of 20.07°C on January 25-26, 2018 to a maximum of 30.51°C on August 22, 2018 (Figure 9.1). At the WFGB 24 m SBE *16plus* location, the minimum temperature logged was 19.59°C, recorded on February 08, 2018. The maximum temperature, recorded on August 10, 2018, was 29.85°C (Figure 9.1).

Data from the WFGB deep station HOBO loggers are presented from January through mid-August of 2018. At the WFGB 30 m station, the minimum temperature logged was 19.67°C, recorded on February 08, 2018. The maximum temperature, recorded on August 10, 2018, was 29.85°C (Figure 9.1). At the WFGB 40 m station, the minimum temperature logged was 19.70°C, recorded on February 08, 2018. The maximum temperature, recorded on August 02, 2018, was 29.41°C (Figure 9.1). At WFGB, the average temperature difference between the 24 m and 30 m stations was -0.07°C and the greatest temperature difference was -1.01 on June 18, 2018. The average temperature difference between the 24 m and 40 m stations was -0.56°C. The greatest difference in temperature recorded was -3.40°C on June 18, 2018. Throughout this study period, no water temperatures exceeding 30°C were recorded by any instruments at depth at WFGB. There was no significant difference between EFGB and WFGB when 2018 daily mean 24 m SBE *16plus* seawater temperatures were compared, and no significant differences in temperatures measured by deep station HOBO loggers were detected between EFGB and WFGB.

Seawater temperature data obtained from loggers at an approximate depth of 24 m have been collected since 1990 (Figure 9.2). Though some data gaps occur due to equipment malfunction and changes within program methodology and/or instrumentation, long-term temperature trends were assessed at EFGB and WFGB. When 2018 data was compared to daily mean seawater temperatures at an approximate depth of 24 m to the 25 year baseline (1990 to 2015), both EFGB (t-test, $df=364$, $t=10.82$, $p<0.002$) and WFGB (t-test, $df=364$, $t=11.25$, $p<0.002$) 2018 seawater temperatures were significantly warmer than the historic 25-year mean.

The Seasonal-Kendall trend test on time-series daily mean seawater temperature data at EFGB resulted in a significantly increasing monotonic trend from 1990 to 2018 ($\tau=0.31$, $z=6.31$, $p=0.001$) after adjusting for correlation among seasons (Figure 9.2). A significantly increasing monotonic trend was also detected at WFGB from 1990 to 2018 ($\tau=0.27$, $z=5.81$, $p=0.002$) after adjusting for correlation among seasons (Figure 9.2).

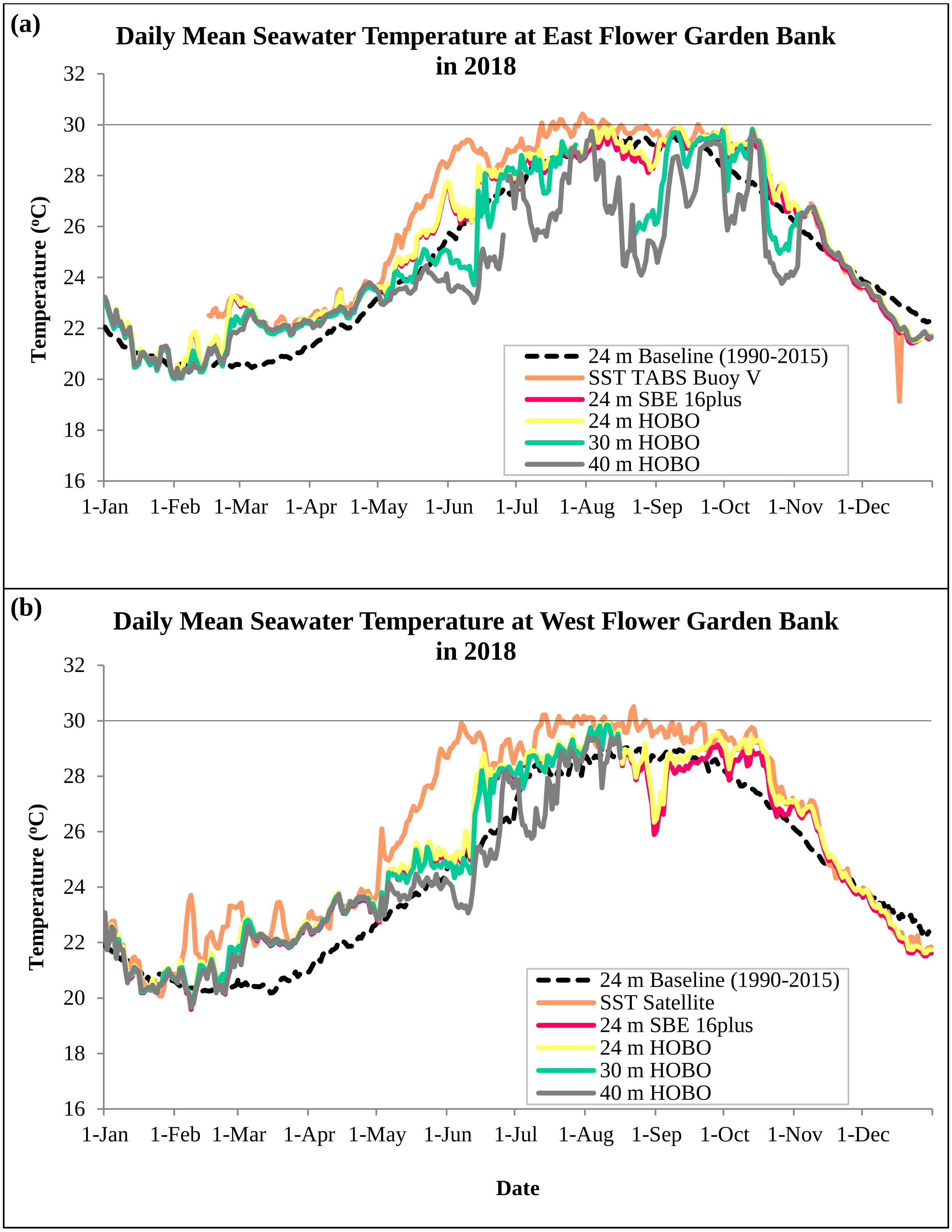

Figure 9.1. Daily mean water temperature (ºC) at (a) EFGB and (b) WFGB from various depths in 2018 and the 25-year daily mean temperature baseline (1990-2015) at 24 m depth. The solid black line at 30ºC is a temperature threshold beyond which coral bleaching is known to occur.

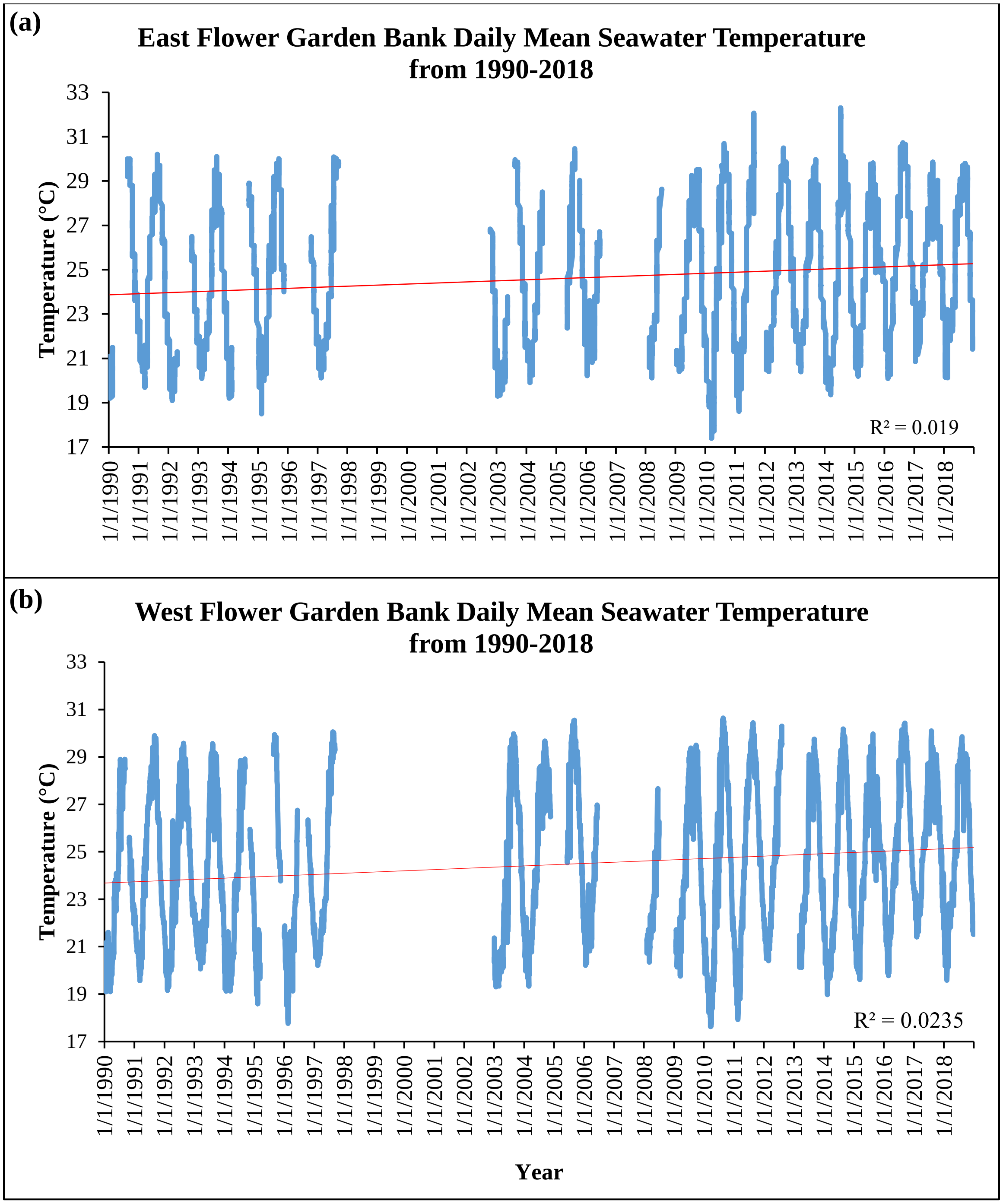

Figure 9.2. Daily mean 12-month seawater temperature (ºC) seasonal variation at (a) EFGB and (b) WFGB from 1990 to 2018 at 24 m depth. Significant trend line in red.

Salinity

Surface salinity, as recorded by TABS Buoy V within the EFGB sanctuary boundaries from February 16, 2018 through December 31, 2018, ranged from a maximum of 36.70 psu on August 24, 2018 to a minimum of 26.24 psu on December 16, 2018 (Figure 9.3). At the EFGB 24 m SBE *16plus* location, the minimum salinity logged was 34.82 psu on June 13, 2018 and the maximum salinity was 36.74 psu on August 08, 2018 (Figure 9.3).

Satellite derived sea surface salinity (SSS) within the WFGB sanctuary boundaries ranged from a maximum of 37.10 psu on April 10, 2018 to a minimum of 31.16 psu on June 9, 2018 (Figure 9.3) At the WFGB 24 m SBE *16plus* location, the minimum salinity logged was 34.99 psu on June 12, 2018 and the maximum salinity was 36.81 psu October 13, 2018 (Figure 9.3). There was a significant difference between EFGB and WFGB 2018 daily mean 24 m SBE *16plus* salinity data (t-test, df=364, t=1.97, $p<0.001$) likely due to lower temperatures at EFGB in mid-May and into June as well as the end of August through November.

Salinity data obtained from loggers at an approximate depth of 24 m have been collected throughout the monitoring program since 2008 with minimal interruptions in data (Figure 9.4). When 2018 data were compared to daily mean salinity at an approximate depth of 24 m from the eight-year baseline (2008-2015), EFGB and WFGB salinity was not significantly different from the eight-year mean.

The Seasonal-Kendall trend test on time-series daily mean salinity data at EFGB resulted in a significantly decreasing monotonic trend from 2008 to 2018 ($\tau=-0.19$, $z=-2.47$, $p=0.046$) after adjusting for correlation among seasons (Figure 9.4). No significant trend was detected at WFGB (Figure 9.4). Results from the Seasonal-Kendall trend test at WFGB were not significant over time after adjusting for correlation among seasons.

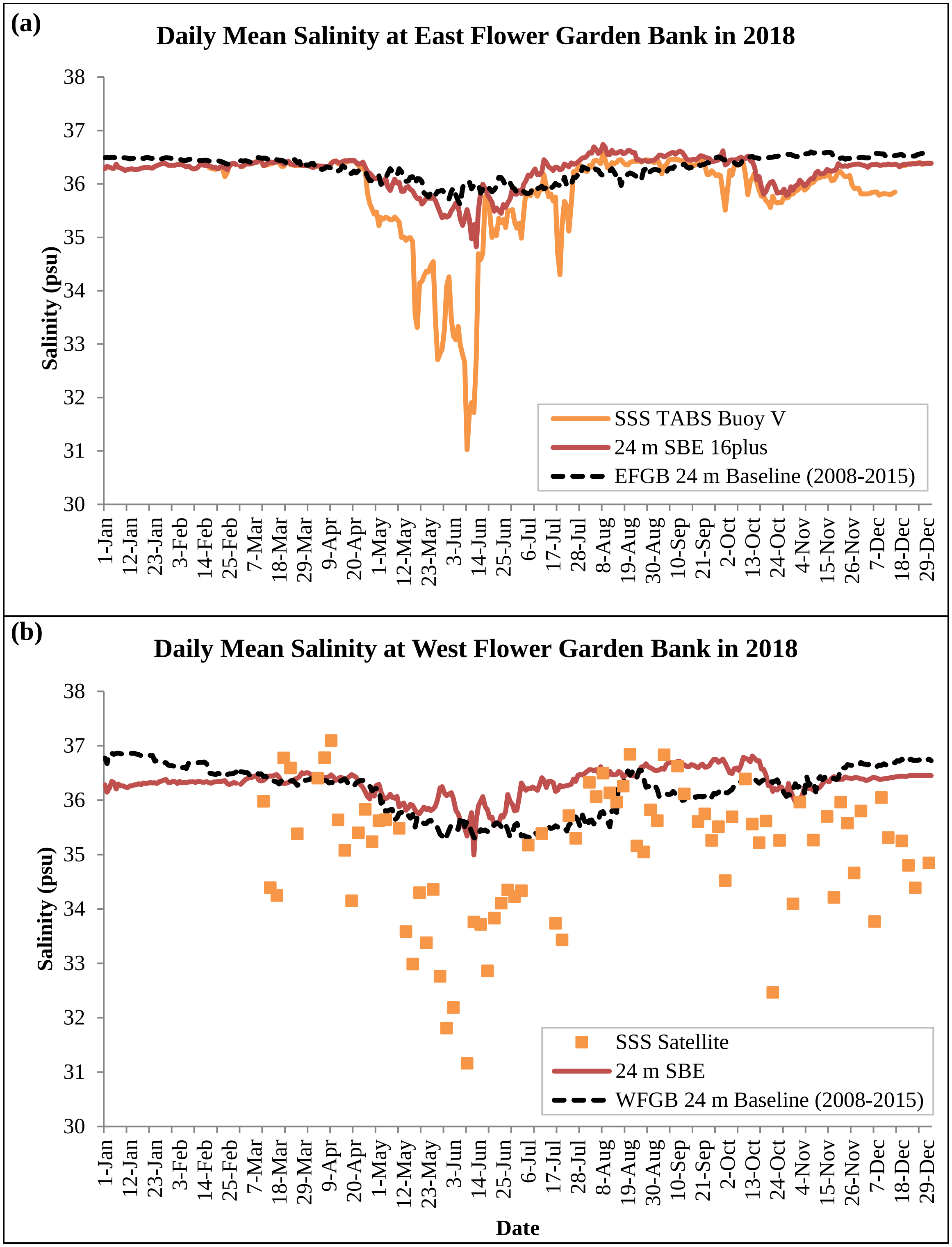

Figure 9.3. (a) Daily mean SSS (psu) at the surface and 24 m station daily mean salinity at EFGB and (b) three-day mean SSS at the surface and 24 m station daily mean salinity at WFGB in 2018 compared to an eight-year daily mean salinity baseline (2008-2015) at 24 m depth.

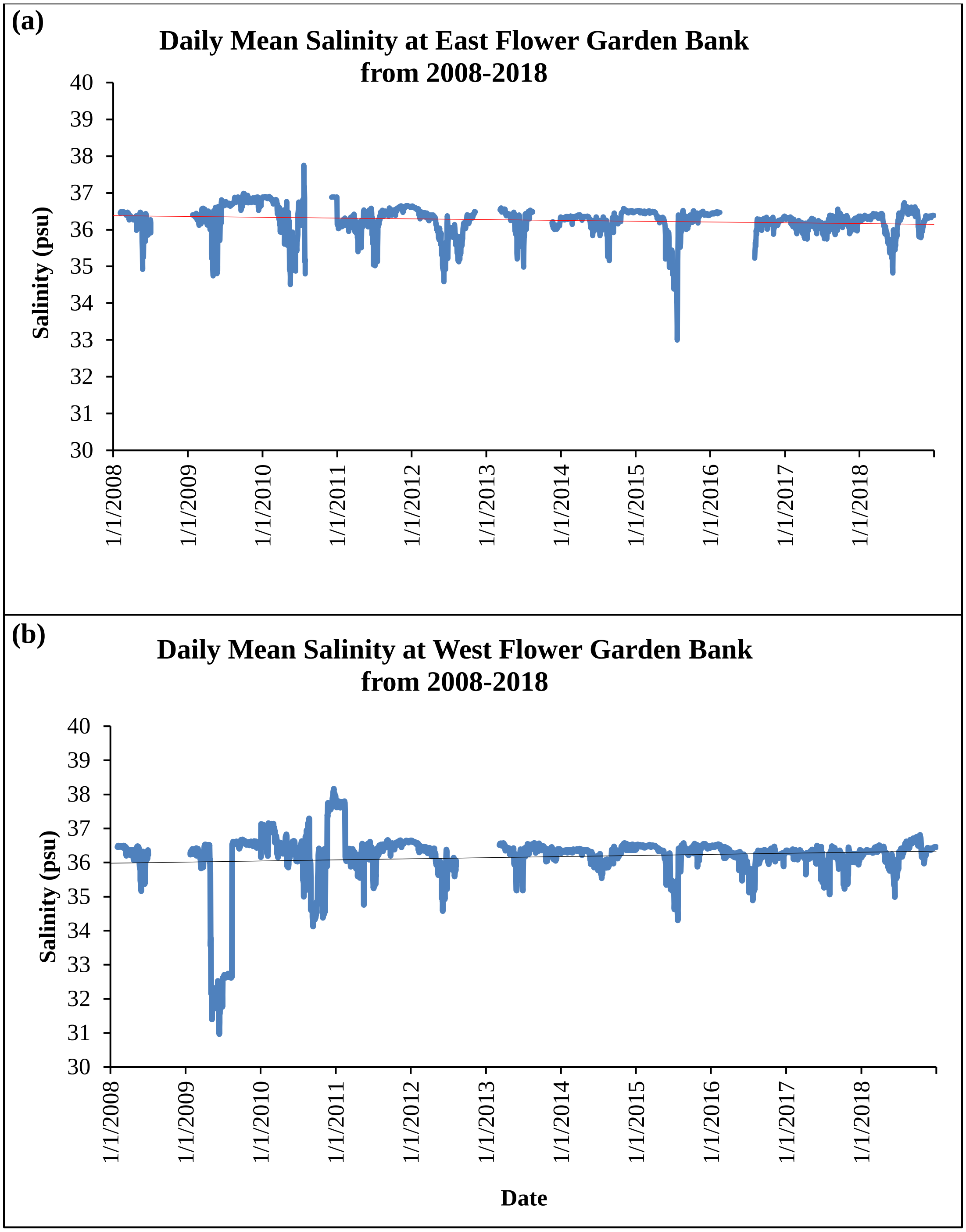

Figure 9.4. Daily mean 12-month salinity seasonal variation at (a) EFGB and (b) WFGB from 2008 to 2018 at 24 m depth. Significant trend line in red at EFGB and non-significant trend line in black at WFGB.

Turbidity

Turbidity was added as a long-term monitoring data parameter in August 2016 (24 m depth). At the EFGB 24 m SBE *16plus* location, the minimum turbidity recorded was 0.036 ntu on Aug 15, 2018 and the maximum turbidity was 0.79 ntu on December 19, 2018 (Figure 9.5). At the WFGB 24 m SBE *16plus* location, the minimum turbidity recorded was -0.07 ntu on November 07, 2018 and the maximum turbidity was 6.31 ntu on October 24, 2018 (Figure 9.5). Upon comparison of 2018 daily mean 24 m SBE *16plus* turbidity data, no significant difference was observed between EFGB and WFGB despite turbidity spikes at WFGB in October and November of 2018. The accuracy of the WFGB instrument appears to have degraded after the spikes in October and November, as subsequent measurements were lower, on average, than those for the rest of the year. Turbidity data from WFGB between July 29 and August 23, 2018 were also removed due to outliers.

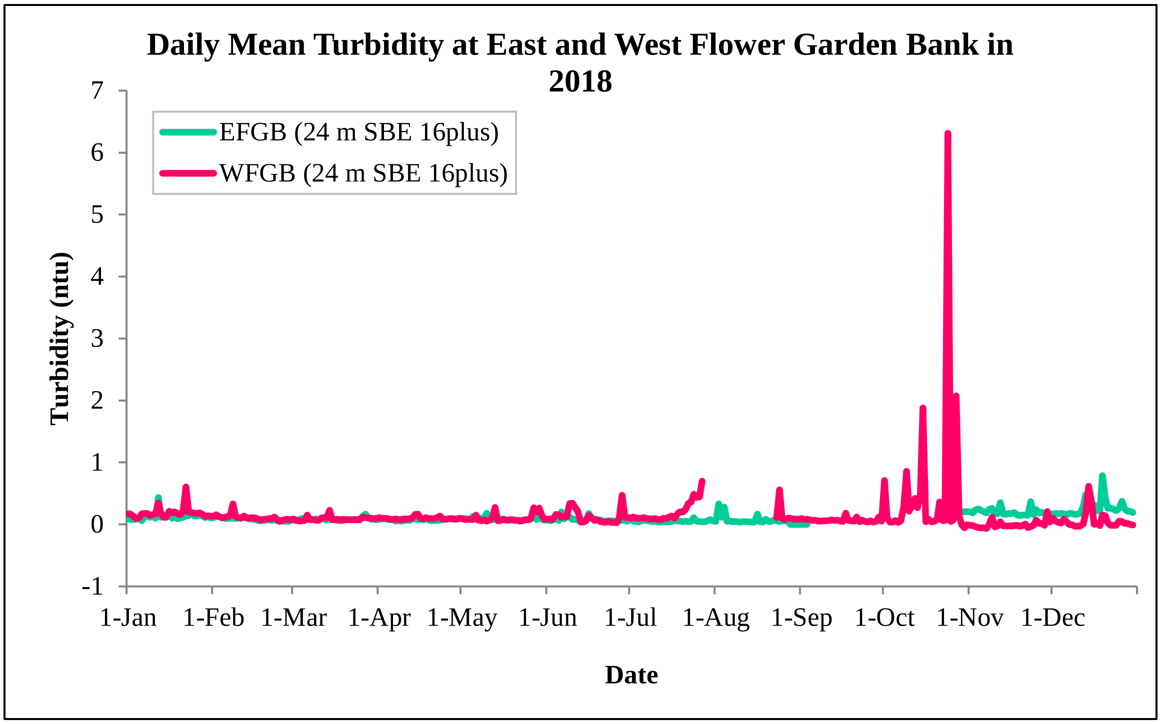

Figure 9.5. Daily mean turbidity (ntu) at EFGB and WFGB at the 24 m depth in 2018.

Water Column Profiles

Water column profile data were summarized by three depth gradients including the reef cap (~18 m), mid-water column (~10 m), and the surface (~1 m). Seawater temperatures displayed an approximate 1°C difference between surface water and reef cap temperatures at both EFGB and WFGB in the August water column profile. The October profile exhibited little stratification since variation in seawater temperature between the reef cap and surface water samples was not observed (Table 9.2 and 9.3). August water column salinity values were slightly higher than the October profile where salinity values were approximately 36 psu and 35 psu, respectively (Table 9.2 and 9.3). Fluorescence was higher at both EFGB and WFGB in October than in August, and pH ranged from approximately 8.33-8.83 throughout the water column among sampling dates (Table 9.2 and 9.3). DO values in August were slightly higher (4.96 to 5.20 ml/L) than October readings (4.60 to 4.64 ml/L) across both banks. August turbidity data were highest at EFGB in the 0.6 ntu range whereas all other turbidity readings fell closer to 0.0 (Table 9.2 and 9.3).

Table 9.2. EFGB depth, temperature, salinity, turbidity, pH, fluorescence, and DO data collected from water column profiles in August and October 2018.

Sample Date	Depth (m)	Temp (ºC)	Salinity (psu)	Turbidity (ntu)	pH (eu)	Fluorescence (mg/m^3)	DO (ml/L)
8/17/2018	17.91	28.77	36.46	0.66	8.33	0.16	5.04
8/17/2018	9.95	29.27	36.49	0.64	8.33	0.13	4.99
8/17/2018	0.99	29.85	36.31	0.66	8.35	0.10	4.96
10/30/2018	16.45	26.84	35.88	0.14	8.82	0.68	4.64
10/30/2018	10.00	26.86	35.87	0.14	8.82	0.67	4.62
10/30/2018	1.02	26.85	35.87	0.10	8.83	0.93	4.61

Table 9.3. WFGB depth, temperature, salinity, turbidity, pH, fluorescence, and DO data collected from water column profiles in August and October 2018.

Sample Date	Depth (m)	Temp (ºC)	Salinity (psu)	Turbidity (ntu)	pH (eu)	Fluorescence (mg/m3)	DO (ml/L)
8/17/2018	21.03	28.63	36.26	-0.12	8.36	0.19	5.20
8/17/2018	10.00	29.47	36.29	-0.12	8.36	0.14	5.04
8/17/2018	1.00	29.99	36.21	-0.11	8.37	0.01	4.96
10/30/2018	20.53	26.98	35.84	0.20	8.80	0.72	4.56
10/30/2018	10.08	26.95	35.72	0.16	8.81	0.71	4.60
10/30/2018	1.04	26.95	35.70	0.14	8.83	0.95	4.61

Water Samples

Nutrient analyses for ammonia, chl *a*, nitrate, nitrite, phosphorus, and nitrogen levels were first taken as part of the long-term monitoring program in 2002. Since that time, nutrients levels have typically been below detectable limits, with the exception of occasional spikes in chl *a*, ammonia, and TKN (Figures 9.6 and 9.7). In 2018, sampling occurred on April 24, August 17, and October 30, 2018. Nitrate levels at WFGB during

October displayed detectable readings at the surface (0.04 mg/L) and midwater (0.06 mg/L); all other samples were below detectable limits.

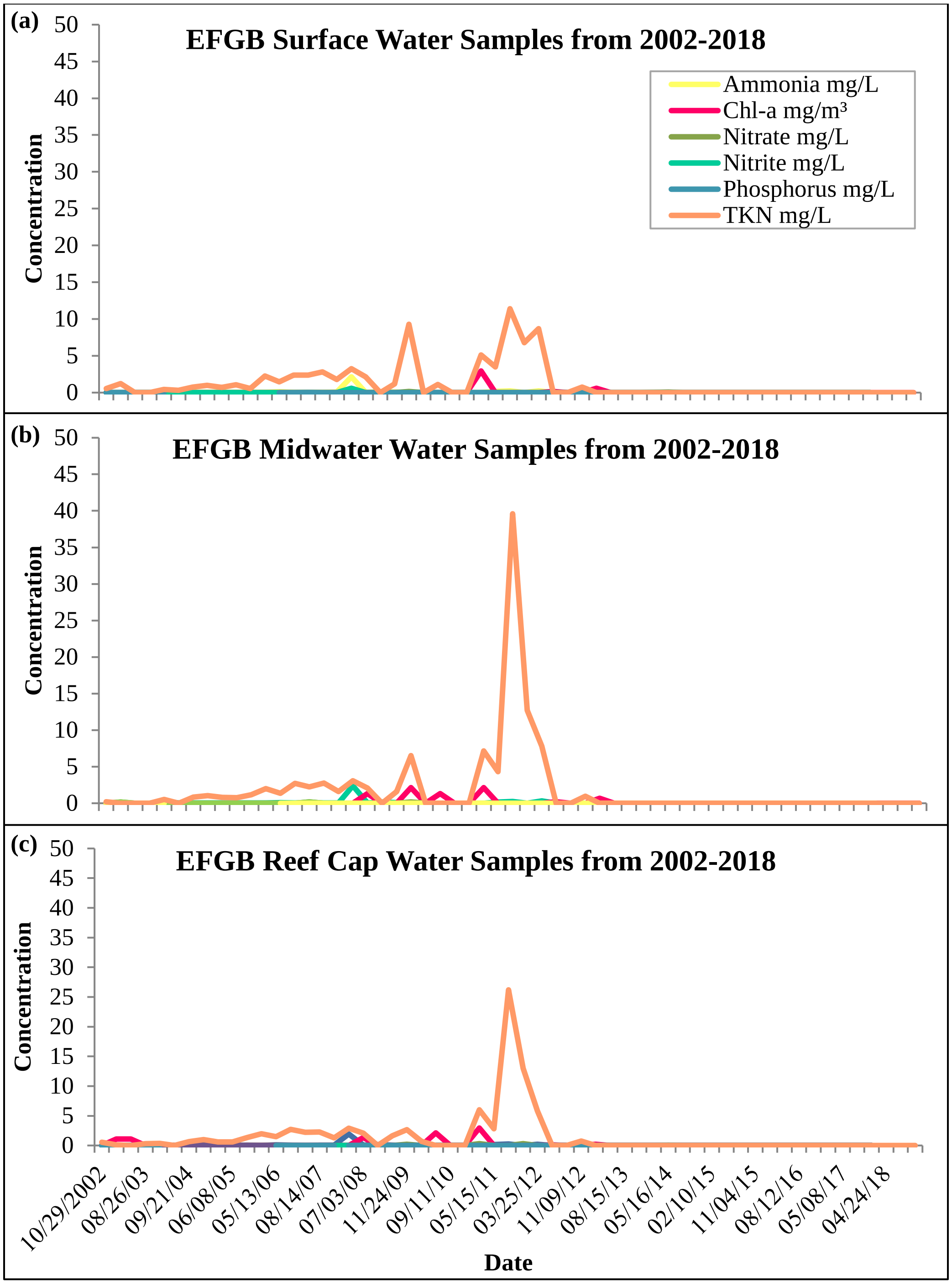

Figure 9.6. Nutrient concentrations from EFGB water samples taken at the (a) surface (1 m), (b) midwater (10 m), and (c) reef cap (16 m) from 2002 to 2018.

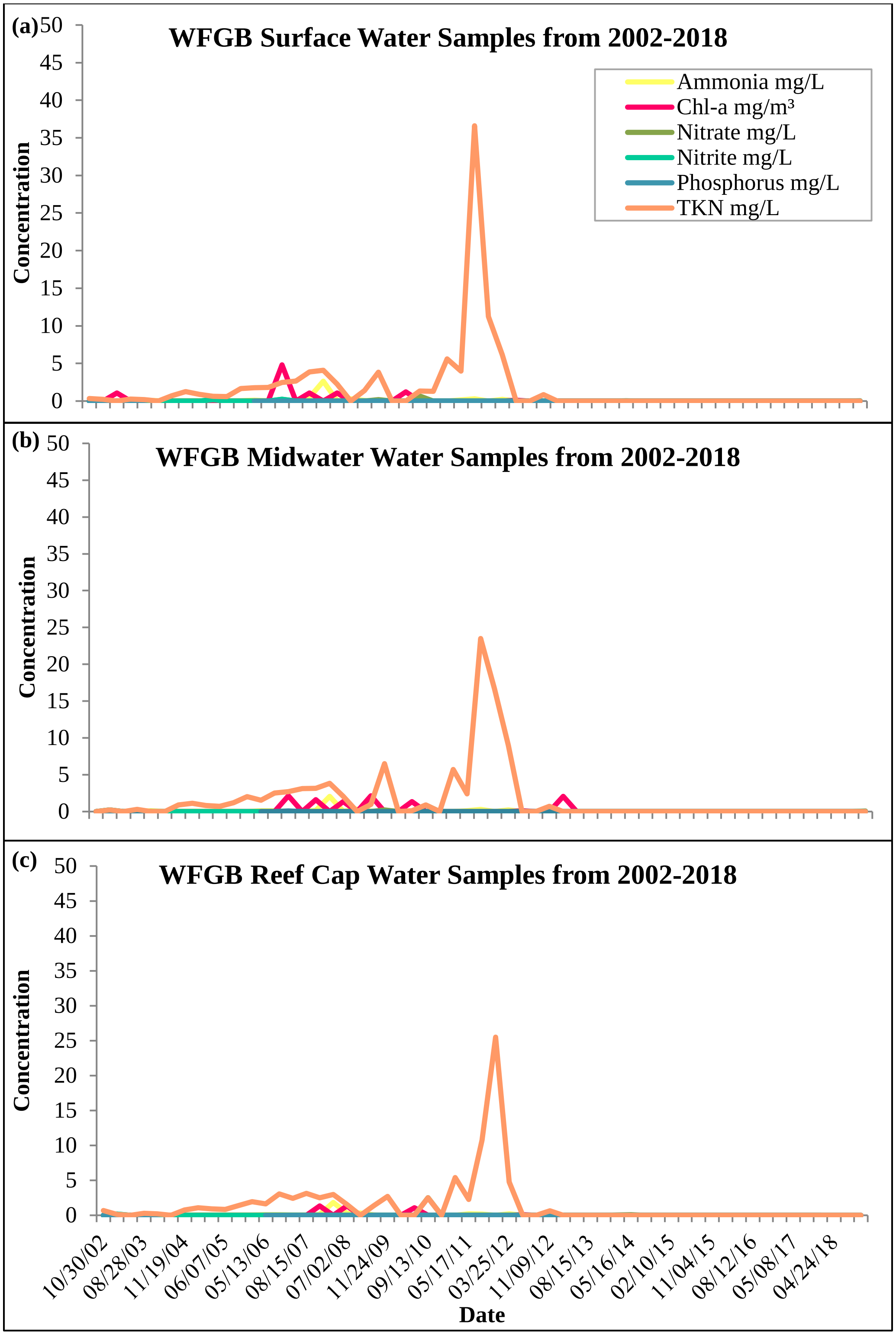

Figure 9.7. Nutrient concentrations from WFGB water samples taken at the (a) surface (1 m), (b) midwater (10 m), and (c) reef cap (16 m) from 2002 to 2018.

Carbonate samples taken during April, August and October at three distinct depth gradients (approximately 20, 10, and 1 m) included pH, alkalinity, CO_2 partial pressure (pCO_2), and total dissolved CO_2 (DIC) (Table 8.4 and 8.5). For EFGB and WFGB, total pH varied little throughout the year. The lowest pCO_2 values, where the air-sea pCO_2 gradients were greatest, were observed in April and October 2018 at both EFGB and WFGB. The lowest $\Omega_{aragonite}$ values and highest DIC were also observed in April 2018.

Table 9.4. EFGB carbonate sample results for 2018 summarized at three depth gradients.

Sample Date	Depth (m)	Salinity (ppt)	Temp (ºC)	pH Total	Alkalinity (µmol/kg)	DIC (µmol/kg)	pH *in situ*	$\Omega_{aragonite}$	pCO_2 (µatm)
4/24/2018	1	36.7	23.6	8.049	2415.2	2095.6	8.070	3.59	387.9
4/24/2018	10	36.71	23.4	8.050	2409.5	2094.9	8.073	3.58	384.2
4/24/2018	20	36.82	23.5	8.050	2414.5	2090.7	8.072	3.58	384.4
8/17/2018	1	36.39	29.70	8.063	2411.4	2076.8	7.993	3.82	471.6
8/17/2018	10	36.49	29.24	8.076	2414.8	2070.7	8.013	3.89	446.7
8/17/2018	20	36.40	28.72	8.075	2408.0	2067.7	8.020	3.86	438.0
10/30/2018	1	35.70	26.95	8.095	2389.9	2045.9	8.066	3.95	384.1
10/30/2018	10	35.73	26.94	8.094	2391.9	2049.8	8.065	3.94	385.5
10/30/2018	20	35.85	26.99	8.089	2391.9	2051.2	8.059	3.90	391.7

Table 9.5. WFGB carbonate sample results for 2018 summarized at three depth gradients.

Sample Date	Depth (m)	Salinity (ppt)	Temp (ºC)	pH Total	Alkalinity (µmol/kg)	DIC (µmol/kg)	pH *in situ*	$\Omega_{aragonite}$	pCO_2 (µatm)
4/24/2018	1	36.615	23.5	8.050	2412.3	2091.7	8.072	3.58	385.4
4/24/2018	10	36.62	23.4	8.050	2410.0	2090.9	8.074	3.57	383.3
4/24/2018	20	36.6	23.4	8.052	2409.3	2089.2	8.075	3.58	380.9
8/17/2018	1	36.21	29.89	8.070	2410.7	2073.0	7.998	3.86	466.1
8/17/2018	10	36.28	29.48	8.080	2412.2	2069.0	8.013	3.92	446.3
8/17/2018	20	36.27	28.66	8.079	2407.2	2069.4	8.024	3.88	433.8
10/30/2018	1	35.86	26.86	8.096	2388.2	2048.5	8.068	3.95	382.4
10/30/2018	10	35.87	26.86	8.091	2387.7	2047.4	8.063	3.90	387.4
10/30/2018	20	35.89	26.84	8.089	2385.3	2045.4	8.061	3.88	388.7

Water Quality Discussion

EFGB and WFGB seawater temperatures at the reef cap in 2018 were warmer than the historical average from February through July, but then dropped below the long-term average in August. WFGB temperatures dropped well below the historical average in August and September before exceeding the historical average again in early October. Although SST as recorded by TABS Buoy V did exceed 30^{o}C, water temperatures at the reef cap depth did not exceed 30^{o}C.

Salinity levels at EFGB and WFGB closely followed the historical averages for most of the study period. WFGB salinity exhibited more variation from the historic baseline than EFGB, where salinity readings from the 24 m logger largely resembled the salinity results from TABS surface Buoy V; however, salinity variability at WFGB was not extreme. Despite annual variation throughout the year, salinity data collected at depth were well within the normal range of variability of salinity for coral reefs located in the Western Atlantic (31–38 psu; Coles and Jokiel 1992). The most likely source of low-salinity water at the banks is a nearshore river-seawater mix, emanating principally from the Mississippi and Atchafalaya River watersheds, that reaches the outer continental shelf and occasionally subjects the banks to nearshore seasonal processes and regional river runoff. Mean salinity reached a low in early June at both banks, according to the 24 m logger, TABS Buoy V, and satellite-derived data, due to coastal runoff from large spring rain events.

Water column profiles in August and October indicated little to no water column stratification; however, nutrient analyses, which are typically below detectable levels, returned measureable, although quite low, nitrate levels within the surface and midwater samples at WFGB in October 2018. Despite these positive nitrate readings ($\leq$0.06 mg/L), laboratory analyses indicated low-nutrient waters in 2018; however, it should be noted that these samples are only taken quarterly and episodic events may escape documentation. Between 2002 and 2011, TKN concentrations were trending upwards, which may have resulted from phytoplankton and bacteria releasing organic nitrogen and ammonia within the food chain subjecting the biological community to seasonal fluctuations. However, TKN can also be affected by both point and non-point sources. When present, the probable sources of nutrients in the water column at the banks were nearshore waters (Nowlin et al. 1998), disturbed sediments (Entsch et al. 1983), or benthic and planktonic organisms (D'Elia and Wiebe 1990). As of 2012, TKN has been below detectable limits at each depth.

Carbonate analysis indicated a thermal control on carbonate systems (*p*CO2 and carbonate saturation state) in the region, with clear seasonal temperature fluctuations. In terms of carbonate chemistry, the lowest $\Omega_{aragonite}$ values and highest DIC values were observed in April 2018, and the aragonite saturation states suggested that EFGB and WFGB were bathed in seawater that was well-buffered at the time of the sampling events. After controlling for temperature, surface seawater pCO_2 did not significantly deviate from atmospheric values throughout annual cycles, and may have a seasonal pattern with peak pCO_2 occurring in late winter to early spring (February to March), and lowest pCO_2 occurring in late summer (August to September). The year 2018 appeared to have a larger air-sea pCO2 gradient (April and October) compared to other years (~70 μatm). Nevertheless, the five-year average of ΔpCO2 suggests that this area had small net air-sea CO_2 flux. Seasonal and spatial distribution of seawater carbonate chemistry in 2018 demonstrates that seawater in the FGBNMS area, despite its relative proximity to land, behaved like an open ocean setting the majority of the time (such as the Bermuda Atlantic Time-series Study) (Bates et al. 2012) in terms of its annual pCO_2 fluctuation and minimal terrestrial influence.

Chapter 10. Conclusions

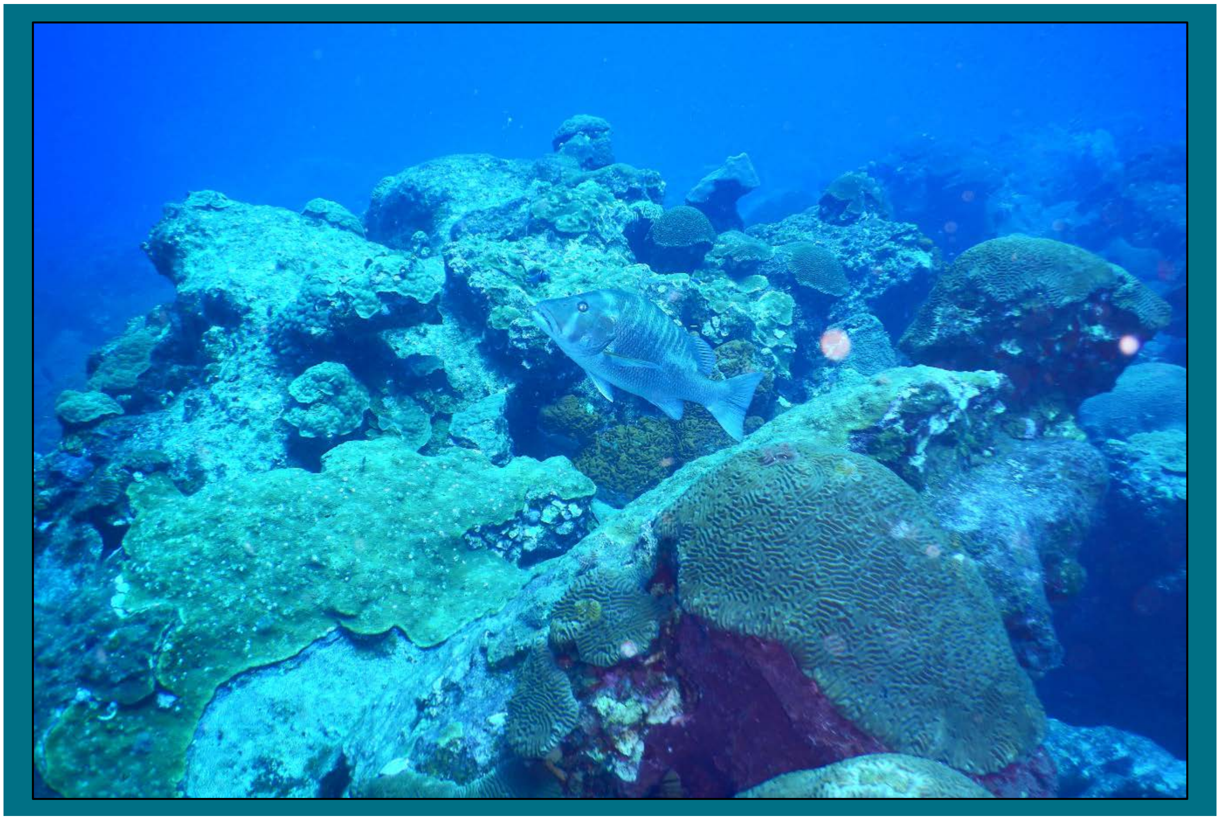

A dog snapper swims over the reef at West Flower Garden Bank in 2018. Photo: Marissa Nuttall/CPC

Despite coral cover declines on most coral reefs of the world in recent decades, mean coral cover within EFGB and WFGB long-term monitoring study sites has ranged from 40–60% for the combined 29 years of monitoring. Even with macroalgae percent cover increasing significantly after the mass mortality of *Diadema antillarum* in the 1980s (with sustained cover of approximately 30% in recent years), unlike many other shallow reefs in the Caribbean region, increases in macroalgae cover have not been concomitant with reduced coral cover at EFGB or WFGB study sites.

Repetitive photostations within study sites indicated increases in coral cover over time at some stations, and stable cover at others. Minimal bleaching and paling was observed in the repetitive stations in 2018. Coral species composition and coral cover changed with depth. Coral cover in the repetitive deep photostations was approximately 70% compared to 50–60% coral cover in the study sites. Macroalgae cover at repetitive deep photostations, while lower than shallower sites, increased over time, following a similar pattern to the repetitive study site photostations and random transects.

Despite the improved methods for collecting marginal growth rates on *Pseudodiploria strigosa* lateral growth stations, it is recognized that these stations have a short lifespan, become covered with biofouling organisms quickly, and do not allow for comparison to other coral reef monitoring programs in the region. Therefore, lateral growth data will no longer be collected after 2018. However, for the duration of data collection from 2014 to 2018, net marginal change was positive in both EFGB and WFGB photostations.

Fish surveys conducted in 2018 indicated an abundant and diverse reef fish community within both EFGB and WFGB study sites, where biomass was uniformly distributed between large and small species. Piscivores had the greatest mean biomass at both EFGB and WFGB, where the high proportion of biomass in the piscivore guild is indicative of an ecosystem with relatively low human impact. Invasive lionfish were documented in fish surveys for the sixth consecutive year, though they were first seen on the banks in 2011. Lionfish densities at EFGB and WFGB study sites continue to remain lower than other locations in the southeast U.S. and Caribbean region. The non-native regal demoiselle was observed in study site surveys at both banks for the first time in 2018.

Water temperatures on the reef cap never exceeded 30ºC in 2018, and salinity averaged 36 psu throughout 2018 at both banks. All nutrient samples taken quarterly in 2018 were below detectable limits, with the exception of elevated nitrate levels at the surface and in midwater at WFGB in October 2018. Carbonate chemistry analysis indicated that the area surrounding EFGB and WFGB acted as a net CO_2 sink.

Overall, one of the most apparent changes since monitoring began in 1989 has been the increase in macroalgae cover. EFGB and WFGB appear unusual compared to other reefs in the region because macroalgae has experienced a sustained increase, yet coral cover has not declined, as it has in so many other places throughout the region. The macroalgae increase on these banks began after the sea urchin die off and may persist because of it;

however, unlike many regional reefs, herbivorous fish have not declined, most nutrients remain below detectable limits, and turbidity remains low. Furthermore, sea urchin populations have slowly been increasing, but remain at a fraction of pre-die off densities. Lastly, it might be suspected that healthy corals, such as those at EFGB and WFGB, are simply better able to compete with algae than stressed corals, perhaps because their marginal tissues more effectively battle for space. It may be that the combination of these factors offset, to some extent, the competitive advantage that macroalgae might otherwise have over corals, and explain the apparent resistance of EFGB and WFGB corals to macroalgae competition.

The ongoing monitoring program at EFGB and WFGB is critical to ensure data are available to understand and distinguish the drivers of ecosystem variation in the northern Gulf of Mexico (Karnauskas et al. 2015). FGBNMS is an ideal sentinel site for the detection and tracking of conditions that are changing because of natural events and human threats. These are places where government, academic, and citizen scientists join, align, and focus capabilities for monitoring, research, data analysis, education, and outreach to raise awareness and inform our actions in response to pressing issues of concern.

Literature Cited

AGRRA (Atlantic and Gulf Rapid Reef Assessment). **2012**. AGRRA Protocols, version 5.4. J.C. Lang, K.W. Marks, P.A. Kramer, P.R. Kramer, and R.N. Ginsburg, eds. 31 p.

Alvarez-Filip, L., J.P. Carricart-Ganivet, G. Horta-Puga, and R. Iglesias-Prieto. **2013**. Shifts in coral-assemblage composition do not ensure persistence of reef functionality. Scientific Reports 3:3486. doi: 10.1038/srep03486

Anderson, M.J., R.N. Gorley, and K.R. Clarke. **2008**. PERMANOVA+ for PRIMER: guide to software and statistical methods. PRIMER-E Ltd. Plymouth, United Kingdom.

Aronson, R.B., P.J. Edmunds, W.F. Precht, D.W. Swanson, and D.R. Levitan. **1994**. Large- scale, long-term monitoring of Caribbean coral reefs: simple, quick, inexpensive methods. Atoll Research Bulletin 421:1–19.

Aronson, R.B. and W.F. Precht. **2000**. Herbivory and algal dynamics on the coral reef at Discovery Bay, Jamaica. Limnology and Oceanography 45:251–255.

Aronson, R.B., W.F. Precht, T.J. Murdoch, and M.L. Robbart. **2005**. Long-term persistence of coral assemblages on the Flower Garden Banks, northwestern Gulf of Mexico: implications for science and management. Gulf of Mexico Science 23:84–94.

Bates, NR, M.H.P Best, K. Neely, R. Garley, A.G. Dickson, and R.J. Johnson. **2012**. Detecting anthropogenic carbon dioxide uptake and ocean acidification in the North Atlantic Ocean. Biogeosciences, 9:2509-2522.

Bauer, L., A. Zitello, S.D. Hile, and T. McGrath. **2015a**. Biogeographic characterization of fish and benthic communities, Jobos Bay, Puerto Rico 2009-06-08 to 2009-06-13 (NODC Accession 0125200). National Oceanographic Data Center, NOAA. Dataset. 12/30/2014.

Bauer, L., S.D. Hile, and T. McGrath. **2015b**. Biogeographic characterization of fish and benthic communities, Vieques, Puerto Rico 2007-05-14 to 2007-05-24 (NODC Accession 0125235). National Oceanographic Data Center, NOAA. Dataset. 12/30/2014.

Bauer, L., S.D. Hile, and T. McGrath. **2015c**. Biogeographic characterization of fish and benthic communities, St Thomas, US Virgin Islands 2012-06-12 to 2012-06-22

(NODC Accession 0125418). National Oceanographic Data Center, NOAA. Dataset. 12/30/2014.

Bohnsack, J.A. and S.P. Bannerot. **1986**. A stationary visual technique for quantitatively assessing community structure of coral reef fishes. NOAA Technical Report NMFS 41:1–15.

Bohnsack, J.A. and D.E. Harper. **1988**. Length-weight relationships of selected marine reef fishes from southeastern United States and the Caribbean. NOAA Technical Memorandum NMFS-SEFC-215. 31 p.

Bridge, T.C., T.J. Done, A. Friedman, R.J. Beaman, S.B. Williams, O. Pizarro, and J.M. Webster. 2011. Variability in mesophotic coral reef communities along the Great Barrier Reef, Australia. Marine Ecology Progress Series 428: 63-75.

Bright, T.J., D.W. McGrail, R. Rezak, G.S. Boland, and A.R. Trippett. **1985**. The Flower Gardens: A compendium of information. U.S. Dept. of the Interior, Minerals Management Service, Gulf of Mexico OCS Region, New Orleans, LA. OCS Study MMS 85-0024. 103 p.

Bright, T.J. and R. Rezak. **1976**. A biological and geological reconnaissance of selected topographical features on the Texas continental shelf. Final Rept. to U.S. Dept. of Interior, Bureau of Land Management. Contract No. 08550-CT5-4. 377 pp.

Bruckner, A.W. and R.J. Bruckner. **1998**. Destruction of coral by *Sparisoma viride*. Coral Reefs 17:350.

Bruckner, A.W., R.J. Bruckner, and P. Sollins. **2000**. Parrotfish predation on live coral: “spot biting” and “focused biting”. Coral Reefs 19:50.

Caldow, C., R. Clark, K. Edwards, S.D. Hile, C. Menza, E. Hickerson, and G.P. Schmahl. **2009**. Biogeographic characterization of fish communities and associated benthic habitats within the Flower Garden Banks National Marine Sanctuary: Sampling design and implementation of SCUBA surveys on the Coral Caps. NOAA Technical Memorandum NOS NCCOS 81. Silver Spring, MD. 134 p.

Caldow, C., K. Roberson, L. Bauer, C.F.G. Jeffrey, S.D. Hile, and T. McGrath. **2015**. Biogeographic characterization of fish and benthic communities, Parguera Region, Puerto Rico 2000-08-21 to 2010-09-21 (NODC Accession 0125202). National Oceanographic Data Center, NOAA. Dataset. 12/30/2014.

Carpenter R.C. and P.J. Edmunds. **2006**. Local and regional scale recovery of *Diadema* promotes recruitment of scleractinian corals. Ecological Letters 9:268–277.

Clark, R., J.C. Taylor, C.A. Buckel, and L.M. Kracklet (eds.). **2014**. Fish and Benthic Communities of the Flower Garden Banks National Marine Sanctuary: Science to Support Sanctuary Management. NOAA Technical Memorandum NOS NCCOS 179. Silver Spring, MD. 317 p.

Clark, R., C.A. Buckel, C. Taylor, S.D. Hile, and T. McGrath. **2015a**. Biogeographic characterization of fish and benthic communities, Flower Garden Banks, Texas 2010-09-10 to 2012-10-02 (NODC Accession 0118358). National Oceanographic Data Center, NOAA. Dataset. 12/30/2014.

Clark, R., S.D. Hile, and T. McGrath. **2015b**. Biogeographic characterization of fish and benthic communities, St Croix, US Virgin Islands 2012-05-07 to 2012-05-18 (NODC Accession 0125237). National Oceanographic Data Center, NOAA. Dataset. 12/30/2014.

Clarke, K.R. **1990**. Comparison of dominance curves. Journal of Experimental Marine Biology and Ecology 138:143-157.

Clarke, K.R., P.J. Somerfield, and R.N. Gorley. **2008**. Testing of null hypotheses in exploratory community analyses: similarity profiles and biota-environment linkage. Journal of Experimental Marine Biology and Ecology 366:56-69.

Clarke, K.R., R.N. Gorley, P.J. Sommerfield, and R.M. Warwick. **2014**. Change in marine communities: an approach to statistical analysis and interpretation, 3rd edition. PRIMER-E: Plymouth, Devon, UK. 260 p.

Coles, S.L. and P.L. Jokiel. **1992**. Effects of salinity on coral reefs. In Pollution in tropical aquatic systems, D.W. Connell and D.W. Hawker, eds. Boca Raton, FL: CRC Press. 147–166 p.

CSA (Continental Shelf Associates). **1989**. Environmental monitoring program for exploratory well #1, lease OCS-G 6264 High Island Area, South Extension, East Addition, Block A-401 near the Flower Garden Bank. Final Report. Jupiter, FL: CSA. 96 p.

CSA (Continental Shelf Associates). **1996**. Long-term monitoring at the East and West Flower Garden Banks. U.S. Dept. of the Interior, Minerals Management Service, Gulf of Mexico OCS Region, New Orleans, LA. OCS Study MMS 96-0046. 77 p.

Dahl, K.A. and W.F. Patterson. **2014**. Habitat-specific density and diet of rapidly expanding invasive red lionfish, *Pterois volitans*, populations in the northern Gulf of Mexico. PLoS One 9:e105852. doi:10.1371/journal.pone.0105852

Darling, E.S., S.J. Green, J.K. O'Leary, and I.M. Côté. **2011**. Indo-Pacific lionfish are larger and more abundant on invaded reefs: a comparison on Kenyan and Bahamian lionfish populations. Biological Invasions 13:2045–2051.

Debose, J.L., M.F. Nuttall, E.L. Hickerson, and G.P. Schmahl. **2012**. A high-latitude coral community with uncertain future: Stetson Bank, northwestern Gulf of Mexico. Coral Reefs 32:255-267.

D'Elia, C.F. and W.J. Wiebe. **1990**. Biogeochemical nutrient cycles in coral-reef ecosystems. In: Dubinsky, Z., ed. Coral reefs. Amsterdam: Elsevier. 49–74 p.

DeMartini, E.E., A.M. Friedlander, S.A. Sandin, and E. Sala. **2008**. Differences in fish-assemblage structure between fished and unfished atolls in the northern Line Islands, central Pacific. Marine Ecology Progress Series 365:199-215.

Dennis, G.D. and T.J. Bright. **1988**. Reef fish assemblages on hard banks in the northwestern Gulf of Mexico. Bulletin of Marine Science 43:280–307.

Dokken, Q.R., I.R. MacDonald, J.W. Tunnell, C.R. Beaver, G.S. Boland, and D.K. Hagman. **1999**. Long-term monitoring of the East and West Flower Garden Banks 1996–1997. U.S. Dept. of the Interior, Mineral Management Service, Gulf of Mexico OCS Region, New Orleans, LA. OCS Study MMS 99-0005. 101 p.

Dokken, Q. R., I.R. MacDonald, J.W. Jr. Tunnell, T. Wade, K. Withers, S.J. Dilworth, T.W. Bates, C.R. Beaver, and C.M. Rigaud. **2003**. Long-term monitoring at the East and West Flower Garden Banks National Marine Sanctuary, 1998–2001: Final report. U.S. Dept. of the Interior, Minerals Management Service, Gulf of Mexico OCS Region, New Orleans, LA. OCS Study MMS 2003-031. 90 p.

Edmunds, P.J. and R.C. Carpenter. **2001**. Recovery of *Diadema antillarum* reduces macroalgal cover and increases abundance of juvenile corals on a Caribbean reef. Proceedings of the National Academy of Sciences 98:5067–5071.

Entsch, B., K.G. Boto, R.G. Sim, and J.T. Wellington. **1983**. Phosphorous and nitrogen in coral reef sediments. Limnology and Oceanography 28:465–476.

Friedlander A and E. DeMartini. **2002**. Contrasts in density, size, and biomass of reef fishes between the northwestern and the main Hawaiian Islands: the effects of fishing down apex predators. Marine Ecology Progress Series 230:253–264.

Froese, R. and D. Pauly. (eds). **2018**. FishBase. World Wide Web electronic publication. Last Accessed: 10/12/2018. www.fishbase.org

Gardner, T.A., I.M. Côté, J.A. Gill, A. Grant, and A.R. Watkinson. **2003**. Long-term region- wide declines in Caribbean corals. Science 301:958–960.

Gittings, S.R. **1998**. Reef community stability on the Flower Garden Banks, northwest Gulf of Mexico. Gulf of Mexico Science 1998:161–169.

Gittings, S.R. and T.J. Bright. **1987**. Mass mortality of *Diadema antillarum* at the Flower Garden Banks, Northwest Gulf of Mexico: effect on algae and coral cover. Abstract. Benthic Ecology Meetings, Raleigh, NC.

Gittings S.R., G.S. Boland, K.J.P. Deslarzes, D.K. Hagman, and B.S. Holland. **1992**. Long-term monitoring at the East and West Flower Garden Banks. U.S. Dept. of the Interior, Minerals Management Service, Gulf of Mexico OCS Region, New Orleans, LA. OCS Study MMS 92-0006. 206 p.

Glynn, P.W. and L. D'Croz. **1990**. Experimental evidence for high temperature stress as the case of El Nino-coincident coral mortality. Coral Reefs 8:181–191.

Goreau, T.F. and J.W. Wells. **1967**. The shallow water Scleractinia of Jamaica: revised list of species and their vertical distribution range. Bulletin of Marine Science 17:442–454.

Graham, N.A.J. and K.L. Nash. **2013**. The importance of structural complexity in coral reef ecosystems. Coral Reefs 32:315-326.

Green, D.H., P.J. Edmunds, and R.C. Carpenter. **2008**. Increasing relative abundance of *Porites astreoides* on Caribbean reefs mediated by an overall decline in coral cover. Marine Ecology Progress Series 359:1-10.

Green, S.J. and I.M. Côté . **2009**. Record densities of Indo-Pacific lionfish on Bahamian coral reefs. Coral Reefs 28:107.

Green, S.J., N.K. Dulvy, A.L.M. Brooks, J.L. Akins, A.B. Cooper, S. Miller, and I.M. Côté. **2014**. Linking removal targets to the ecological effects of invaders: a predictive model and field test. Ecological Applications 24:1311-1322. doi:10.1890/13-0979.1

Hagman, D.K. and S.R. Gittings. **1992**. Coral bleaching on high latitude reefs at the Flower Garden Banks, NW Gulf of Mexico. Proceedings of the 7th International Coral Reef Symposium 1:38-43.

Helsel, D.R. and R.M. Hirsch. **2002**. Statistical methods in water resources. In: Techniques of water-resources investigations of the United States Geological

Survey. Book 4, Hydrologic analysis and interpretation. Washington DC: U.S. Geological Survey. 522 p.

Helsel, D.R., D.K. Mueller, and J.R. Slack. **2006**. Computer program for the Kendall family of trend tests: U.S. Geological Survey Scientific Investigations Report 2005–5275. 4 p.

Heron, S.F., J.A. Maynard, R. van Hooidonk, and C.M. Eakin. **2016**. Warming trends and bleaching stress of the world's coral reefs 1985-2012. Scientific Reports 6:3842.

Hipel, K.W. and A.I. McLeod. **1994**. Time series modelling of water resources and environmental systems. http://www.stats.uwo.ca/faculty/aim/RPackages.htm

Hughes, T.P., J.T. Kerry, M. Alvarez-Noriega, J.G. Alveraz-Romero, et al. **2017**. Global warming and recurrent mass bleaching of corals. Nature 543:373-377.

Jackson, J.B.C., Donovan, M.K., Cramer, K.L., Lam, V.V. (eds). **2014**. Status and Trends of Caribbean coral reefs: 1970-2012. Global Coral Reef Monitoring Network, IUCN, Gland, Switzerland. 304 p.

Johnston, M.A., M.F. Nuttall, R.J. Eckert, J.A. Embesi, N.C. Slowey, E.L. Hickerson, and G.P. Schmahl. **2013**. Long-term monitoring at the East and West Flower Garden Banks National Marine Sanctuary, 2009-2010, volume 1: technical report. U.S. Dept. of Interior, Bureau of Ocean Energy Management, Gulf of Mexico OCS Region, New Orleans, LA. OCS Study BOEM 2013-215. 362 p.

Johnston, M.A., M.F. Nuttall, R.J. Eckert, J.A. Embesi, N.C. Slowey, E.L. Hickerson, and G.P. Schmahl. **2015**. Long-term monitoring at the East and West Flower Garden Banks National Marine Sanctuary, 2011–2012, volume 1: technical report. U.S. Dept. of Interior, Bureau of Ocean Energy Management, Gulf of Mexico OCS Region, New Orleans, LA. OCS Study BOEM 2015-027. 194 p.

Johnston, M.A., M.F. Nuttall, R.J. Eckert, J.A. Embesi, T.K. Sterne, E.L. Hickerson, and G.P. Schmahl. **2016a**. Rapid invasion of Indo-Pacific lionfishes *Pterois volitans* (Linnaeus, 1758) and *P. miles* (Bennett, 1828) in Flower Garden Banks National Marine Sanctuary, Gulf of Mexico, documented in multiple data sets. Bioinvasions Records 5:115-122.

Johnston, M.A., M.F. Nuttall, R.J. Eckert, J.A. Embesi, T.K. Sterne, E.L. Hickerson, G.P. Schmahl. **2016b**. Persistence of Coral Assemblages in Flower Garden Banks National Marine Sanctuary, Gulf of Mexico. Coral Reefs 35:821-826.

Johnston, M.A., R.J. Eckert, M.F. Nuttall, T.K. Sterne, J.A. Embesi, D.P. Manzello, E.L. Hickerson, and G.P. Schmahl. **2017a**. Long-term monitoring at the East and West Flower Garden Banks National Marine Sanctuary, 2013–2015, volume 1: technical report. U.S. Dept. of Interior, Bureau of Ocean Energy Management, Gulf of Mexico OCS Region, New Orleans, LA. OCS Study BOEM 2017-058. 186 p.

Johnston, M.A., T.K. Sterne, R.J. Eckert, M.F. Nuttall, J.A. Embesi, R. Walker, X. Hu, E.L. Hickerson, and G.P. Schmahl. **2017b**. Long-term monitoring at East and West Flower Garden Banks, 2016 Annual Report. Marine Sanctuaries Conservation Series ONMS-17-09. U.S. Department of Commerce, National Oceanic and Atmospheric Administration, Flower Garden Banks National Marine Sanctuary, Galveston, TX. 132 pp.

Johnston, M.A., M.F. Nuttall, R.J. Eckert, R.D. Blakeway, T.K. Sterne, E.L. Hickerson, G.P. Schmahl, M.T. Lee, J. MacMillan, and J.A. Embesi. **2018a**. Localized coral reef mortality event at East Flower Garden Bank, Gulf of Mexico. Bulletin of Marine Science 95:239-250.

Johnston, M.A., T.K. Sterne, R.D. Blakeway, J. MacMillan, M.F. Nuttall, X. Hu, J.A. Embesi, E.L. Hickerson, and G.P. Schmahl. **2018b**. Long-term monitoring at East and West Flower Garden Banks, 2017 Annual Report. Marine Sanctuaries Conservation Series ONMS-18-02. U.S. Department of Commerce, National Oceanic and Atmospheric Administration, Flower Garden Banks National Marine Sanctuary, Galveston, TX. 124 pp.

Johnston, M.A., E.L. Hickerson, M.F. Nuttall, R.D. Blakeway, T.K. Sterne, R.J. Eckert, and G.P. Schmahl. **2019**. Coral bleaching and recovery from 2016 to 2017 at East and West Flower Garden Banks, Gulf of Mexico. Coral Reefs 38:787-799. doi: 10.1007/s00338-019-01788-7

JPL MUR MEaSUREs Project. **2015**. GHRSST Level 4 MUR Global Foundation Sea Surface Temperature Analysis (v4.1). Ver. 4.1. PO.DAAC, CA, USA. Dataset accessed [2019-10-18] at https://doi.org/10.5067/GHGMR-4FJ04.

Karnauskas, M., M.J. Schirripa, J.K. Craig, G.S. Cook, C.R. Kelble, J.J. Agar, B.A. Black, D.B. Enfield, D. Lindo-Atichati, B.A. Muhling, K.M. Purcell, P.M. Richards, C. Wang. **2015**. Evidence of climate-driven ecosystem reorganization in the Gulf of Mexico. Global Change Biology 21:2554-2568. doi: 10.1111/gcb.12894

Knowlton, N. and J.B.C. Jackson. **2008**. Shifting baselines, local impacts, and global change on coral reefs. PLoS Biology 6:e54.

Kohler, K.E. and S.M. Gill. **2006**. Coral point count with Excel extensions (CPCe): A Visual Basic program for the determination of coral and substrate coverage using random point count methodology. Computers and Geosciences 32:1259–1269.

Kramer, P.A. **2003**. Synthesis of coral reef health indicators for the western Atlantic: results of the AGRRA program (1997–2000). Atoll Research Bulletin 496:1–58.

Morris, J.A. Jr. and P.E. Whitfield. **2009**. Biology, ecology, control and management of the invasive Indo-Pacific Lionfish: an updated integrated assessment. NOAA Technical Memorandum NOS NCCOS 99. 57 p.

Mumby, P.J., A.J. Edwards, J.E Arias-González, K.C. Kindeman, P.G Blackwell, A. Gall, M.I. Gorczynska, A.R. Harborne, C.L. Pescod, H. Renken, C.C.C. Wabnitz, and G. Llewellyn. **2004**. Mangroves enhance the biomass of coral reef fish communities in the Caribbean. Nature 427:533-536.

Mumby, P.J. and R.S. Steneck RS. **2011**. The resilience of coral reefs and its implications for reef management. In: Dubinsky Z, Stambler N, eds. Coral reefs: an ecosystem in transition. Springer, Netherlands. 509–519 p.

Nowlin, W.D., A.E. Jochens, R.O. Reid, and S.F. DiMarco. **1998**. Texas-Louisiana shelf circulation and transport processes study: synthesis report. Volume II: Appendices. U.S. Dept. of the Interior, Minerals Management Service, Gulf of Mexico OCS Region, New Orleans, LA. OCS Study MMS 98-0036. 288 p.

Nuttall, M.F., M.A. Johnston, R.J. Eckert, J.A. Embesi, E.L. Hickerson, and G.P. Schmahl. **2014**. Lionfish (*Pterois volitans* [Linnaeus, 1758] and *P. miles* [Bennett, 1828]) records within mesophotic depth ranges on natural banks in the Northwestern Gulf of Mexico. Bioinvasions Records 3:111-115.

Nuttall, M.F., R.D. Blakeway, J. MacMillan, T.K. Sterne, X. Hu, J.A. Embesi, E.L. Hickerson, M.J. Johnston, G.P. Schmahl, and J. Sinclair. **2018**. Stetson Bank Long-Term Monitoring: 2017 Annual Report. National Marine Sanctuaries Conservation Series ONMS-19-03. U.S. Department of Commerce, National Oceanic and Atmospheric Administration, Flower Garden Banks National Marine Sanctuary, Galveston, TX. 94 p.

Odum, E. and H. Odum. **1971**. Fundamentals of ecology. Saunders Co., Philadelphia. 624 p.

Ogden, J. and R. Wicklund (eds). **1988**. Mass bleaching of coral reefs in the Caribbean: a research strategy. National Undersea Research Program Research Report 88-2. US Department of Commerce. Washington, D.C. 51 p.

ONMS (Office of National Marine Sanctuaries). **2008**. Flower Garden Banks National Marine Sanctuary Condition Report 2008. U.S. DOC, NOAA, ONMS, Silver Spring, MD. 49 p.

ONMS (Office of National Marine Sanctuaries). **2011**. Florida Keys National Marine Sanctuary Condition Report 2011. U.S. DOC, NOAA, ONMS, Silver Spring, MD. 105 p.

Pattengill, C.V. **1998**. The structure and persistence of reef fish assemblages of the Flower Garden Banks National Marine Sanctuary. Doctoral dissertation, Texas A&M University, College Station, TX. 176 p.

Pattengiill-Semmens, C.V. and B.X. Semmens. **1998**. An analysis of fish survey data generated by nonexpert volunteers in the Flower Garden Banks National Marine Sanctuary. Gulf of Mexico Science 16:196-207.

Pittman, S., S.D. Hile, and T. McGrath. **2015**. Biogeographic characterization of fish and benthic communities of East End Marine Park, St. Croix, US Virgin Islands 2010-10-18 to 2011-11-10 (NODC Accession 0125270). National Oceanographic Data Center, NOAA. Dataset. 12/30/2014.

Precht, W.F., R.B. Aronson, K.J.P. Deslarzes, M.L. Robbart, A. Gelber, D. Evans, B. Gearheart, and B. Zimmer. **2006**. Long-term monitoring at the East and West Flower Garden Banks, 2002–2003: Final report. U.S. Dept. of the Interior, Minerals Management Service, Gulf of Mexico OCS Region, New Orleans, LA. OCS Study MMS 2004–031. 182 p.

Precht, W.F., R.B. Aronson, K.J.P. Deslarzes, M.L. Robbart, B. Zimmer, and L. Duncan. **2008**. Post-hurricane assessment at the East Flower Garden Bank long-term monitoring site: November 2005. U.S. Dept. of the Interior, Minerals Management Service, Gulf of Mexico OCS Region, New Orleans, LA. OCS Study MMS 2008-019. 39 p.

REEF (Reef Environmental Education Foundation). **2014**. Reef Environmental Education Foundation. World Wide Web electronic publication. Last Accessed: 4/24/2014. www.reef.org

Roberson, K. S. Viehman, and R. Clark. **2014**. Development of Benthic and Fish Monitoring Protocols for the Atlantic/Caribbean Biological Team: National Coral Reef Monitoring Program. NOAA Coral Reef Conservation Program. 8 p.

Roberson, K., C. Caldow, C.F.G. Jeffrey, S.D. Hile, and T. McGrath. **2015**. Biogeographic characterization of fish and benthic communities, St Croix and St

John, US Virgin Islands 2001-02-06 to 2010-10-29 (NODC Accession 0125236). National Oceanographic Data Center, NOAA. Dataset. 12/30/2014.

Robertson, D.R., N. Simoes, C. Gutiérrez Rodríguez, V.J. Piñeros, H. and Pérez-España. **2016**. An Indo-Pacific damselfish well established in the southern Gulf of Mexico: prospects for a wider, adverse invasion. Journal of the Ocean Science Foundation 19:1–17.

Robertson, D.R., O. Dominguez-Dominguez, B. Victor, and N. Simoes. **2018**. An Indo-Pacific damselfish (*Neopomacentrus cyanomos*) in the Gulf of Mexico: origin and mode of introduction. PeerJ 6:e4328. https://doi.org/10.7717/peerj.4328

Rooker, J.R., Q.R. Dokken, C.V. Pattengill, and G.J. Holt. **1997**. Fish assemblages on artificial and natural reefs in the Flower Garden Banks National Marine Sanctuary, USA. Coral Reefs 16:83–92.

Ruzicka, R., K. Semon, M. Colella, V. Brinkhuis, J. Kidney, J. Morrison, K. Macaulay, J.W. Porter, M. Meyers, M. Christman, and J. Colee. **2009**. Coral Reef Evaluation and Monitoring Project Annual Report. NOAA/NOS MOA-2001-683/7477. 111 p.

Sale, P.F. **1991**. The ecology of fishes on coral reefs. Academic Press, Inc., San Diego, California. 754 p.

Sandin S, J. Smith, E. DeMartini, E. Dinsdale, S. Donner, A. Friedlander, T. Konotchick, M. Malay, J. Maragos, D. Obura. **2008**. Baselines and degradation of coral reefs in the northern Line Islands. PLoS ONE 3:e1548.

Schmahl, G.P., E.L. Hickerson, and W.F. Precht. **2008**. Biology and ecology of coral reefs and coral communities in the Flower Garden Banks region, northwestern Gulf of Mexico. In: Riegl, B. and R. Dodge, eds. Coral Reefs of the USA. Springer Netherlands. 221–261 p.

Simons, R.A. **2019**. ERDDAP. https://coastwatch.pfeg.noaa.gov/erddap. Monterey, CA: NOAA/NMFS/SWFSC/ERD.

Singh, A., H. Wang, W. Morrison, H. Weiss. **2012**. Modeling fish biomass structure at near pristine coral reefs and degradation by fishing. Journal of Biological Systems 20:21-36.

SOKI Wiki. **2014**. Abundance biomass curve (ABC method) - Indicators - Confluence, SOKI, Antarctic Climate and Ecosystems Co-operative Research Centre. Last Accessed: 12/8/ 2014. http://www.soki.aq/x/foFm

Steneck, R.S., S. Arnold, and H. DeBey. **2011**. Status and trends of Bonaire's reefs 2011 and cause for grave concerns. University of Maine and NOAA National Marine Fisheries Service, Silver Spring, MD. 137 p.

Toth, L.T., R.V. Woesik, T.J.T. Murdocj, S.R. Smith, J.C. Ogden, W.F. Precht, and R.B. Aronson. **2014**. Do no-take reserves benefit Florida's corals? 14 years of change and stasis in the Florida Keys National Marine Sanctuary. Coral Reefs 33:565-577. doi: 10.1007/s00338-014-1158-x

van Hooidonk, R., J.A. Maynard, J. Tamelander, J. Gove, G. Ahmadia, L. Raymundo, G. Williams, S. Heron, and S. Planes. **2016**. Local-scale projections of coral reef futures and implications of the Paris Agreement. Nature Scientific Reports 6:39666.

Wang, H., W. Morrison, A. Singh, H. Weiss. **2009**. Modeling inverted biomass pyramids and refuges in ecosystems. Ecological Modeling 220:1376-1382.

Yau, Chi. **2016**. R tutorial with Bayesian statistics using OpenBUGS. Accessed 10/24/2016. www.r-tutor.com

Zimmer, B., L. Duncan, R.B. Aronson, K.J.P. Deslarzes, D. Deis, M.L. Robbart, W.F. Precht, L. Kaufman, B. Shank, E. Weil, J. Field, D.J. Evans, and L. Whaylen. **2010**. Long-term monitoring at the East and West Flower Garden Banks, 2004–2008. Volume I: Technical report. U.S. Dept. of the Interior, Bureau of Ocean Energy Management, Regulation, and Enforcement, Gulf of Mexico OCS Region, New Orleans, LA. OCS Study BOEMRE 2010-052. 310 p.

Acknowledgments

Flower Garden Banks National Marine Sanctuary (FGBNMS) would like to acknowledge the many groups and individuals that provided invaluable support to make this monitoring effort successful, including the Bureau of Ocean Energy Management (BOEM), Cardinal Point Captains, Texas A&M University Galveston, Moody Gardens Aquarium, Scripps Institution of Oceanography, the National Marine Sanctuary Foundation, NOAA Coast Watch, and the NOAA Dive Center. In particular, we acknowledge BOEM COR, Mark Belter, for his support and dedication to this project and Dr. Xinping Hu from TAMU-CC for providing ocean carbonate data. Finally, our sincere thanks are extended to the editors and reviewers of this document who helped improve this report.

Researchers and volunteers that assisted with 2018 field operations, data collection, and data processing include:

Raven Blakeway
Robert Brewer
John Embesi
Jake Emmert
Vianne Euresti
Keith Hanson
Rebekah Hernandez
Emma Hickerson
Chris Isom
Michelle Johnston
Clayton Leopold
Sarah Linden
Jimmy MacMillan
David McBee
Marissa Nuttall
Kelly O'Connell
Dustin Picard
G.P. Schmahl
Brian Zelenke

Cardinal Point Captains - R/V *Manta* Crew:
Justin Blake
Jose Bosquez
Karol Brewer
Cassidy Brown
Nicole Cherichella

This study was funded through an interagency agreement between the Bureau of Ocean Energy Management and the National Oceanic and Atmospheric Administration's National Ocean Service, Office of National Marine Sanctuaries, through Flower Garden Banks National Marine Sanctuary under contract number M14PG00020. Field work in 2018 was carried out under permit FGBNMS-2018-001.

Glossary of Acronyms

ANOSIM – analyis of similarities
BOEM – Bureau of Ocean Energy Management
CCL – Carbon Cycle Laboratory
Chl-*a – chlorophyll-a*
CPCe – Coral Point Count® with Excel® extensions
CTB – crustose coralline algae, fine turf algae, and bare rock
CTD – conductivity, temperature, and depth
DIC – total dissolved CO_2
DO – dissolved oxygen
EFGB – East Flower Garden Bank
EPA – Environmental Protection Agency
FGBNMS – Flower Garden Banks National Marine Sanctuary
LTM – long-term monitoring
MMS – Minerals Management Service
NOAA – National Oceanic and Atmospheric Administration
PCO – principal coordinates ordination
pCO_2 *–* CO_2 *partial pressure*
PERMANOVA – permutational multivariate analysis of variance
SIMPER – similarity percentages
SSS – sea surface salinity
SST – sea surface temperature
TABS – Texas Automated Buoy System
TAMU – Texas A&M University
TAMU-CC – Texas A&M University Corpus Christi
TKN – total Kjeldahl nitrogen
QA/QC – quality assurance/quality control
WFGB – West Flower Garden Bank

National Marine Sanctuaries

America's Underwater Treasures